EFFECTS OF METFORMIN ON OLANZAPINE INDUCED WEIGHT GAIN IN MALE WISTAR RATS: THE CHANGE OF HYPOTHALAMIC NEUROHORMONES INVOLVED IN BODY WEIGHT REGULATION

A THESIS SUBMITTED TO
THE GRADUATE SCHOOL OF NATURAL AND APPLIED SCIENCES
OF
MIDDLE EAST TECHNICAL UNIVERSITY

BY

GİZEM KURT

IN PARTIAL FULFILLMENT OF THE REQUIREMENTS
FOR
THE DEGREE OF MASTER OF SCIENCE
IN
BIOLOGY

JULY 2014

Approval of the thesis :

EFFECTS OF METFORMIN ON OLANZAPINE INDUCED WEIGHT GAIN IN MALE WISTAR RATS: THE CHANGE OF HYPOTHALAMIC NEUROHORMONES INVOLVED IN BODY WEIGHT REGULATION

submitted by **GİZEM KURT** in partial fulfillment of the requirements for the degree of **Master of Science in Biology Department, Middle East Technical University** by,

Prof. Dr. Canan Özgen _____
Dean, Graduate School of **Natural and Applied Sciences**

Prof. Dr. Orhan Adalı _____
Head of Department, **Biology**

Assoc. Prof. Dr. Tülin Yanık _____
Supervisor, **Biology Dept., METU**

Examining Committee Members:

Prof. Dr. Semra Kocabıyık _____
Biology Dept., METU

Assoc. Prof. Dr. Tülin Yanık _____
Biology Dept., METU

Assoc. Prof. Dr. Mesut Muyan _____
Biology Dept., METU

Assoc. Prof. Dr.Çağdaş Devrim Son _____
Biology Dept., METU

Assoc. Prof. Dr. Mehmet Ak _____
Meram Medical School, Necmettin Erbakan University

Date: 24.07.2014

I hereby declare that all information in this document has been obtained and presented in accordance with academic rules and ethical conduct. I also declare that, as required by these rules and conduct, I have fully cited and referenced all material and results that are not original to this work.

Name, Last Name: GİZEM KURT

Signature:

ABSTRACT

EFFECTS OF METFORMIN ON OLANZAPINE INDUCED WEIGHT GAIN IN MALE WISTAR RATS: THE CHANGE OF HYPOTHALAMIC NEUROHORMONES INVOLVED IN BODY WEIGHT REGULATION

Kurt, Gizem

M.S., Department of Biology

Supervisor: Assoc. Prof. Dr. Tülin Yanık

July 2014, 148 pages

Obesity, resulting from the extreme weight gain, is one of the biggest health problems nowadays because it causes disruption of the metabolism and metabolic problems, including type 2 diabetes mellitus, dyslipidemia and cardiovascular disease. Atypical (second generation) antipsychotic drugs, which are highly in use, have adverse effects including weight gain. Ongoing researches for the treatment of antipsychotics induced-weight gain are present and one of the promising agents is metformin, an anti-diabetic drug. However, hypothalamic targets and cellular

action mechanisms of metformin in the antipsychotic-treated brain is still unknown. The main regulator of the appetite, weight balance and energy homeostasis is the hypothalamus, and hypothalamic neurohormones; proopiomelanocortin (POMC), anorexigenic, and neuropeptide Y (NPY), orexigenic, are potent. The aim of this study was to investigate the underlying hypothalamic mechanisms of the metformin treatment of atypical antipsychotic olanzapine-induced weight gain in male Wistar rats. Our hypothesis was the treatment of olanzapine increases the orexigenic peptide and decreases the anorexigenic peptide expression levels in the hypothalamus whereas metformin which can pass the brain blood barrier (BBB) might reverse those possible effects. Our results indicated that *POMC* expression in the hypothalamus decreased in all olanzapine groups regardless of the metformin administration. In addition, metformin could not fully restore the significantly increased hypothalamic *NPY* expression resulting from olanzapine treatment.

Key Words: olanzapine, metformin, neuropeptide Y, proopiomelanocortin, weight gain

ÖZ

METFORMİNİN ERKEK WİSTAR SIÇANLARDA OLANZAPİN KAYNAKLI KİLO ALIMINA ETKİLERİ: VÜCUT KİLO KONTROLÜNDE ROL ALAN HiPOTALAMİK NÖROHORMONLARDAKİ DEĞİŞİM

Kurt, Gizem

Yüksek Lisans, Biyoloji Bölümü

Tez Yöneticisi: Doç. Dr. Tülin Yanık

Temmuz 2014, 148 sayfa

Aşırı kilo alımı sonucu oluşan obezite günümüzdeki en büyük sağlık sorunlarından biri olarak metabolizmanın bozulmasına ve tip 2 diyabet, dislipidemi ve kardiyovasküler riskler gibi metabolik problemlere sebebiyet vermektedir. Yaygın olarak kullanılan ikinci jenerasyon antipsikotik ilaçların yan etkilerinden biri de aşırı kilo alımıdır. Antipsikotiklerin sebep olduğu kilo alımını önlemek için araştırmalar sürdürülmektedir. Kilo alımı tedavisinde etkili olduğu görülen

ajanlardan biri de antidiyabetik ilaç metformindir. Buna rağmen, metforminin hipotalamustaki hedefleri ve etki mekanizması halen belirsizliğini korumaktadır. Vücudun kilo dengesi ve enerji metabolizması ağırlıklı olarak hipotalamusun kontrolündedir. Hipotalamik nöropeptitlerden anoreksijenik proopiomelanokortin (POMC) ve oreksijenik nöropeptit Y (NPY) iştah, kilo ve enerji metabolizması kontrolünde rol alan etkin elemanlardandır. Bu çalışmamızın amacı, olanzapinin sebep olduğu kilo alımının ve kilo alımının tersine çevrilmesi için uygulanan metformin tedavisinin altında yatan hipotalamik mekanizmaları araştırmaktır. Hipotezimize göre, olanzapin kullanımı hipotalamustaki oreksijenik peptit gen ifadesi düzeylerini artırırken, anoreksijenik olanların gen ifadesini azaltacaktır. Beyin-Kan Bariyerini (BBB) geçebilen metformin ise aynı peptitler üzerinden tam tersi etki oluşturacaktır. Elde ettiğimiz bulgular, tüm olanzapin gruplarında, hipotalamik *POMC* ifadelerinde anlamlı bir azalmaya işaret etmiştir. Buna ek olarak, hipotalamik *NPY* düzeylerinde olanzapine kullanımına bağlı gözlemlediğimiz anlamlı artış, metformin kullanımıyla tam olarak control düzeylerine geri dönmemiştir.

Anahtar Kelimeler: olanzapin, metformin, nöropeptit Y, proopiomelanokortin, kilo alımı

To the Kemalist Turkey where the science and the wisdom

will be the only sources to shed light to our paths

ACKNOWLEDGEMENTS

First of all, I would like to express my gratitude to my thesis advisor Assoc. Prof. Dr. Tülin Yanık for her excellent guidance, all the advices and criticisms, eye-opening discussions and friendly support. I am also deeply grateful to Assoc. Prof. Dr. Mehmet Ak for sharing his knowledge and help as well as all the contributions to this study.

Secondly, I would also like to convey my thanks to the members of my thesis committee Prof. Dr. Semra Kocabıyık, Assoc. Prof. Dr. Mesut Muyan and Assoc. Prof. Dr. Çağdaş D. Son for their suggestions and constructive criticisms.

Moreover, I am thankful to my laboratory mates, especially Serhat Özdemir for his contributions to this study as well as Feride Kaşıkçı, Hikmet Taner Teker and Barış Ulum for their help, discussions and friendship. In addition, I felt lucky to have two of the hardworking undergraduate students, Bilge Büyükdemirtaş and Müge Sak, working in this laboratory and grateful for their encouragement and support.

I would also like to thank The Scientific and Technological Research Council of Turkey (TÜBİTAK) for the scholarship they provided during my graduate study. In addition, I would like to thank Middle East Technical University Scientific Research Coordinatorship (METU-BAP) and Gülhane Military Medical Academy (GATA) for financially supporting the project through BAP-08-11-2012-015 collaborative grant.

I also feel blessed and am grateful to have friendship and endless support of Tuğba Dursun and Ayda Çiğlez that helped me get through the hardships.

I am indebted to Aktan Alpsoy for his patience with my odd non-stop working h when I am obsessed with an experiment, and helping me clarify my mind when I entered into a vicious circle of ideas.

The last but not the least, I am well aware that without the psychological and loving support of my family, I could not be where I am now. Thus, as every successful step I took, this one also belongs to them as much as it belongs to me.

TABLE OF CONTENTS

LIST OF TABLES

TABLES

LIST OF FIGURES

FIGURES

LIST OF ABBREVIATIONS

5-HT	5-hydroxytryptamine (serotonin)
5-HT1B	Serotonin 1B receptors
5-HT2C	Serotonin 2C receptors
α-MSH	Alpha-melanocyte stimulating hormone
AC	Adenylate cyclase
ACTH	Adrenocorticotropic hormone
AgRP	Agouti-related peptide
AMPK	Adenosine monophosphate-activated protein kinase
ARC	Arcuate nucleus
BBB	Blood-brain barrier
cDNA	Complementary DNA
cAMP	Cyclic adenosine monophosphate
CART	Cocaine- and amphetamine-regulated Transcript
CLIP	Corticotropin-like-intermediate lobe peptide
CNS	Central nervous system
CPE	Carboxypeptidase E
CSF	Cerebrospinal fluid
CYP450	Cytochrome P450
da-α–MSH	Desacetyl α–MSH
D	Dopamine receptor
DAG	Diacylglycerol
DIO	Diet-induced obesity

DMH	Dorsomedial hypothalamus
EP	Endorphin
EPS	Extrapyramidal side effects
ER	Endoplasmic reticulum
FoxO1	Forkhead box protein O1
GABA	Γ-Amino Butyric Acid
GAPDH	Glyceraldehyde 3-phosphate dehydrogenase
gDNA	Genomic DNA
GLP-1	Glucagon-like peptide 1
GPCR	G-protein coupled receptor
HFD	High-fat diet
ICV	Intracerebroventricular
IFN	Infundibular nucleus
InsR	Insulin receptor
IRS	Insulin receptor substrate
JAK	Janus kinase
JP	Joining peptide
KO	Knockout
LepR-B	Leptin receptor isoform b
LH	Lateral hypothalamus
LPH	Lipotropin
MCR	Melanocortin receptor
mTOR	Mammalian target of Rapamycin
N-AT	N-acetyltransferase
NMS	Neuroleptic malignant syndrome
NPY	Neuropeptide Y
PACE4	Paired aminoacid coverting enzyme 4
PAM	Peptidyl α-amidating monooxygenase
PC	Prohormone convertase

PI3K	Phosphatidylinositol-4,5-bisphosphate 3-kinase
PKB / AKT	Protein kinase B
PKC	Protein kinase C
PLC	Phospholipase C
PNS	Peripheral nervous system
POMC	Proopiomelanocortin
PRCP	Prolylcarboxypeptid
PVN	Periventricular nucleus
RT-qPCR	Quantitative real-time polymerase chain reaction
RSP	Regulated secretory pathway
S6K1	S6 kinase 1
SERT	Serotonin reuptake transporters
SNP	Single nucleotide polymorphism
STAT 3	Signal transducer and activator of transcription 3
T2DM	Type 2 diabetes mellitus
TGN	Trans golgi network
VTA	Ventral tegmental area
WHO	World health organization
Y	NPY receptor

CHAPTER 1

INTRODUCTION

1.1 WEIGHT CONTROL MECHANISMS & OBESITY

1.1.1 Weight Control Mechanisms

In a healthy organism, energy stores and the food intake are strictly regulated by the involvement of peripheral signals and central nervous system (CNS). When a disruption in that regulation occurs, most of the time it presents itself in the phenotype as a decrease or an increase in the weight, defective glucose and lipid metabolism, and in many other ways having prominent effects on the overall homeostasis. Therefore, it is very important to understand that regulation to be able to overcome defects for the well-being of the organism.

1.1.1.1 Peripheral Signals

Although the main controller of the feeding behavior lies within the brain, still without signals coming from the periphery it would be ineffective. The brain senses both short-term and long-term signals to regulate energy homeostasis and

feeding behavior of the organism. Those signals include both neuronal ones coming from afferent sensory relays and humoral ones coming from adipose tissue, gut, intestines, pancreas and liver. In addition, circulating nutrient levels including glucose and amino acid levels are also processed as signals (Morris *et al.*, 2009; Perboni *et al*., 2009). Even though there are many peripheral signals take part in the control of body weight, the most important potent ones are leptin, originating from the adipose tissue, and insulin, is released from the pancreatic β-cells (Morton *et al*., 2006; Crespo *et al*., 2014).

In the proceeding sections, detailed information about the effects of insulin and leptin will be presented in the context of the thesis.

1.1.1.2 Hypothalamus & Arcuate Nucleus

By the help of a main controller which integrates and interprets all the signals received from the periphery, weight of the organism can be regulated. Although many brain regions, such as the cortex, the brainstem, the limbic system and the amygdala, take part in the regulation of body weight, still the hypothalamus is the main controller of the energy and appetite mechanisms and hence the body weight. The hypothalamus is located in the forebrain which consists of many nuclei for different psychological behaviors. Specifically, within the hypothalamus the arcuate nucleus (ARC) of the hypothalamus is the most curial player for feeding mechanisms (Morris *et al*., 2009; Crespo *et al.*, 2014). Since the ARC resides near the mediobasal hypothalamus where blood-brain barrier (BBB) is not so strict so that this position enables it to easily inspect and control the energy status of the organism (Sasaki *et al*., 2010) (Varela *et al.*, 2012).

Two very special sets of neurons existing in the ARC sense both short term and long term signals from the periphery. The first set is the anorexigenic neurons that

are called proopiomelanocortin (POMC) and cocaine- and amphetamine-regulated transcript (CART) which inhibit food intake when activated. The second set is the orexigenic neurons that are namely neuropeptide Y (NPY) and agouti related peptide (AgRP) neurons which promote hunger once activated (Crespo *et al.*, 2014).

In this study, the hypothesis was based on changes of *POMC* and *NPY* expressions in the hypothalamus upon atypical anti-psychotic usage; therefore, they were further explained in the following sections while AgRP and CART were not of interest.

1.1.1.2.1 Proopiomelanocortin (POMC)

POMC is a 241 aminoacid long, 31kDa prohormon with a 26 aminoacid N-terminal signal sequence in the pre-POMC form (Wardlaw, 2011; von Bohlen und Halback & Dermietzel, 2006). In human genome, 8kb *POMC* gene is located on the short arm of chromosome 23 as a single copy with 3 exons and 2 introns (Wang & Majzoub, 2011). It is highly conserved among species (von Bohlen und Halback & Dermietzel, 2006).

POMC is the precursor of several bioactive peptides with melanotrophic, corticotropic (Wang & Majzoub, 2011) and opioid activities (Zhang, *et al.*, 2009) having critical roles in appetite regulation, energy homeostasis, glucose and lipid metabolism, stress response and pigmentation (Gantz & Fong, 2003). It is processed tissue-specifically depending on the availability of its processing enzymes in the tissues and gives rise to peptides including adenocorticotropin hormone (ACTH), alpha-melanocyte stimulating hormone (α-MSH), beta- and gamma-lipotropin (β- and γ-LPH) and endorphins (EPs) as can be seen in Figure 1-1 (Wardlaw, 2011; von Bohlen und Halback & Dermietzel, 2006).

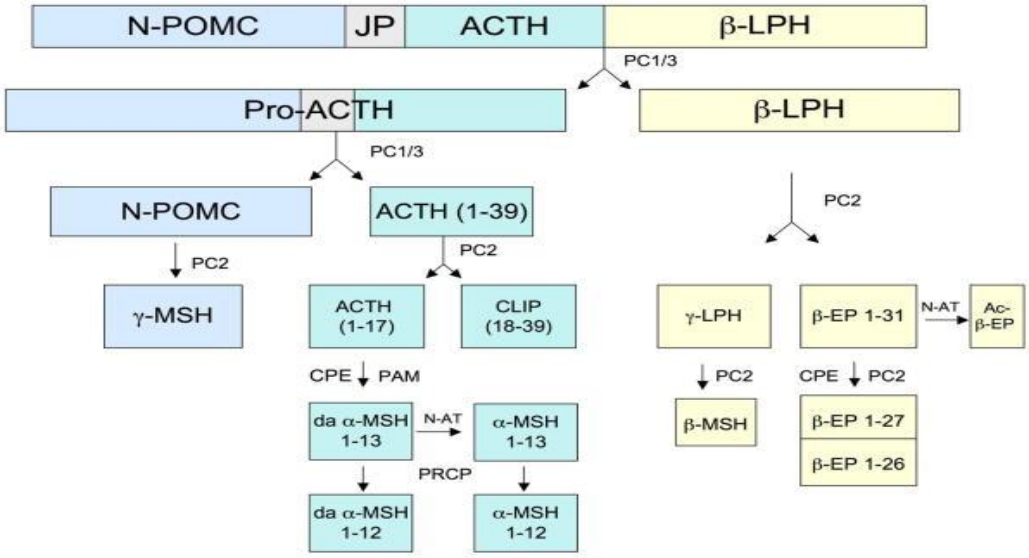

Figure 1-1 Processing of POMC. JP: joining peptide; LPH: lipotropin; EP: endorphin; CLIP: corticotropin-like-intermediate lobe peptide; MSH: melanocyte stimulating hormone; ACTH: adenocorticotropin hormone, da-α–MSH: desacetyl α–MSH; PC1/3 and PC2: prohormone convertases 1/3 and 2; CPE: carboxypeptidase E; N-AT: N-acetyltransferase; PAM: peptidyl α-amidating monooxygenase; PRCP: prolylcarboxypeptid. Retrieved from (Wardlaw, 2011).

POMC is expressed in arcuate nucleus of hypothalamus, pituitary, solitary tract, medulla within the CNS and in several peripheral tissues (von Bohlen und Halback & Dermietzel, 2006; Wang & Majzoub, 2011). After *POMC* mRNA is translated into rough endoplasmic reticulum (ER), the prepropeptide is directed towards the trans golgi network (TGN) and then the regulated secretory pathway (RSP) vesicles. During its passage through ER, TGN and RSP vesicles, it is cleaved and modified by enzymes including prohormone convertases (PC 1/3 and PC2),

carboxypeptidase E (CPE) (Wardlaw, 2011), paired aminoacid coverting enzyme 4 (PACE4) and finally amidating and N-acetylating enzymes (Millington, 2007; Wang & Majzoub, 2011).

1.1.1.2.1.1 POMC and Control of Feeding

POMC knockout mice were obese (Perboni *et al.*, 2009) whereas POMC overexpressing mice specifically in the ARC and the ventral tegmental area (VTA) showed decreasing weight gain and adiposity (Andino, *et al.*, 2011). Parallel to those observations, transgenic lean and obese mice with forced expression of α-MSH were reported to show a decrease in body weight and adipose tissue (Savontaus *et al.*, 2004). In general, during the satiate state, the expression of *POMC* was inhibited whereas in case of hunger, the expression and secretion are promoted.

1.1.1.2.1.2 Melanocortin Receptors and Energy Homeostasis

Five distinct melanocortin receptors (MCRs) ranging from MC1R to MC5R have been identified (Gantz & Fong, 2003; Dores *et al.*, 2014). All MCRs are G-protein coupled receptors (GPCRs) with seven transmembrane spanning domains and they trigger intracellular signal cascades that increase cAMP concentrations through activation of Adenylate Cyclase (AC) and activate Protein Kinase C (PKC) and Diacylglycerol (DAG) (Gantz & Fong, 2003; Millington, 2007; Dores *et al.*, 2014).

Melanocortin Receptor 1 (MC1R) is found in melanocytes and mainly involve in skin pigmentation. It is also present in keratinocytes, fibroblasts, endothelial cells,

leukocytes, testis, corpus luteum, placenta and periaqueductal gray neurons in brain (von Bohlen und Halback & Dermietzel, 2006; Wang & Majzoub, 2011; Gantz & Fong, 2003). α-MSH is the potent ligand for MC1R (see Table 1-1). Melanocortin Receptor 2 (MC2R) is highly specific for ACTH as can be seen on Table 1-1 (von Bohlen und Halback & Dermietzel, 2006; Gantz & Fong, 2003). It is present in adrenal cortex and its activation by ACTH stimulates release of glucocorticoids like cortisol and corticosterone so that they act on stress mechanisms and immune system (Dores *et al.*, 2014). MC2R is also found in adipose tissue (Gantz & Fong, 2003). Melanocortin Receptor 3 (MC3R) is detected in several parts of CNS some of which are hypothalamus, cortex, amygdala, ventral tegmental area, thalamus and periventricular nucleus, and in periphery such as stomach, intestine and placenta (von Bohlen und Halback & Dermietzel, 2006). All melanocortins have similar affinities for MC3R. Melanocortin Receptor 4 (MC4R) is observed all over the CNS with the increased population density in hypothalamus, hippocampus and hindbrain (De Jonghe *et al.*, 2011). In humans, MC4R is only found in the brain while it is found in the periphery in some animals (Wang & Majzoub, 2011). α-MSH and ACTH is the selective ligand for MC4R. Melanocortin Receptor 5 (MC5R) is expressed in both CNS and peripheral tissues. In CNS, it is detected in cortex, hippocampus, hypothalamus, cerebellum, pituitary, substantia nigra (von Bohlen und Halback & Dermietzel, 2006). In the periphery, it is present in many tissues including adrenal glands with high expression and skin, skeletal muscle, stomach, lung, kidney, liver, mammary glands, lymph nodes, ovary, uterus, testis with low expression (Wang & Majzoub, 2011; von Bohlen und Halback & Dermietzel, 2006). The most potent ligand for MC5R is observed to be α-MSH (see Table 1-1).

Table 1-1 Melanocortin receptors, ligands and antagonists. MC1-5R: Melanocortin Receptor 1-5; MSH: Melanocyte Stimulating Hormone; ACTH: Adenocorticotropin Hormone; AgRP: Agouti Related Peptide. Modified from (Gantz & Fong, 2003)

Receptor ID	**Potency of Ligands**	**Antagonists**
MC1R	α-MSH = ACTH > β-MSH > γ-MSH	Agouti
MC2R	ACTH	Agouti
MC3R	α-MSH = ACTH = β-MSH = γ-MSH	Agouti, AgRP
MC4R	α-MSH = ACTH > β-MSH > γ-MSH	Agouti, AgRP
MC5R	α-MSH > ACTH > β-MSH > γ-MSH	

MC1R, MC2R and MC5R are not as critical as MC3R and MC4R for the control of food intake. Disruption of MC1R was reported to be neutral in terms of energy homeostasis while MC2R and MC5R losses were observed to cause detrimental impacts on gluconeogenesis, hypoglycemia and adrenal atrophy without resulting in an obese phenotype (Jonghe *et al.*, 2011). In contrast to insubstantial impacts of MC1R, MC2R and MC5R on feeding behavior, MC3R and MC4R have prominent influences on regulation of weight. MC3R gene knockout mice show increased fat amount with decreased lean weight without any significant change in body weight (Wang & Majzoub, 2011). In parallel with the effects of MC3R, MC4R-null mice are obese, hyperphagic, hyperinsulinemic and hyperglycemic (Perboni *et al.*, 2009; Wang & Majzoub, 2011). In addition, lipid uptake by white adipose tissue and fat accumulation as well as triglyceride synthesis were observed to elevated in MC4R knockout mice (Nogueiras, *et al.*, 2007). Furthermore, agonists and antagonists of MC4R cause significant decrease and increase, respectively, in body weight (Perboni *et al.*, 2009). Several MC4R mutations in human as well as rodents

constitute a considerable percentage for resulting in monogenic obesity (Millington, 2007; Morris & Hansen, 2009; Wang & Majzoub, 2011).

1.1.1.2.2 Neuropeptide Y (NPY)

NPY is a peptide composed of 36 amino acid residues. It is expressed in both peripheral nervous system (PNS) and CNS including the ARC, periventricular nucleus (PVN) and nucleus of solitary tract with high expression. In addition, it is also produced and secreted by pancreatic β cells, and act to inhibit insulin secretion (Burcelin *et al.*, 2001). 7,2 kb long human *NPY* gene, which is composed of 4 exons and 3 introns, is found on the 7^{th} chromosome (Morris & Hansen, 2009; von Bohlen und Halback & Dermietzel, 2006). Similar to POMC, it is synthesized in pro-NPY form and cleaved by the PCs to yield the mature form.

1.1.1.2.2.1 NPY and Control of Feeding

NPY is a potent neuropeptide to induce food intake as confirmed by several *in-vivo* studies. It was shown that NPY injection to hypothalamus causes a strong appetite increase (Beck, 2006). It shortens the time in between feeding so that more food is ingested and NPY –KO mice showed delayed feeding. (Beck, 2006). Hunger state stimulates expression and secretion of NPY, and in turn NPY acts on other brain regions to stimulate feeding. Normal mice showed elevation of food intake upon decreased glucose levels while NPY-KO mice showed feeding response to a lower extend (Beck, 2006). On the other hand, at satiety both expression and secretion of NPY are inhibited (von Bohlen und Halback & Dermietzel, 2006). Recently, van den Heuvel *et al*. (2014) showed that hypothalamic *NPY* levels do not change with meal composition variations. Acute

and chronic administration of NPY to rats resulted in hyperphagia with the prolonged exposure resulting in obese phenotype. (von Bohlen und Halback & Dermietzel, 2006). In addition, several polymorphisms of *NPY* were found to be associated with metabolic syndrome (Crespo *et al.*, 2014).

1.1.1.2.2.2 NPY Receptors and Signaling

There are 6 distinct NPY receptors identified as Y1, Y2, Y4, Y5, Y6 and Y7 (von Bohlen und Halback & Dermietzel, 2006). Y1, Y2, Y4 and Y5 were detected in the human CNS as well as in rodents (Morris & Hansen, 2009). They are GPCRs linked to adenylate cyclase (AC) and phospholipase C (PLC) pathways leading to elevated intracellular Ca^{2+} concentrations in neurons (von Bohlen und Halback & Dermietzel, 2006). Y1 and Y5 receptors are thought to involve in induction of feeding behavior (van den Heuvel, *et al.*, 2014) as well as emotionality and stress response (Heiling, 2004). Y1 receptors found in spinal cord were associated to mediate anti-hyperalgesic effect of NPY upon inflammation (Taylor, *et al.*, 2014). Agonists of Y1 receptor were shown to stimulate feeding as oppose to Y1 antagonist-induced inhibition of feeding (Beck, 2006). In addition, Y1 KO mice were shown to have and increased leptin and insulin levels and an obese phenotype which was not due to hyperphagia but due to decreased energy expenditure (Burcelin *et al.*, 2001). Y2 receptors are located on the presynaptic membrane and involve in regulation of NPY release (Martire *et al.*, 1995; Beck, 2006). Y5 receptor was found in PVN and LH and thought to support Y1 receptor action on food intake (Beck, 2006).

1.1.1.2.3 Effects of Signaling Pathways on NPY and POMC

Actions of POMC and NPY neurons are mainly modulated by leptin and insulin. Besides ghrelin, circulating glucose levels, peptide YY, β- endorphin, serotonin, glutamate, melanin-concentrating hormone and orexins are also important signaling mechanism for those neurons. Furthermore, γ-amino butyric acid (GABA), which is a suppressor neurotransmitter, secreted from AgRP/NPY neurons and AgRP, NPY also have negative effects on POMC neurons and MCRs as well (Gantz & Fong, 2003). In addition, acetylcholine is also thought to have an impact on both NPY and POMC neurons since nicotine activates those neurons in the ARC and increases expression of both MC4R and POMC (Picciotto & Mineur, 2013).

1.1.1.2.3.1 Insulin and Leptin Action on POMC and NPY Neurons

Adipokine leptin and insulin are secreted depending on feeding status and the long-term energy stores of the organism. Secreted amount of leptin from the adipocytes is correlated with the size of adipose mass. After food intake, increased circulatory nutrient levels stimulate secretion of insulin and leptin at the same time. Both signals pass through the BBB to act on the CNS in order to promote satiety. In other words, both insulin and leptin are anorexigenic peripheral signals that act mainly on ARC in order to inhibit feeding (Belgardt *et al.*, 2009; Perboni *et al.*,2009).

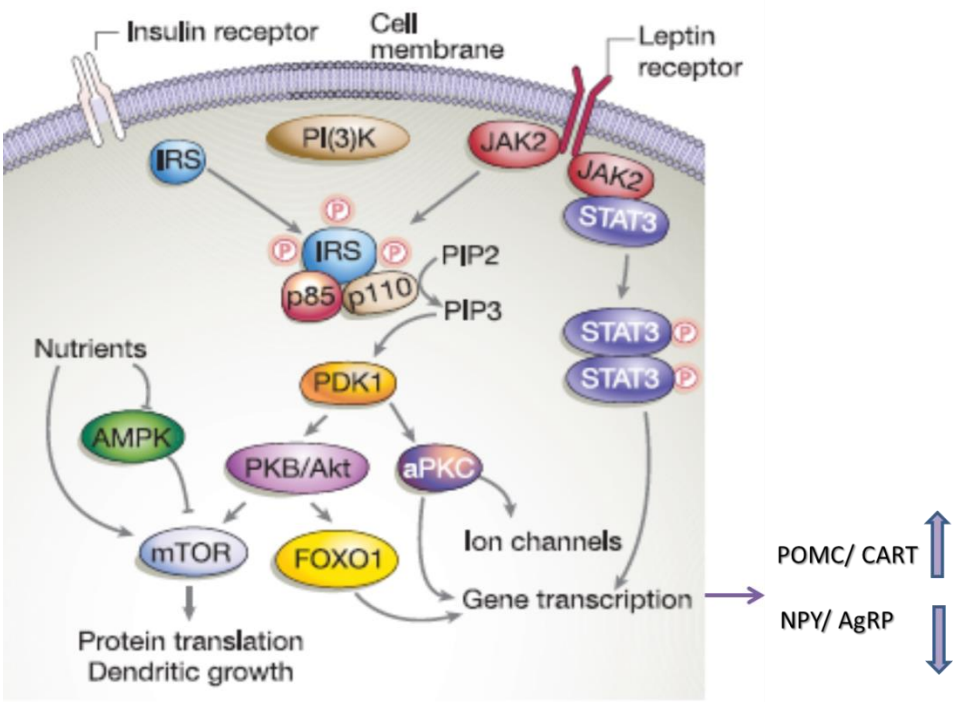

Figure 1-2 Insulin and leptin signaling pathway in hypothalamus. Modified from Morton *et al.*2006.

Combination of several different researches has revealed more or less the basic intracellular signal transduction routes which are triggered by insulin and leptin within the POMC and NPY neurons. As indicated in the Figure 1-2, the action of leptin in ARC is mediated by one of its receptors; the leptin receptor isoform B (ObRb or LepR-B), (Münzberg *et al.*,2005) while the action of insulin is mediated by insulin receptors (InsR) found on POMC and NPY neurons in ARC (Varela & Horvath, 2012). Leptin receptors are class 1 cytokine receptors that act through JAK-STAT pathway (Münzberg *et al.*, 2005). Once bound to its ligand leptin, Janus Kinases (JAK) , which are a type of intracellular tyrosine kinases

phosphorylate the intracellular LepR-B domain and activate kinase activity of the receptor. In turn, they phosphorylate signal transducer and activator of transcription 3 (STAT3) which is then dimerized and translocated into nucleus. After entry into the nucleus, the dimer binds to *POMC* gene promoter in POMC neurons and activates the *POMC* expression and depresses the NPY expression in NPY neurons (Münzberg *et al.*,2005; Varela & Horvath, 2012). Apart from activation of JAK-STAT3 pathway to regulate the gene expression in POMC and NPY neurons, it also activates phosphatidylinositol-4,5-bisphosphate 3-kinase (PI3K) pathway. Similarly, the downstream signaling cascade of the InsR is PI3K in which leptin and insulin signaling pathways merge. Activation of InsR due to binding of insulin leads to phosphorylation of insulin receptor substrate (IRS) which, in turn, causes the activation of PI3K. Then, at the several steps further from the activation of PI3K, another important intracellular kinase, Protein Kinase B (PKB or AKT) is activated which links insulin and leptin signaling to other pathways, such as mTOR pathway and AMP-activated protein kinase (AMPK) and regulates transcription factors, such as Forkhead box protein O1 (FoxO1) which are found to be related to obesity (Belgardt *et al.*, 2009; Varela & Horvath, 2012). The active form of FoxO1 stimulates food intake by inhibiting the *POMC* gene promoter whereas promoting the *NPY* expression (Sasaki & Kitamura, 2010). Furthermore, mammalian target of rapamycin (mTOR), which is a serine-threonine kinase promotes cell growth and proliferation, and its downstream target S6 Kinase 1 (S6K1) were also shown to involve in leptin and insulin signaling cascades within the hypothalamic neurons (Dann, *et al.*, 2007; Varela & Horvath, 2012). Cota *et al.* reported that activation of S6K1 was decreased upon fasting in mice and inhibition of mTOR pathway by use of rapamycin, an inhibitor of mTOR, boosted food intake in pre-fed mice. In addition, it was also indicated that intracerebroventricular (ICV) leptin administration activated mTOR pathway which could be reversed by the rapamycin treatment (Cota, *et al.*, 2006). On the other hand, another research done by mTOR upstream suppressor knockout mice

specifically in hypothalamic POMC neurons indicated that mTOR overactivation led to inhibition of POMC neurons and a hyperphagic obese phenotype in mice, which was rescued by rapamycin administration (Mori, *et al.*, 2009). Nevertheless, studies indicate that leptin and insulin also act through mTOR pathway to regulate energy intake. Moreover, the AMPK pathway, which senses the intracellular AMP/ATP concentrations, is blocked by leptin and insulin actions. The AMPK pathway is activated by the decrease in cellular energy status which is indicated by an increased AMP/ATP ratio in the cell (Belgardt *et al.*, 2009).

1.1.1.2.3.2 GABA Action on POMC Neurons

GABA is the major inhibitory neurotransmitter. GABAergic neurons are found throughout the brain and their density is high especially in thalamus, hippocampus and cerebral cortex. There are 3 receptor subtypes that 2 of which, $GABA_A$ and $GABA_C$, are ionotropic; that is they are ion channels, and increases the permeability of Cl^- ions, and one of them, $GABA_B$, which is a kind of metabotropic receptor, a GPCR that acts through cAMP pathway (von Buhlen und Halback & Dermietzel, 2006). In the ARC, majority of the NPY/AgRP neurons co-express and release GABA which is known to regulate food intake (Delgado, 2013). The impact of GABA on feeding is orexigenic. According to Cowley *et al.*2001, NPY neurons impose an inhibition on POMC neurons in the ARC through secretion of GABA and consequent hyperpolarization of POMC neuron, which was achieved by the leptin action on NPY neuron and the repression of GABA release. Also, Vong *et al.* 2011 demonstrated another pathway in which leptin exerts its anorexigenic act that inhibited GABAergic NPY/AgRP neurons to attain inhibition of POMC neurons. Through a mouse model in which GABA release was disrupted by LepR-B neurons reported to be concentrated in the ARC, the dorsomedial hypothalamus (DMH) and lateral hypothalamus (LH), and it was

found that hypothalamic POMC expression was elevated while NPY expression was reduced compared to controls. Interestingly, it was observed that those mice demonstrated obese phenotype with the high fat diet (HFD) group showing early onset obesity while chow-fed mice had late onset obesity (Xu *et al.*, 2012). Recently Ito *et al.* 2013, showed that specific $GABA_B$ receptor deletion from POMC neurons and HFD caused body weight increase accompanied by a decrease in insulin sensitivity in male mice whereas not in female mice. They also reported that hypothalamic mRNA expression of POMC was declined in male knockout (KO) mice fed with HFD while hypothalamic NPY expression did not alter compared to controls.

1.1.1.2.3.3 Serotonin Action on POMC and NPY Neurons

Serotonin (5-Hydroxytryptamine or 5-HT) is a neurotransmitter which involves in regulation of cognitive processes, emotions, sexual and feeding behaviors. It has 7 receptor families ranging from 5-HT1 to 5-HT7 some of which are GPCRs and some are channel-type receptors. Among them, central serotonin 2C receptors (5-HT2C) are known to involve in body weight regulation as well as glucose homeostasis. 5-HT2C receptors are GPCRs that activate PLC so that PKC and Ca^{2+}/Calmodulin pathways are triggered (Ohno *et al.*, 2013; von Buhlen und Halback & Dermietzel, 2006). There are evidences that 5-HT2C receptor agonists inhibit feeding whereas antagonists cause the contrary impact on feeding behavior (Reynolds & Kirk, 2010). Moreover, when 5-HT2C receptor is systemically knocked out in mice, hyperphagia and weight gain were observed (Tecott, *et al.*, 1995). In addition, 5-HT2C subtype is found in POMC neurons in the ARC and activation of those receptors increases POMC expression (Berglund, *et al.*, 2013). In 2013, Berglund *et al.* reported that specific pre- and postnatal deletion of 5-HT2C receptors from POMC neurons resulted in increased blood glucose, insulin

and glucagon levels accompanied by insulin resistance in mice without change in body weight in normal chow fed whereas significantly increase in body weight in high fat and high sugar diet accompanied by hyperphagia under both diet groups. In addition, it was observed that although the hyperphagia was common, the difference in weight gain in those diet groups was due to the compensation of this behavior with elevated energy expenditure in chow diet fed knock out group which was also elevated but could not compensate the excess energy intake due to excess eating in high calorie diet (Berglund, *et al.*, 2013). Another receptor isoform, 5-HT1B was detection NPY/AgRP neurons in the ARC (Heisler, *et al.*, 2006). Heisler *et al*. 2006 reported that agonist action on 5-HT1B caused hyperpolarization of NPY/AgRP neurons in the ARC and inhibited release of neuropeptides from those cells. In addition, they showed that serotonin agonist-induced decrease in food intake was diminished and hyperphagia was induced when mice treated with 5-HT1B antagonist. Serotonin reuptake transporters (SERT) are important for clearance of available serotonin from the synaptic cleft and SERT-KO mice were reported to be obese (Chen *et al.*, 2012). Recently, Borgers *et al*. (2014) showed that SERT is expressed extensively among the infundibular nucleus (IFN), which is the human equivalent of the ARC, in co-localization with POMC and NPY/AgRP neurons. (Borgers, *et al.*, 2014). In addition, they also reported that the SERT immunoreactivity was decreased in overweight individuals.

1.1.2 Obesity

Obesity is defined as the extravagant accumulation of fat within the body which leads to metabolic health problems and mortality. According to World Health Organization (WHO), obesity is no longer restricted to rich-income countries; in fact, it is now a world-wide epidemic with exceeding 1 billion adults in 2008 and

40 million children under the age 5 in 2012 (WHO, 2014). As the number of obese and overweight individual has risen, it has passed way beyond being just a health issue, but it also became an economic problem of the societies. That is because obesity results in a dysregulated metabolism and associate with many diseases including type 2 diabetes mellitus, dyslipidemia, hypertension, cardiac problems, reproductive disorders and cancer, and the cost to treat them all reaches to extremes (Varela & Horvath, 2012; WHO, 2014).

1.1.2.1 Etiology

Obesity occurs from either one of the genetic, endocrine, behavioral and environmental factors or from contribution of several of them. Basically, it is due to the chronic increase in energy intake accompanied by a drop in energy expenditure so that excess energy is stored as fat. There are several possible reasons for that condition to occur. First of all, while the cost of healthy food and availability of many high-fat and high-carbohydrate and cheap food increased, as well as physical activity in populations decreased, the imbalance of energy received and expensed is supported. Secondly, mutations or deletions in critical genes, such as genes for leptin, LepR, POMC, MC4R, CART, might directly result in obesity (monogenic obesity) or common genetics variants or single nucleotide polymorphisms (SNPs) in combination with other environmental and possible epigenetic factors may lead to predisposition to obesity (polygenic obesity) (Nguyen & El-Serag, 2010; Hinney *et al.*, 2010; Genne-Bacon, 2014). Furthermore, several drugs including second generation antipsychotics causes significant weight gain and may lead to obesity which will be covered later in this chapter in detailed.

1.1.2.2 Treatment Approaches

In order to overcome obesity problem several approaches, mostly a few applied together, are used. Those can be

- Life style interventions, such as implementation of a healthy diet, regular exercise program and psychological backup (WHO, 2014),
- Pharmaceutical approaches (Harvey & Ogden, 2014; Sherson *et al.*, 2014)
- And if those not work then bariatric surgery; that is the reducing size of stomach or removal of a part of it to hinder nutrient absorption (Sherafat-Kazemzadeh *et al.*, 2013; Gonzalez-Campoy, *et al.*, 2014).

As the pharmacological intervention, drugs with different action mechanisms are used as single agents or in combinations with each other for obesity treatment. Distinct mechanisms that available drugs target are limitation of energy intake by suppression of appetite or hormone supplements, suppression of nutrient trafficking by either burdening digestion or absorption in gastrointestinal tract, and affecting insulin action, lipolysis and energy expenditure (Sherafat-Kazemzadeh, *et al.*, 2013).

1.2 OLANZAPINE

1.2.1 Olanzapine and Its Metabolism

Olanzapine is an atypical (2^{nd} generation) antipsychotic drug which is prescribed for the treatment of psychiatric disorders including schizophrenia, bipolar disorder and depression. Its chemical nomenclature is 2-methyl-4-(4-methyl-1-piperazinyl)-10H-thieno [2,3-b] [1,5]benzodiazepine with the closed formula of $C_{17}H_{20}N_4S$.

Injectable and oral tablet forms are present in the market and sold under the trade names such as Zyprexa (Eli Lilly, US), Rexapin (Abdi Ibrahim, Turkey), Apzet (Tripharma, Turkey), Olanzapine Phizer (Phizer, UK). Reported adverse effects include hyperglycemia, hyperlipidemia, weight gain, suicide thoughts, neuroleptic malignant syndrome (NMS), tardive dyskinesia, hypotension, dysphagia, seizures, cognitive and motor impairment, elevation of prolactin levels and increased mortality in elderly with dementia-related psychosis (Eli Lilly, 2013) (Phizer, 2011)**.** Olanzapine is mainly metabolized by cytochrome P450 (CYP450) and glucuronidation. In addition, CYP1A2, CYP2D6 and the falvin-containing monooxigenase system also contributes to the olanzapine metabolism (FDA Center for Drug Evaluation and Research, 1999).

1.2.2 Olanzapine Mode of Action

Olanzapine blocks firing of dopaminergic and serotonergic pathways through antagonizing dopamine receptors (D1-D5) as well as serotonin 5-HT2-A/C, 5-HT3 and 5-HT6 receptors with a stronger preference for 5-HT2 compared with D2 receptors (Eli Lilly, 2013; Phizer, 2011). Moreover, it has affinity for cholinergic muscarinic receptors M1-M5, α1 adrenergic receptor and histamine H1 receptor (Phizer, 2011) and to a smaller extend, it binds to 5-HT1-B (Reynolds & Kirk, 2010).

1.2.3 Olanzapine-Induced Weight Gain

Treatment of psychotic diseases has reached to another level by introduction of second generation (atypical) antipsychotics which not only antagonize with dopaminergic system like the typical ones, but also work on serotonergic

pathways, and with the reduced extrapyramidal side effects (EPS) compared to typical antipsychotics (Reynolds & Kirk, 2010). On the other hand, atypical antipsychotics induce weight gain as a side effect (Correll *et al.*, 2011) and associated with cardiometabolic problems, dyslipidemia and impaired glucose tolerance (Reynolds & Kirk, 2010). The metabolic dysfunction might be related to the original disease mechanisms, as in higher prevalence of type 2 diabetes mellitus (T2DM) observed among schizophrenia patients long before use of second generation antipsychotics (Papanastasiou, 2013). Still, if the psychotic patients are more prone to develop metabolic disorders then it is another reason to prevent the increase in weight as the extreme weight gain results metabolic disorders. Even though differences have been observed among the individuals related to food intake increases and weight gain, different studies proved atypical antipsychotic side effect of increase in weight, the amount of which is related to the chosen drug (Teff & Kim, 2011). Moreover, olanzapine and clozapine are found to be the drugs associated with the highest weight gain with olanzapine reaching around 18% of the original weight over a year (Reynolds & Kirk, 2010). In fact, it was reported that 2 weeks olanzapine administration to healthy subjects caused significantly increase in food intake (Fountaine, *et al.*, 2010).

Studies done on rats have yielded gender-dependent results in terms of weight gain for olanzapine studies. Mainly, female-chosen studies have shown results indicating increased body weight. In addition, when strains were compared, Wistar rats gained more weight compared to Sprague-Dawley rats as an outcome of olanzapine administration (van der Zwaal *et al.*, 2014). Apart from overall body weight gain, reduction in muscle mass and increases in adiposity was observed in male rats. Reports about decreases in locomotor activities and hyperphagia were also present as well as increases in meal amounts for both genders (van der Zwaal *et al.*, 2014).

1.2.3.1 Treatment Strategies for Olanzapine-Induced Weight Gain

In general, the treatment approaches for the atypical antipsychotic drug-induced and specifically for olanzapine-induced weight gain can be categorized into 3 broad groups as

- Changing into another atypical antipsychotic drug,
- Usage of adjunctive non-pharmacologic treatments and
- Prescription of adjunctive medications.

In the first approach, simply another antipsychotic with not as weight gain inducing as the already used one is prescribed to the patient. Change of drugs seems plausible and improvement of metabolic parameters of patients were reported in such switching cases; however, in the switching scenario the risk of whether the new medication adheres to the patient and the possibility of him/her dropping out of the new treatment followed by the disease relapse present. The second strategic group consists of behavioral interventions including controlled diet, increased physical activity and cognitive intervention. Although that strategy is the most preferable one, still the continuation of the intervention solely depends on the patient and his/her living conditions. Finally, the last group is composed of utilization combined drug treatments to manage the weight gain. Some of the medications that can be used with treatment includes metformin (with the most positive outcomes so far), reboxetine, betahistine, topiramate, intranasal PYY, fenfluramine, sibutramine, each agent with differing action mechanisms (Maayan & Correll, 2010). In the preceding parts of the introduction, available knowledge about the action mechanism of metformin and its use in drug-induced weight gain treatment with the emphasis on olanzapine-induced weight gain treatment will be explained in depth.

1.2.4 Effects of Olanzapine on NPY and POMC Pathways

In a study published in 2006, impact of olanzapine in region-specific brain *NPY* expression levels were demonstrated after 36-day of drug administration to female Sprague-Dawley rats. In that study, it was found out that olanzapine administration increased NPY expression, and after 48h *NPY* levels turned back to normal (Huang *et al.*, 2006). Parallel to that study, Weston-Green *et al.* reported that after 2-week olanzapine treatment of female Sprague-Dawley rats, mRNA expression levels of *NPY* was significantly increased in the ARC (Weston-Green *et al.*, 2012). In the same study, *POMC* expression levels were also reported to be significantly decreased in ARC and increase in body weight of olanzapine-treated rats were significant compared to controls. Furthermore, those studies are also supported by Ferno *et al.* (2011) who showed short-term (6 days) olanzapine treatment resulted in significant up regulation of *NPY* and significant downregulation of *POMC* accompanied by increased food consumption and weight gain. On the contrary to those findings, Davoodi *et al.* (2009) reported no difference in hypothalamic *POMC* and *NPY* expressions after acute and 7-day olanzapine administration to female Sprague-Dawley rats. Similarly, Guesdon *et al.* (2010) found no change in *NPY* in the ARC when they conducted a research on male Wistar rats for 2-weeks by olanzapine administration directly to the third ventricle via mini-pumps.

1.2.5 SNP Studies on Olanzapine Treatments

Although induction of weight gain by atypical antipsychotics is observed widely, still there are variations due to life style choices and genetic background of human subjects. Putting subjective choice of individuals apart, several polymorphisms found in leptin, leptin receptor and serotonin receptor genes were observed to be associated with the weight gain side effect (Lee & Bishop, 2011). Especially, a

single nucleitide polymorphism found in 5-HT2C receptor gene C759T highly correlates with the weight gain side effect. Specifically, it was reported that presence of T allele protects against obesity while C allele doubles the risk of obesity (Zhang & Malhotra, 2011).

1.3 METFORMIN

1.3.1 Metformin and Its Metabolism

Metformin is one of the biguanide drugs with the ability to lower blood glucose levels. Due to its safety profile, it is widely used in the treatment of type 2 diabetes mellitus; that is insulin-independent diabetes mellitus (Pernicova & Korbonits, 2014). The pharmacologic nomenclature of metformin is N-,N-dimethylimidodicarbonimidic diamide with the closed formula of $C_4H_{11}N_5$ (Bristol-Mayers Squibb Company, 2013) It available in the market as metformin hydrocloride in different forms and under different names including Glucophage (MERCK, Germany/ Bristol-Mayers, US), Carbophage (MERCK, Germany), Metfull (Vitalis, Turkey), Riomet (Ranbaxy , US), Gluforce (Biofarma, Turkey).

Metformin is not metabolized by liver; instead it is discarded directly by kidney. In human, plasma half-life of the drug is detected to be about 6.2 h. According to the prescription information common adverse effects of metformin in human are listed as diarrhea, nausea, flatulence, asthenia, indigestion, abdominal discomfort and headache. Moreover, a quite low possibility but lethal side effect is that: due to insufficient renal function leading to metformin accumulation in body, in every 100 000 patients 3 of them show lactic acidosis; that is increase in blood lactate and pH levels, with a half chance results in death (Bristol-Mayers Squibb Company, 2013).

Apart from lowering glucose levels in blood, metformin is also reported to lower risk of cardiovascular mortality (Kravchuk *et al.*, 2011), heart failure (Sachdanandam, *et al.*, 2009) reverses leptin resistance (Cittadini, *et al.*, 2012), injury of renal podocytes (Kim *et al.*, 2012) and ocular inflammation (Kalariya *et al.*, 2012). In addition, it is also prescribed for weight gain management with the drugs causing obesity such as antipsychotic drugs which will be covered in the following sections.

1.3.2 Metformin Mode of Action

In the periphery, metformin acts through decreasing glucose production by inhibiting gluconeogenesis in the liver and increasing insulin sensitivity as well as glucose internalization and use in the targeted tissues (Pernicova & Korbonits, 2014; Bristol-Mayers Squibb Company, 2013). In addition, it hinders glucose absorption in the intestines (Sherafat-Kazemzadeh *et al.*, 2013).

To be more precise, in the liver it enhances signaling through insulin InsR and IRS-2. In addition, it promotes translocation of glucose transporters to the plasma membrane and so internalization of glucose. Therefore, it contributes to suppression of gluconeogenesis. Similar effects on insulin signaling and glucose internalization were also observed in skeletal muscle cells. Furthermore, several enzymes involved in glycolysis and gluconeogenesis pathways were modulated by metformin (stimulated and inhibited, respectively) and metformin counteract the actions of glucagon. In addition, biguanides are known to interfere with the glucagon signaling in the liver as indicated by decreased cAMP levels and decreased activity of cAMP-dependent protein kinase (PKA) (Pernicova & Korbonits, 2014). Moreover, mitochondrion is a direct target of metformin. An *in-vitro* study conducted by Stephenne and his colleagues in 2011 demonstrated that AMPK activity in rat and human hepatocytes was increased depending on dosage

and timing, and that was accompanied with a significant increase in AMP-to-ATP ratio in cells. In addition, it was also reported that due to mitochondrial respiratory chain complex 1 inhibition by metformin, the cellular energy status was dropped (indicated by increased AMP:ATP ratio) and resulted in AMPK activation (Stephenne, *et al.*, 2011). An overall proposed model for metformin interference with intracellular signaling can be observed in Figure 1-3. In addition, metformin is also known to act on pancreas by stimulation of glucagon-like peptide 1 (GLP-1) actions, which promotes insulin secretion while opposes glucagon secretion (Pernicova & Korbonits, 2014).

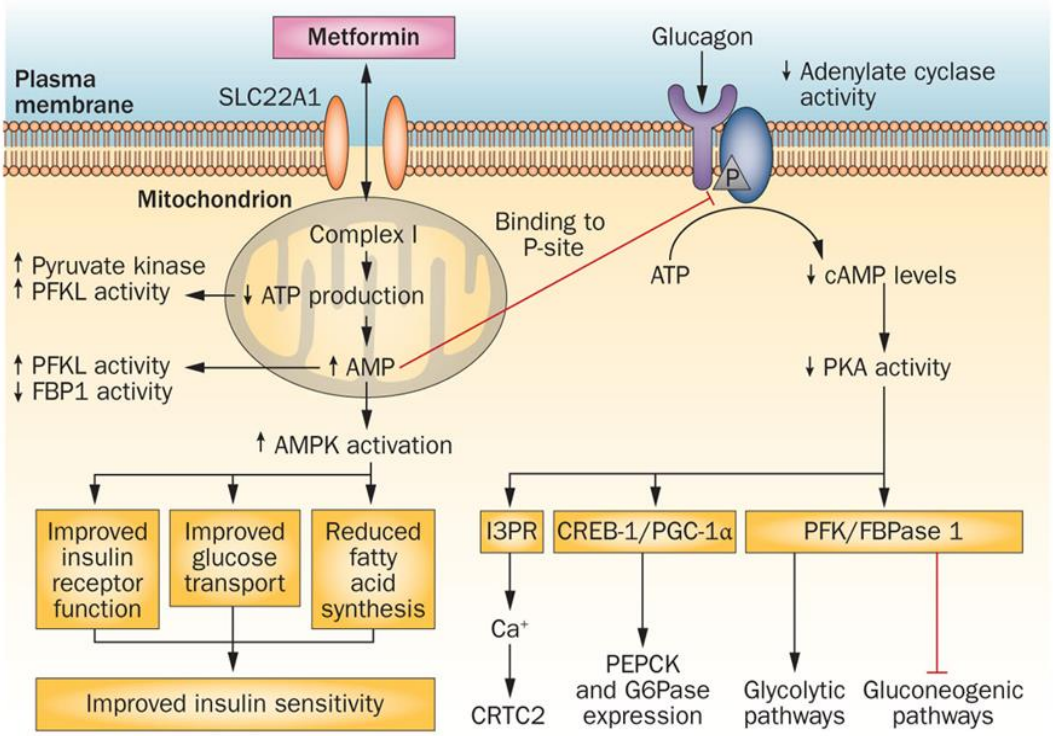

Figure 1-3 Metformin action in hepatocytes. Retrieved from (Pernicova & Korbonits, 2014).

1.3.3 Metformin Use in Olanzapine-Induced Obesity Treatment

Human studies of metformin conducted up to now, draw a controversial picture of the effectiveness against antipsychotic-induced weight gain. However, that might probably due to the limited number of studies with enough patient number for power of the tests, presence of few controlled and placebo included studies, and being unable to control the human behavior (Lee & Jeong, 2011). The report of Baptista and his colleagues in 2006 showed no difference in weight gain of 3,5-month metformin treated and placebo treated adult patients co-treated with olanzapine (Baptista, *et al.*, 2006). In the following year, another report came out by Baptista *et al.* 2007 about a 3-month long adult study with olanzapine-pretreated patients prescribed metformin or placebo, which yielded no significant results in terms of weight loss. On the other hand, Wu *et al.* 2008 reported significant results after a 3-month old research conducted with adult patients that had not received olanzapine before that start of the experiment. They found that metformin prescribed olanzapine treatment patients gained significantly less weight (about 5kg less) compared to placebo receiving ones (Wu, *et al.*, 2008). There are also other studies conducted with adolescents and children. Metformin treatment in 15 patients from total of 19 resulted in significant weight loss (Morrison *et al.*, 2002), but there was no control group in the study and some of the patients received combination of drugs. Moreover, in a placebo controlled 4-month long trial with children receiving antipsychotics including olanzapine, it was found that the weight gain was stopped in metformin receiving group while the placebo group continued to gain weight (Klein *et al.*, 2006).

Studies conducted on olanzapine-induced weight gain treatment by metformin in rats were quite recent compared to human studies. An acute research investigating possible reversal of olanzapine-induced glucose intolerance in female Sprague-Dawley rats by 3 different anti-diabetic drugs, including metformin, reported that

metformin improves glucose tolerance (Boyda, *et al.*, 2012). The same group also studied drug combinations and metformin was found to significantly decrease blood glucose levels after acute olanzapine treatment (Boyda, *et al.*, 2014). However, in both studies olanzapine only administered acutely and only the effect on serum glucose levels were determined. Hu *et al.* 2014 reported that when female Sprague-Dawley rats were treated with olanzapine and olanzapine in combination with metformin for 2 weeks, metformin significantly prevents weight gain without affecting the hyperphagic status of rats and prevents brown fat loss due to olanzapine treatment. They also found that in the liver, adipose and skeletal muscle expression of genes related to energy expenditure (including AMPK) were down regulated by olanzapine (Hu, *et al.*, 2014). Their study was focused on the periphery, not on CNS.

1.3.4 Effects of Metformin on Hypothalamus

Although peripheral action mechanisms of metformin on metabolism have been studied the past decades, researches about its effects on central nervous system are relatively recent. Until the work of Lv *et al.* 2012, metformin passage through Blood Brain Barrier (BBB) was not shown. In their study conducted with diabetic male Sprague-Dawley rats, metformin, which was administered orally, was detected in the cerebrospinal fluid (CSF) (Lv, *et al.*, 2012). Observation of metformin in the brain implies possible effects of metformin on central weight control mechanisms. In accordance with that idea, in the same study it was also indicated that after 4 weeks of oral metformin administration, *NPY* expression levels in the hypothalami, measured by quantitative real-time polymerase chain reaction (RT-qPCR), were significantly dropped whereas *POMC* expression levels remained the same. In addition, it was shown by application of western blot method that although phosphorylated AMPK levels did not changed,

phosphorylated STAT3 levels increased in metformin-treated diabetic rats (Lv, *et al.*, 2012). Even though, presence of metformin in CNS was shown in 2012, the researches on the possibility of metformin acting on hypothalamus started before that. In cultured primary rat hypothalamic neurons, metformin treatment significantly lowered the expression of *NPY* and phosphorylation of AMPK while had no effect on *POMC* expression under glucose starvation (Chau-Van *et al.*, 2007). In contrast to Chau-Van *et al.* 2007, Duan *et al.* 2013 showed that acute central metformin administration to rats increased hypothalamic AMPK phosphorylation with decreased *NPY* expression and *POMC* expression was unaffected. The decrease in *NPY* levels were directly related to increased AMPK phosphorylation since under blocked AMPK phosphorylation *NPY* levels remained high. In another short-term *in-vivo* study investigating directly the possible role of hypothalamus in metformin induced appetite suppression by acute ICV brain injection, it was found out that hypothalamic AMPK and STAT3 phosphorylation increased as the administered metformin amount was increased, but no change was reported for PI3K levels (Lee *et al.*, 2012). Moreover, as opposed to the other studies, in the same work of Lee *et al.* 2012, hypothalamic *POMC* expression was reported to increase significantly following acute metformin administration whereas *NPY* expression was not altered significantly.

It is clear that there is inconsistency in the literature between the reported data about the effect of metformin on hypothalamic weight control mechanisms. Also, there is a lack of information in the literature about the effect of long-term metformin administration on hypothalamic mechanisms.

The studies on effects of metformin on hypothalamus were not restricted to the intracellular signaling pathways and *POMC* and *NPY* expression levels. A research conducted on male Long-Evans rats with diet-induced obesity (DIO) and resistant to DIO shed light on another effect of metformin on hypothalamus (Aubert *et al.*, 2011). Interestingly, significantly elevated leptin receptor gene expression in the

ARC with decreased body weight was observed after 2-weeks intraperitoneal metformin administration which implies a possible role of metformin on central weight control through improvement of leptin signaling in the ARC neurons. Parallel to those, another study was showed that metformin treatment of HFD induced leptin resistant rats for 4-weeks improved leptin sensitivity and induced weight loss (Kim, *et al.*, 2006) which supports increased hypothalamic *POMC* expression and STAT3 phosphorylation with no significant change in hypothalamic *NPY* expression (Lee *et al.*, 2012).

1.3.5 SNPs Studies on Metformin Treatments

Similar to the polymorphism associations in olanzapine studies, the leptin receptor and leptin gene SNPs were found to be associated with antipsychotic induced weight gain side effect (Fernandez, *et al.*, 2010). In addition, associations of metformin transporters and AMPK subunits were found to interfere with the metformin treatment response in T2DM patients (Jablonski, *et al.*, 2010).

1.4 AIM OF THE STUDY

Even though olanzapine causes the highest weight gain as a side effect compared to other atypical antipsychotics, it is more superior for the treatment of psychotic disorders (van der Zwaal *et al.*, 2014). Therefore, it is curial to understand underlying mechanism of the side effect to develop new treatment approaches. Metformin is found to be one of the most potent treatment approaches for the weight gain induced by olanzapine use. Metformin as well as olanzapine action on CNS and metformin efficacy assessments on olanzapine-induced weight gain treatment in human trials are present. However, direct investigations of underlying

mechanism of metformin action in treatment of weight gain side effect of olanzapine are recent and only focused on peripheral parameters. It was implied from the studies that metformin may also act on the CNS and can pass through BBB. Although several brain regions and neuropeptides involved in energy intake control, the main controller of the body weight lies within the hypothalamus. With the known potencies of the POMC and NPY on feeding, it is plausible to think that both the metformin and olanzapine co-actions on POMC and NPY neurons in the ARC may be the point where their actions intervene and the overall outcome, prevention of weight gain or loss of body weight might be achieved. To our knowledge no direct research conducted to prove that hypothesis in animals. Thus, the aim of this study was to investigate possible opposing actions of chronic olanzapine and metformin administration in the hypothalamus focusing on the ARC by studying the POMC and NPY neurohormones expressions. Since intracellular signaling pathways have intervening branches, metformin might interfere directly or indirectly with olanzapine-induced changes in hypothalamic weight regulatory neuron populations. Another goal was to determine whether co-administration of metformin in the beginning of olanzapine treatment was more effective on inhibition of weight gain than the co-administration after the side effect appears or not. The outcome of which is quite important for the human prescriptions.

CHAPTER 2

MATERIALS AND METHODS

2.1 ANIMAL STUDIES

For the rat studies, overall experimental scheme was presented in Figure 2-1. All the solutions and buffers used were in materials and methods chapter were prepared as in Appendix A.

2.1.1 Animal Handling

Fifty 4-week old male Wistar rats were purchased from KOBAY (Turkey). Male rats but not female ones were used due to the complex hormonal cycling of the female system (Naftolin *et al.*, 1990; Brown & Clegg, 2010) that may interfere with the results and in order to match the previous study done with male humans (Ak *et al.*, 2013) .They were randomly assigned to cages as 3 or 4 animals per cage and housed in 22 $\pm$ 2^{o}C with 60% humidity and 12 hour light/ dark cycle (lights were automatically turned on at 7:30 am and off at 7:30 pm). Drinking water and regular chow diet were supplied *ad libitum*. Following a week of acclimatization period, all animals were randomly assigned to groups and weighted. For each

animal, an identification (ID) code number was assigned as "C#R#" in which "C" stands for cage, "R" stands for rat while first number shows the cage number and the second one represents rat's individual number for that cage. To illustrate, C13R4 stands for the number 4 rat in 13th cage. All samples derived from that animal were represented with that ID. Those animal codes were also used in the following sections as explained. All the assigned IDs according to the divided groups were shown in Table F-1.

2.1.2 Drug Dosages and Preparations

Olanzapine was a generous gift from Eli Lilly (USA) and metformin was bought as METFULL 1000mg effervescent tablets (Vitalis, Turkey). The drugs were prepared fresh just before the administration. Since olanzapine is soluble under acidic conditions (FDA Center for Drug Evaluation and Research, 1999) and a dose (2mg/kg) of it was dissolved in 1 mL 0,1M acetic acid (Sigma-Aldrich, Germany) solution (Yanik *et al.*, 2013). After that, the drug in 10 mL of 10% sucrose (Sigma-Aldrich, Germany) solution, were added and pH was adjusted to 7,50 – 8,00 by 1M sodium hydroxide (NaOH) (Applichem, Germany) solution. The final volume was added up to 12 mL with 10% sucrose solution since the calculations of drug amounts were done as if 12 animal per group. Similarly, 11 mL 10% sucrose solution was mixed with 1mL dH_2O per control group in order to make the final sucrose concentrations equal for all groups and rule out the impact of sucrose on animals. For each group, 2 doses a day (4mg/kg/day) were prepared and administered. The amount of drug in water was updated weekly depending on both the animal weights and average drunk water per day for every group. Metformin tablets were readily dissolved in drinking water (METFULL tablet prospectus) as daily doses in amounts depending on the weekly average drunk water per group. The pH was adjusted 6,80 with 4M NaOH in order to eliminate

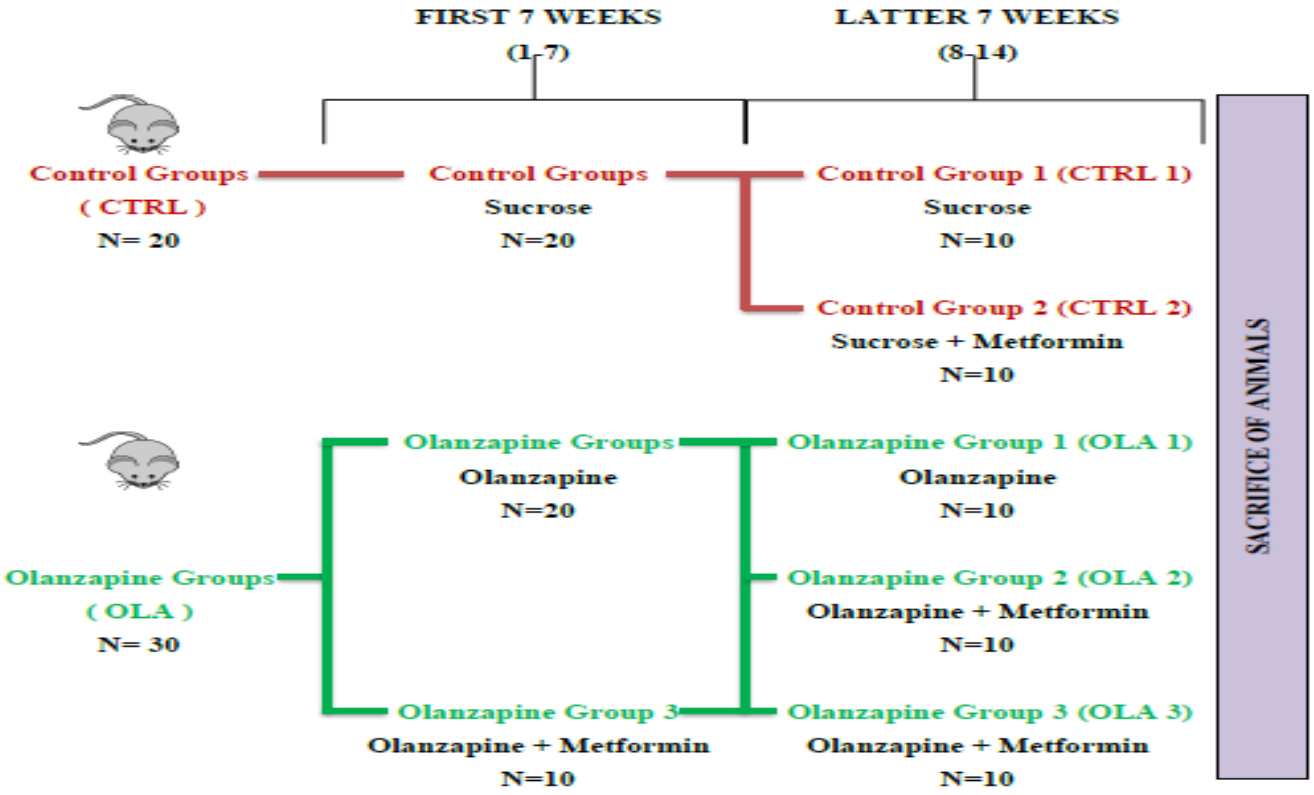

Figure 2-1 The rat groups and drug administration scheme according to time schedule. There were total of 5 groups. CTRL: control (1,2), OLA: olanzapine groups (1, 2, 3). The duration of the drug treatments (1-7 weeks and 8-14) were also indicated. For each group N: 10

pH differences between other groups' drinking water as much as possible. Because one of the highest solubility of metformin is at that pH 6,80 (Block, Schemling, Couto, Mourao, & Bresolin, 2008), which is close to pH of drinking water compared to the low pH after the tablets were dissolved. It was administered as 250mg/kg/day in drinking water as described above and the amount of drug in water was updated weekly depending on both the animal weights and average drunk water per day for every group.

2.1.3 Drug Administration

Animals in all groups received olanzapine and sucrose solutions as 1mL / dose twice a day in syringes. Supplying orally administered solutions in syringes by making them attractive with a vehicle such as sucrose is advantages (Schleimer et al, 2005). First of all, because animals voluntarily drink the solutions, experimental stress was minimized. Secondly, disadvantages of other oral methods such as gavage in long term experiment (eg. irritation of the esophagus due to repeated application) were eliminated. In the first 2 days of the experiment, rats were familiarized with the syringe by the help of 10% sucrose solution. They were readily drinking the solution (Figure 2-2). Then, on the third day, drug administrations were started with the half of the doses. Following that period, olanzapine and sucrose solutions were administered twice a day to the corresponding groups as in Figure 2-1. First doses were supplied at 9:00 am while the second ones were supplied at 7:00 pm. Overall, drugs were administered for 14 weeks (Figure 2-1).

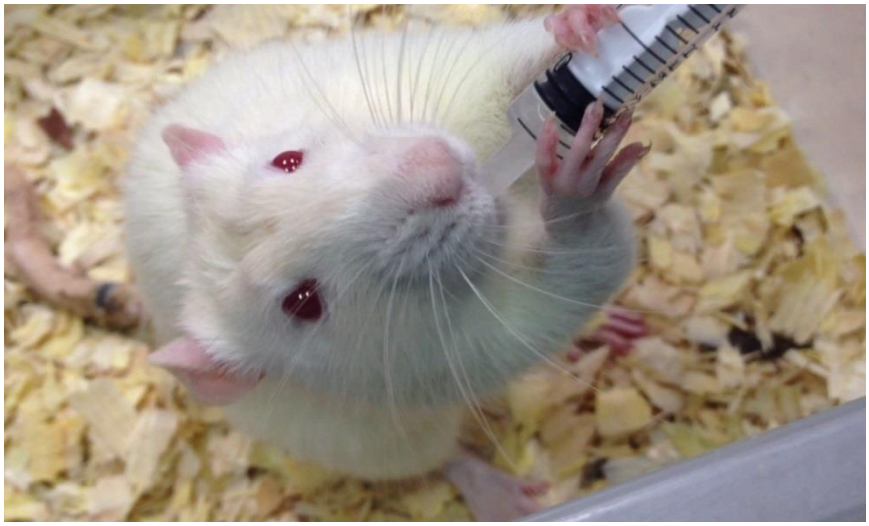

Figure 2-3 Administration of olanzapine to a rat.

2.1.4 Weight and Meal Size Measurements

All animals were weighted weekly. Weights were recorded and used for both analysis of changes and calculation of drug amounts. Similarly, each cage was supplied with a predetermined amount of regular chow diet (200 g) every day at the same hour (6:00 pm). The remaining chow was weighted for every next day at the same hour to find out how much meal was consumed. The values were recorded and analyzed (Figure 3-1). In addition, daily food intake recordings of groups were graphed all together and trend lines of each group was drown. Since the slope of trend lines reflects the direction of food consumption, they were also calculated. A positive slope was assumed to indicate increased daily feeding whereas a negative one was assumed as decrease in food intake. On the other hand, a slope almost equals to zero; that is, parallel to throughout the all experiment was evaluated as unchanged daily food intake.

2.1.5 Animal Sacrifications and Sample Collections

All the materials including collection tubes, pipette tips, scissors, forceps, bistoury etc. and needed amount of dH_2O to prepare solutions were sterilized by treatment of Diethylpyrocarbonate (DEPC) (Sigma-Aldrich, Germany) for overnight (o/n) in order to inactivate RNases. Then, all of them were autoclaved to inactivate DEPC and materials were dried in the oven before use. The working areas and micropipettes were cleaned by RNase Away (Thermo Scientific, USA).

All animals were sacrificed at the end of the 14^{th} week. In the beginning of the procedure, each animal was slightly sedated with carbon dioxide (CO_2) gas for 10 sec and decapitated by the guillotine.

2.1.5.1 Hypothalamus Collection

As soon as beheading, the brain was removed from the skull and washed with 1X Phosphate Buffer Saline (PBS) (Sigma-Aldrich, Germany) solution. Then, the hypothalamus was recovered from the brain (Figure 2-3) and immediately stored in 500 µL RNA*later* RNA stabilization reagent (Qiagen, Germany). The sample tubes filled with RNA*later* were stored at $+4^oC$ o/n (16 h) according to the manufacturer and the tissues were placed in fresh DEPC-treated tubes. The hypothalami were then stored at -80^oC until used.

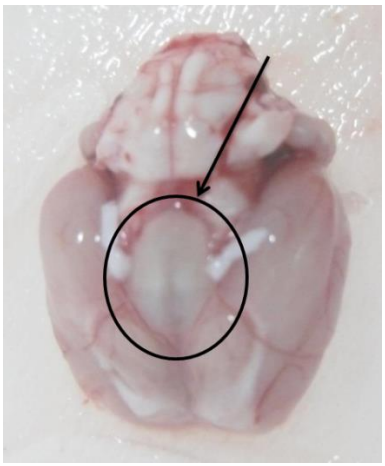

Figure 2-4 Removed and upside down positioned brain of one of the experimental animals. The black circle and arrow specify the location of hypothalamus.

2.1.5.2 Blood Collection and Serum Preparation

Trunk blood from each sacrificed animal were collected in 10 mL red capped blood collection tubes and centrifuged at 1 600g in Selecta Centrofriger BL-II centrifuge (General Laboratory Coorporation, Yemen) for 10 min. The serum samples (supernatant) were aliquoted into autoclave-sterilized 1,5 mL eppendorfs and stored at -80^{o}C for longer storage.

2.2 BLOOD SERUM STUDIES

2.2.1 Serum Triglyceride Levels

Triglyceride levels in collected rat serums were determined by use of Abcam Triglyceride Quantification Kit (USA) according to manufacturer's instructions for colorimetric assay were followed. The procedure relies on the conversion of triglycerides into free fatty acids and glycerol by lipase and detection of glycerol amount by the specific probe that changes color which is reflected at absorbance at 570nm wavelength. Clear flat bottom 96-well plates (Corning, USA) were used and standard curves were constructed individually for each plate. Samples were diluted with assay buffer to give absorbance in the range and the dilutions were decided according to trial of different dilutions with the kit before the actual measurement. Each sample was loaded into 3 different wells. One of each sample was used as no Lipase control to eliminate background coming from glycerol in the samples. The samples that were out of the reading range were re-diluted and measured again. The calculations were done according to the standard curves.

2.2.2 Serum Leptin Levels

Serum leptin amounts were determined by use of mouse/rat enzyme-linked immune absorbent assay (ELISA) kit (Phoenix Pharmaceuticals, Inc, USA). The manufacturer's protocol was followed with some modifications. Briefly, antibody-coated plate was blocked with the blocking buffer containing 5% bovine serum albumin (BSA) (Thermo Scientific, USA) and 0,025% Tween20 (BioShop, Canada) in PBS. Simply, all the wells were filled with blocking buffer at maximum amount they can hold and the plate was allowed to stand 2 h at room temperature. After blocking, wells were washed thoroughly with the provided wash buffer 3 times. The standards and samples (1:20 dilution) were prepared and loaded as duplicates (100µL/well). The loaded plate was incubated at room

temperature for 1 hour with constant shaking (about 300 rpm). After the incubation, wells were washed 3 times with 350 µL wash buffer. Then, 100µl of the diluted biotin-labelled anti-rat/mouse leptin antibody solution were added and incubated at room temperature for 1 hour with shaking. Wash steps were repeated and the wells were incubated with 100µl of Streptavidin-HRP conjugate solution at room temperature for 30 min with shaking. Following incubation, wells were washed twice with wash solution and then once with dH_2O. Then, 100µL substrate solution was added and plate was covered with aluminum folio to prevent light entrance. Following 10 min room temperature incubation, color development was stopped by addition of stop solution and the absorbance at 450nm wavelength was read within 5 min. Finally, leptin standard curve was constructed and the leptin concentrations of serum samples were calculated by the equation derived from the linear range of the curve.

2.3 EXPRESSION STUDIES

All the materials, solutions and water used for all RNA and cDNA procedures were either DEPC-treated to remove RNases or purchased as nuclease-free to prevent degradation of RNAs. All the centrifugations were done at $+4^oC$ in Selecta Centrofriger BL-II unless it was indicated otherwise.

2.3.1 Total Hypothalamic RNA Isolation

For determination of expression levels of target genes, *NPY* and *POMC*, as well as the internal reference gene, glyceraldehyde 3-phosphate dehydrogenase (*GAPDH*),

total RNA was isolated by use of TRI Reagent (Sigma-Aldrich, Germany) according to the manufacturer's instructions with some modifications. First of all, hypothalami were removed from -80^{o}C, 1 mL ice-cold 1X PBS solution was added into each tube immediately and centrifuged at 10 000g for 40sec to get rid of the remnants of RNA*later*. As soon as the centrifugation ended each sample was taken into a new 1,5mL centrifuge tube and immersed into 1mL TRI Reagent and kept on ice. Then, each sample was homogenized by the teflon-glass homogenizator at a speed of 2500rpm by the help of a drill on ice. The samples were incubated at room temperature for 10 min and then centrifuged at 12 000g for 10 min to remove insoluble materials. Supernatants were taken into new 1,5mL centrifuge tubes. 200mL ice-cold pure Chloroform (Sigma-Aldrich, Germany) was added into each tube, then mixed by vigorous inversions for 30 sec and incubated at room temperature for 3 min. To achieve phase separation, tubes were centrifuged at 12 000g for 15 min. The mixture in tubes separated into 3 phases as the upper aqueous RNA phase, the interphase in the middle with DNA and the lower organic phase with proteins. The upper phases were carefully removed without touching the interphase by pipetting and transferred into new centrifuge tubes. From the remaining phases, the organic phases were also collected by the help of gel-loading pipette tips into new centrifuge tubes and stored at -80^{o}C until protein isolation. Following, again 200 mL ice-cold pure Chloroform was added into each collected aqueous phase. The tubes were mixed by vigorous inversions for 30 sec and incubated at room temperature for 7 min. Similarly, phases were separated by centrifugation at 12 000g for 15min and the aqueous phases were collected into new centrifuge tubes while the rest of the contents were discarded. Then, 500mL ice-cold pure molecular biology grade Isopropanol (2-Propanol) (Sigma-Aldrich, Germany) was added into tubes which were inverted slowly to mix the contents until the whitish clouds disappeared. One mL RNase-free glycogen (Sigma-Aldrich, Germany) was added to each sample as co-precipitant to enhance precipitation of RNA by Isopropanol (Life Technologies Corporation, 2010). The

samples were incubated at -20^{o}C for minimum 40 min which was followed by centrifugation at 12 000g for 25 min. The supernatant was discarded and the centrifugation was repeated for 1 minute to collect all the remnant solutions to discard. One mL freshly prepared 75% ice-cold ethanol (EtOH) (Sigma-Aldrich, Germany) was added onto each pellet to wash and the tubes were inverted slowly to detach the pellet from the tube. The tubes were centrifuged at 7 500g for 5 min and the EtOH was discarded and the step was repeated once more. After removing the EtOH from the tubes, the tubes were spun down again for 1 minute to collect all the EtOH remnants as much as possible. Following the last spin, the caps of the tubes were opened in front of a Bunsen burner flame and all samples were allowed to air dry (for 10-15 min). Finally, 40 µL nuclease-free water (Thermo Scientific, USA) was poured onto each dried pellet. The tubes were allowed to stand for 5 min on ice and then an additional 5-10 min with gentle occasional pipetting until the pellets were fully dissolved. After determination of the concentrations, the RNA samples were stored at -80^{o}C until used.

2.3.2 DNase Treatment of RNA Samples

Although the genomic DNA (gDNA) was expected to remain at the interphase during phase separation, still it could contaminate RNA samples, which would interfere with the results. In our pilot studies, it was observed that DNA contamination could not be fully avoided. Hence DNase treatment (Ambion DNA-*free* Kit, Life Technologies, USA) was utilized to remove contaminant gDNA from the RNA samples. Briefly, 10ug nucleic acid from all samples were taken into separate microcentrifuge tubes and diluted to 44 µL final volume. Then 5 µL DNase I Buffer and 0,5 µL DNase I enzyme was added into each tube, mixed gently by pipetting and spun down shortly with a bench top mini centrifuge. Tubes were incubated at 37^{o}C for 30 min in the microtube heater (Thermoline Scientific

DMB-2, Australia) and at the end of 30 min, 0,5 µL DNase I enzyme was added again and incubated at 37^{o}C for 30 min. Then, 5 µL DNase inactivation reagent was added in the tubes and incubated at room temperature for 2 min by occasional mixing by pipetting. Finally, the tubes were centrifuged at 10 000g for 1,5 min at room temperature and supernatants were taken into new DEPC-treated microcentrifuge tubes. The samples were stored at -80^{o}C until used.

2.3.3 RNA Cleanup and Concentration

In order to get rid of any contaminants that might interfere with the following procedures, RNA samples were cleaned up and concentrated by use of ZYMO RNA Clean and Concentrator – 5 kit (ZYMO RESEARCH, USA) according to the manufacturer's instructions with slight modifications. All the centrifugations were performed at 12 000g in RT unless indicated otherwise. Fifty µL DNase-treated RNA samples were thawed on ice and 100 µL RNA binding buffer was mixed with each sample. Then, 150 µL pure EtOH (Sigma-Aldrich, Germany) was added into each tube and mixed. After that, the solutions were transferred into the Zymo-Spin IC Columns placed in a collection tube and spun for 1 minute. Flow-through in the collection tubes were decanted and 400 µL RNA prep buffer was added into each column. The tubes were centrifuged again for 1 min and the collection tubes were emptied again. The RNA-bound columns were washed with 700 µL EtOH-added RNA wash buffer by centrifugation them for 1 minute. The flow-through was discarded. The wash step was repeated by use of 400 µL EtOH-added RNA wash buffer followed by a 2-minute spun and the collection tubes were emptied again. Without addition of any solution, columns were centrifuged for 1 minute to get rid of any remaining buffer. The columns were removed from the collection tubes and placed onto RNase-free microcentrifuge tubes.15 µL nuclease-free water was added onto each column and they were incubated at room temperature for 2

min. Finally, RNA samples were eluted by centrifugation at 10 000g for 1 minute and stored at -80^{o}C until used.

2.3.4 Nucleic Acid Concentration by NanoDrop

Nucleic acid concentrations of RNA samples immediately after the total RNA isolation and after the cleanup protocols were determined by the NanoDrop 2000 UV-Vis Spectrophotometer (Thermo Scientific, USA) with utilization of 2 μL sample for each measurement. Absorbance ratios of 260/280 nm wavelengths as well as 260/230 nm wavelengths were determined by the NanoDrop. Since maximum absorption of nucleotides are at 260 nm wavelength, NanoDrop calculates the concentration of nucleic acid sample by Beer Lambert Law and absorbance of it at that wavelength.

RNA purity was determined by 260/280 and 260/230 absorbance ratios since maximum absorbance of proteins were around 280nm while contaminant reagents generally give the highest absorbance around 230nm. Although the ratios can change depending on the solvent composition, in general for a pure RNA sample, 260/280 ratio is expected to be around 2,0 while 260/230 ratio is expected to be in between 1,8 -2,2 (Fleige & Pfaffl, 2006).

2.3.5 Visualization of RNA Samples by Agarose Gel Electrophoresis

Although 260/280 ratios give a hint about the quality of RNA samples, still the samples were needed to be run in agarose gel to detect both the integrity of RNA and gDNA contaminants, if any. The RNA samples before any treatment and after DNase and cleanup treatments were run in 1% agarose (Sigma-Aldrich, Germany) gel pre-stained with Ethidium bromide (EtBr) (Sigma-Aldrich, Germany), for 50min at 80V. In order to differentiate the sizes of bands, RiboRuler High Range

RNA Ladder (Thermo Scientific, USA) was used. Samples were diluted 1:1 with nuclease-free water and mixed with 2X loading dye supplied with the ladder. Four µL of the sample-dye mixture was loaded into each well. After the run, bands were visualized by exposing to ultraviolet (UV) light in Vilber Lourmat UV Imager (Belgium).

2.3.6 Synthesis of Complementary DNA (cDNA) by Reverse Transcription

Thermo Scientific RevertAid First Strand cDNA Synthesis Kit (USA) was used for synthesis of cDNA from DNase treated and cleaned up RNA samples. All cDNA synthesis were done from 0,5 µg RNA. After the thawing, the RNA were pipetted into a 0,2 mL PCR tubes, and 1 µL random hexamer primer (100 µM) provided by the kit was also added. Then, the volumes were added up to 12 µL with nuclease-free water. After gently mixing the tubes were incubated at 65°C for 5 min in BioRad T100 Thermal Cycler (USA) to open up possible secondary structures formed by RNAs. Next, the tubes were taken on ice and the contents were spun down by a bench-top mini centrifuge. Four µL 5X reaction buffer, 1 µL RiboLock RNase inhibitor (20 u/µl), 2 µL 10 mM deoxyribonucleotide triphosphate (dNTP) mixed and 1 µL RevertAid M-MuLV reverse transcriptase (M-MuLV RT) (200 u/µl) were added into each tube to yield a 20 µL final volume/tube. To determine whether remnants of gDNA would also amplified in Quantitative Real-Time Polymerase Chain Reaction (RT-qPCR) or not, negative controls (no RT) for several samples were also prepared by excluding M-MuLV RT from the reaction mixture and adding up the volume with nuclease-free water. The components of 5X reaction buffer can be seen in Appendix A. The reaction mixtures were mixed by pipetting and spun down. They were kept at 25°C for 5 min followed by 60-minute incubation at 42°C and termination of reaction by heating to 70°C for 5

min. The products were stored at -20°C for immediate use in RT-qPCR application.

2.3.7 Quantitative Real-Time Polymerase Chain Reaction (RT-qPCR) Application

RT-qPCR is the most reliable method for the determination of the nucleic acid amounts when the procedures and standards are followed carefully. Although the nature of the used fluorophore can change, the detection simply relies on the increase in fluorescence signal during the amplification of the template DNA species. In this study, SYBR Green, which intercalates itself into the double strands regardless of the sequence, was used. As the more DNA was amplified, the more dye binds to them so that the signal increases. Moreover, the detection depends on the starting amount of the sample because the higher amounts mean the earlier start of the detection of the fluorescence. By defining a threshold fluorescence level above which the detections were significant (not the false background signals), and by calculating and comparing the amount increase (fold change) depending on the cycle at which the samples passed the threshold; that is, Ct values (Cq or TOB), and the efficiency of the reaction, the initial amount of targets can be quantified relatively or absolutely (Bustin, *et al.*, 2009). In addition, a melt analysis was performed at the end of each run which would help the interpretation of the quality of the products. The melt analysis simply depends on the fact that as the more DNA double strand separates from each other owing to the stepwise temperature increase, the more the fluorescence signal drops. At the point where the half of the strands was separated from each other, a sharp decrease was observed. The temperature at which the half of the double strand is opened up is called melting temperature (Tm) and represented as a peak by the program. The Tm depends on the length and composition of DNA species so that the same DNA

species can be observed as the overlapped peaks whereas different species give distinct peaks. Therefore, performed melt curve analysis is critical for the assessment of the quality and specificity of the amplification. (Dorak, 2006). All the RNA steps were confirmed based on MIQE guidelines, except only one reference gene was used for normalization in this study (Dorak, 2006).

For RT-qPCR protocol, SYBR Green JumpStart *Taq* ReadyMix without $MgCl_2$ produced by Sigma-Aldrich (Germany) was used. The components of the SYBR mixture are shown in Appendix A. The intron-spanning primers' sequences (Iontek, Turkey) used were listed at Table 2-2. The optimized reaction conditions were detailed in Tables 2-3, 2-4, 2-5 and 2-6. All the reactions were conducted in thin-walled clear 0,2 mL PCR tubes (Greiner Bio-One, USA) using RotorGene Q (Qiagen, Germany).

To construct a standard curve for each gene, different serial dilutions from cDNA products were used. Because the sample results should be in working dilution range to be able to perform quantitation and comparison, depending on the results of dilution series all samples were diluted as 1/100 from their cDNAs. In addition, in each run, at least 1 no-RT control and 1 no template control (NTC) samples were used and analyzed to detect whether gDNA was amplified and/or whether there is DNA contamination in the other components, respectively. Optimally, at every run, it is best to include standard dilution series to make sure all the reactions for a single gene have the same efficiency. However, since 36-tube rotor was available and the number of samples was high, at least 2 components of the constructed standard curve were analyzed at the vacancies in the rotor in order to compare the reactions with the standard curves.

Table 2-1 Primer sequences used in RT-qPCR protocols. *GAPDH*: glyceraldehyde-3-phosphate dehydrogenase gene in *Rattus norvegicus* (NM_017008), *POMC*: proopiomelanocortin gene in *Rattus norvegicus* (NM_139326), *NPY*: neuropeptide Y gene in *Rattus norvegicus* (NM_012614).

Primer ID	Sequence
GAPDH forward primer	5' – TCCCATTCTTCCACCTTT – 3'
GAPDH reverse primer	5' – TAGCCATATTCATTGTCATACC – 3'
POMC forward primer	5' – AACATCTTCGTCCTCAGA – 3'
POMC reverse primer	5' – CGACTGTAGCAGAATCTC – 3'
NPY forward primer	5' – AATGAGAGAAAGCACAGAAA – 3'
NPY reverse primer	5' – AAGTCAGGAGAGCAAGTT – 3'

Table 2-2. RT-qPCR components for *GAPDH* reaction. $MgCl_2$: Magnesium Chloride.

Reaction Components	Volume in 1 Tube (µL)
SybrGreen Mix	10
GAPDH forward primer (5uM stock)	1,6
GAPDH reverse primer (5uM stock)	1,6
$MgCl_2$ (25mM)	2,4
cDNA (df: 1/100)	4
Nuclease-free dH_2O	0,4
TOTAL	**20**

Table 2-3. RT-qPCR components for *POMC* reaction.

Reaction Components	Volume in 1 Tube (µL)
SybrGreen Mix	10
POMC forward primer (5uM stock)	0,8
POMC reverse primer (5uM stock)	0,4
$MgCl_2$ (25mM)	2,4
cDNA (df: 1/100)	4
Nuclease-free dH_2O	2,4
TOTAL	**20**

Table 2-4. RT-qPCR components for *NPY* reaction.

Reaction Components	Volume in 1 Tube (µL)
SybrGreen Mix	10
NPY forward primer (5uM stock)	0,4
NPY reverse primer (5uM stock)	0,4
$MgCl_2$ (25mM)	2,4
cDNA (df: 1/100)	4
Nuclease-free dH_2O	2,8
TOTAL	**20**

Table 2-5. Optimized RT-qPCR reaction conditions of *GAPDH* , *POMC* and *NPY* genes.

	Temperature (°C)	Duration	Cycle #	Temperature (°C)	Duration	Cycle #	Temperature (°C)	Duration	Cycle #
Initial Denaturation	94	15min		94	15min		94	15min	
Denaturation	94	20sec		94	20sec		94	20sec	
Annealing	57	30sec		63	30sec		53	15sec	
Extension	72	30sec	35	72	20sec	45	72	20sec	50
Melt	50-99			50-99			50-99		
Gene of Interest	***GAPDH* Reaction**			***POMC* Reaction**			***NPY* Reaction**		

2.3.7.1 Visualization of RT-qPCR Products by Agarose Gel Electrophoresis

The RT-qPCR products were run in 3% agarose gel pre-stained with EtBr. To detect sizes of the products O'GeneRuler low range DNA ladder (Thermo Scientific, USA) was loaded into 1 well and run with the samples. Simply, samples were mixed with 6X loading dye provided with the ladder as 1:5 dye:sample ratio and 8 µL sample-dye mixture was loaded into each well. Then they were run at 80V for 65 min. At the end, bands were visualized under UV light.

2.3.8 Relative Quantification of Target RNAs

The results obtained from the RT-qPCR reactions were analyzed by calculations of delta Ct values and fold change ratios. First of all efficiencies of the reactions for each gene was determined by construction of a standard curve from different cDNA dilutions of a chosen control sample (C1R3). Then, from the drawn change in Ct versus initial copy number curve, the reaction efficiency was calculated as

$$\text{Reaction Efficiency} = 10^{-1/slope} - 1$$

When the efficiency is 100% (or 1), it means the sample doubles at each amplification cycle (Qiagen, 2009).

Since no absolute control was used to construct the standard curves, relative quantification was applied. Although there are other mathematical methods of quantification (Pfaffl, 2006) owing to the close reaction efficiencies for all genes, the calculation of fold changes was done by the method proposed by Liwak *et al.* 2001. The formulation is as follows:

$$\Delta Ct = Ct\ (\text{target gene}) - Ct\ (\text{reference gene})$$

$$\Delta\Delta Ct = \Delta Ct\ (\text{treatment}) - \Delta Ct\ (\text{control})$$

$$\text{Ratio (fold change)} = 2^{-\Delta\Delta Ct}$$

2.4 STATISTICAL ANALYSIS

Statistical analysis of weight change, meal size, serum triglyceride and serum leptin levels, and RT-qPCR data were done by use of GraphPad Prism 6 Software. Before each analysis, outliers in the data were removed. One-way Analysis of Variance (ANOVA) for whole groups and unpaired t-test for individually analyzed

groups by taking significance value (p) as 0.05 were applied. For significant outcomes, Tukey's post hoc test was applied by the same program to verify differences between groups. In addition, descriptive data were also calculated and shown as arithmetic mean $\pm$ standard error (SEM) for all analysis.

CHAPTER 3

RESULTS AND DISCUSSION

3.1 ANIMAL STUDIES

3.1.1 Meal Size and Weight Changes

The results of meal size measurements and weight gain after the 14-week period indicated that groups that did not take metformin, which were CTRL 1 (slope of trendline:-0.0002) and OLA1 (slope of trendline:-0.0052) had consumed the same amount of meal throughout the experiment. In other words, rats in both of those groups consumed the same amount of food after 14 weeks as they had consumed in the first week implied by the parallel food curves to the x-axis of the graph (Figure 3-1). On the other hand, when the metformin-received groups were compared, all of them showed decrease in appetite (Figure 3-1). Specifically, OLA 2 group showed the sharpest decrease with the trend line slope of -0.0328, which was pursued by OLA 3 group with the slope of -0.0306. In addition, CTRL 2 group presented the mildest decrement among metformin groups (slope: -0.0133) which may indicate that the food intake inhibition by metformin might be more pronounced in the olanzapine treatment compared to sole metformin administration. Moreover, metformin may have a more potent impact on food

consumption when prescribed later in the olanzapine treatment. Furthermore, as indicated in the Figure 3-2, those differences between groups were statistically significant (****p<0,0001) with the exclusion of CTRL 1 vs OLA 1 and CTRL 2 vs OLA 2. To be more precise, average meal size per rat for CTRL 1 was 34.35 $\pm$ 0.22 g/ day and for OLA 1 was 35.00 $\pm$ 0.25 g/day. In addition, every rat in CTRL 2 group averagely ate 31.64 $\pm$ 0.25 g/day and every one in OLA 2 group ate 31.75 + 0.24 g/day, which were quite similar. The similarity between those groups was quite interesting which may imply that olanzapine may not have effect on food intake. The role of food choice rather than food amount was not evaluated in this study, but that could be considered for the future studies. Also, even though metformin caused a sharper drop in the amount of food consumed in OLA 2 group compared to CTRL 2, the higher food consumption prior to the metformin administration might have result in a leveling off with the controls. In other words, although the negative impact of metformin on appetite was observed to be more potent when administration started later, it may not differ from the controls in overall amount of ingested food was considered. In fact, the decrease in energy intake might be more pronounced in the olanzapine group treated with metformin from the start, which also differed from all of the other groups (average meal size/rat: 29.92 $\pm$ 0.34 g/day). Nevertheless, to prove that hypothesis, a much longer term study needed to be performed. In addition, when all the olanzapine groups were compared with each other, it may be implied that appetite decreasing effect of metformin was more when started metformin treatment from the beginning of the study. Moreover, if the meal size differences of CTRL1 - CTRL2 and OLA1 - OLA2 were compared to each other, it may be deduced that metformin might have more pronounced effect on appetite when co-administered with olanzapine.

In order to observe the effect of different amount of food consumptions of the rats on the body weight, animals were weighted weekly (Figure 3-3). In the beginning of the study, average weight of groups had not differed from each other. Starting from the 7^{th} week, the significant differences between weights were started to be

observed. However, only significant difference observed in the end (week 14) was between OLA 3 and CTRL 1 group. The other groups did not differ from each other statistically. However, the observations of adiposity around the internal organs (Figure 3-4) showed that, CTRL1, CTRL2 and OLA 3 groups had less abdominal fat while OLA 1 group animals showed quite high abdominal fat compared to all groups. OLA 2 animals were observed to have less fat than OLA 1 animals and more fat than OLA 3 animals. Those observations might imply that although overall animal weights did not differ from each other in olanzapine groups, still the body fat composition may be effected. In other words, the adiposity levels may have increased while the lean mass of animals may have decreased in olanzapine groups which might result in no difference. However, the adiposity levels could not be determined and remained as observations so that the possibility of changes in body compositions could not be studied. In addition, since the rats were outbred animals, there was a possibility of interference due to genetic variances (especially ones resulting in predisposition to eat more and gain weight). In other words, the animal numbers per group may have not been enough to compensate outcomes due to intragroup differences.

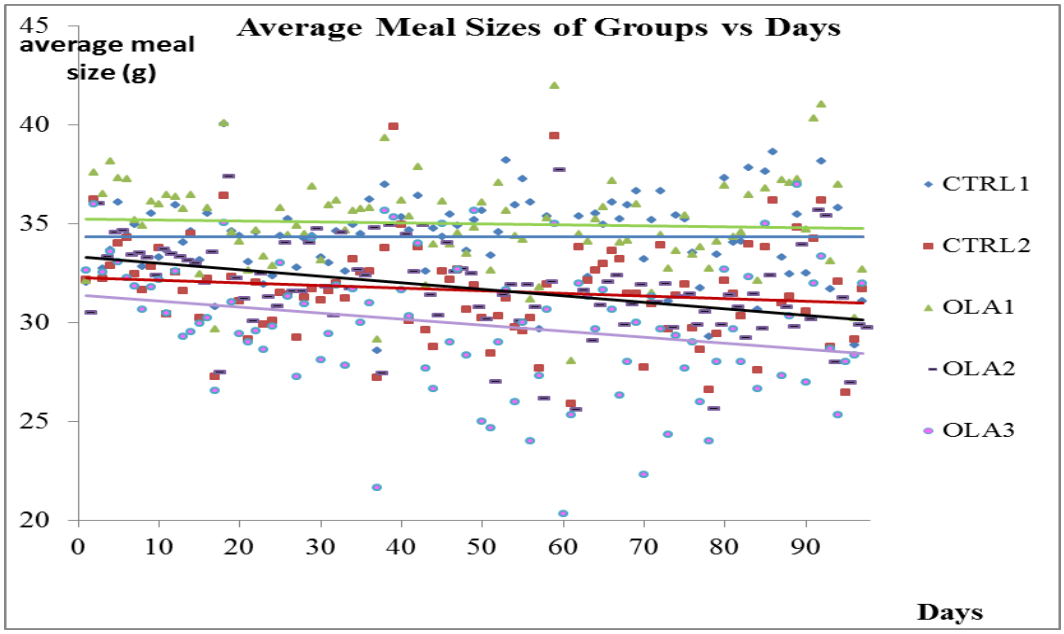

Figure 3-1 Average meal size/animal of groups according to day.

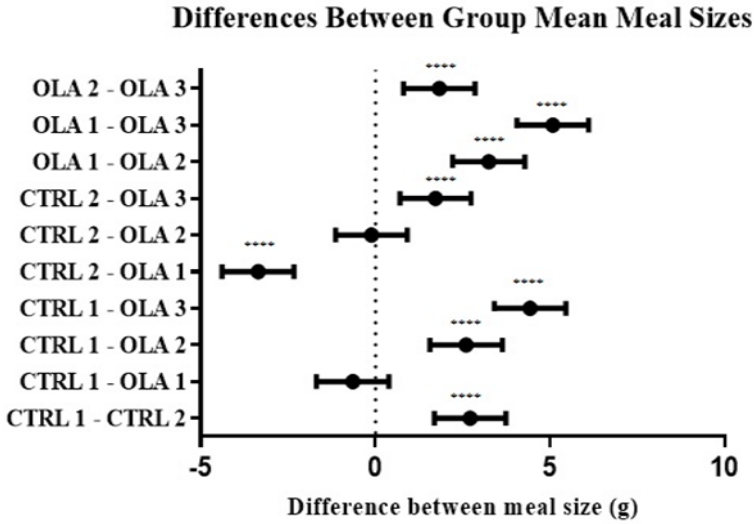

Figure 3-2 The mean meal size differences among all groups for 14 weeks. **** p<0.0001**.** The values indicated as Mean ± SEM.

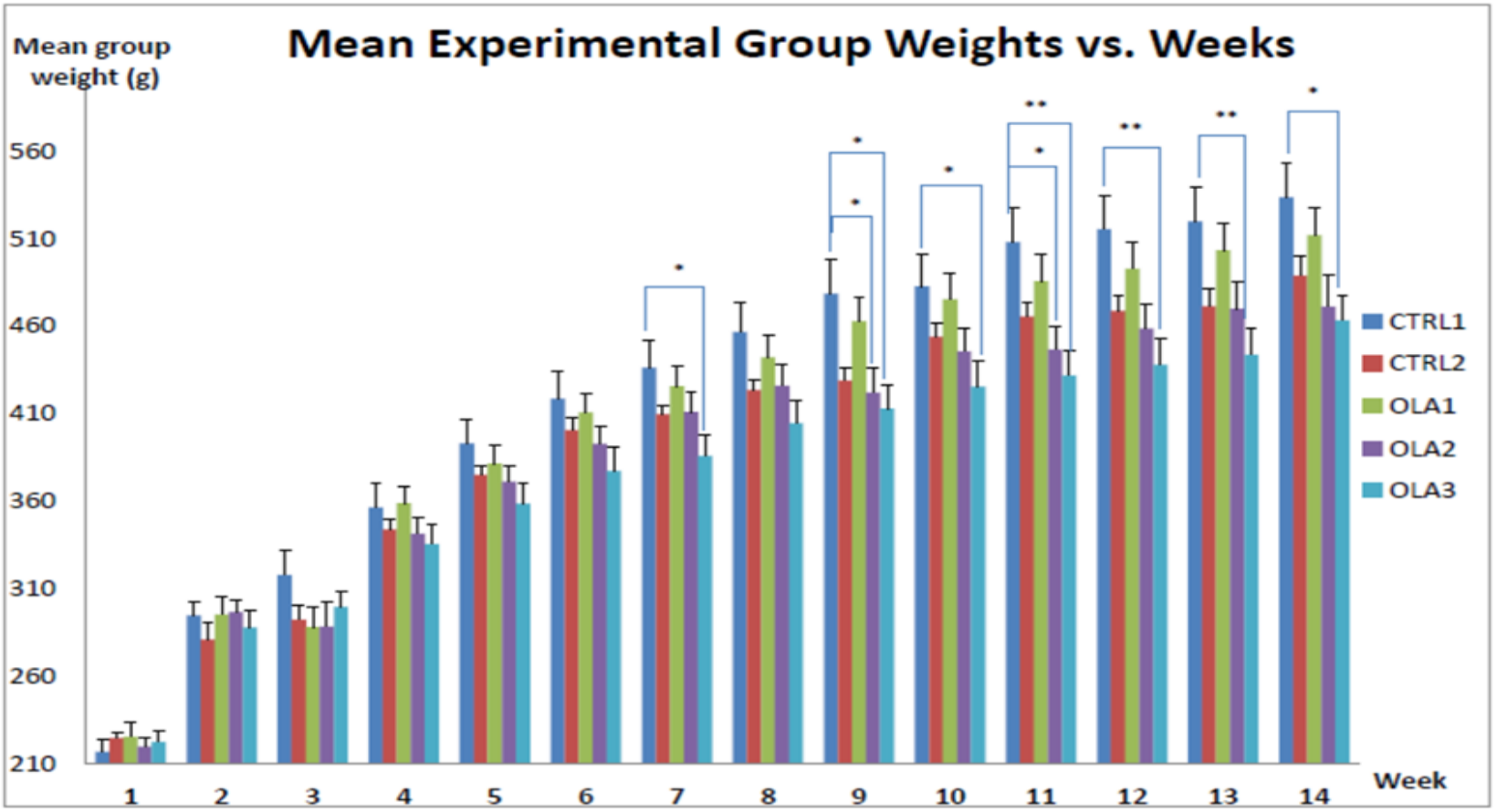

Figure 3-3 Weekly mean rat weights of groups. *p<0.05, **p<0.01. The values indicated as Mean ± SEM.

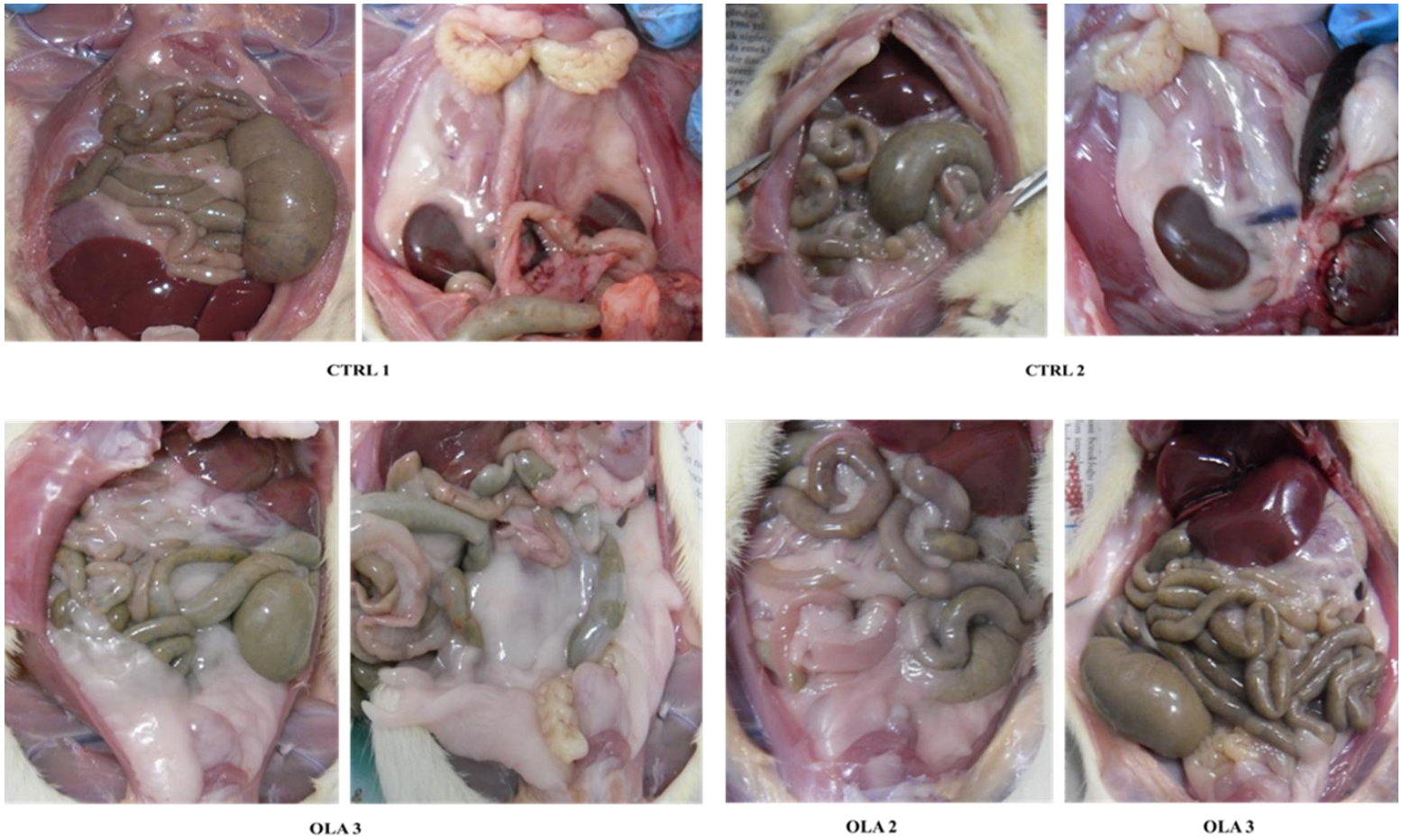

Figure 3-4 Representative pictures of abdominal adiposity of rats.

3.2 BLOOD SERUM STUDIES

3.2.1 Serum Triglyceride Levels

Serum triglyceride levels are a measure of lipid profile and elevation of levels is an indication of dyslipidemia (Papanastasiou, 2013). Therefore, to estimate the effects of the treatments on lipid metabolism, triglyceride levels of the animals were detected. By use of the equations derived from the standard curves lipid and the absorbance values of the samples, serum triglyceride concentrations were calculated. There was no significant difference between groups (Figure 3-5). The group means of triglyceride levels were as 0.97 $\pm$ 0.11 mM for CTRL 1, 1.28 $\pm$ 0.06 mM for CTRL 2, 1.26 $\pm$ 0.12 mM for OLA 1, 1.20 $\pm$ 0.14 mM for OLA 2 and, lastly, 1.26 $\pm$ 0.08 mM for OLA 3.

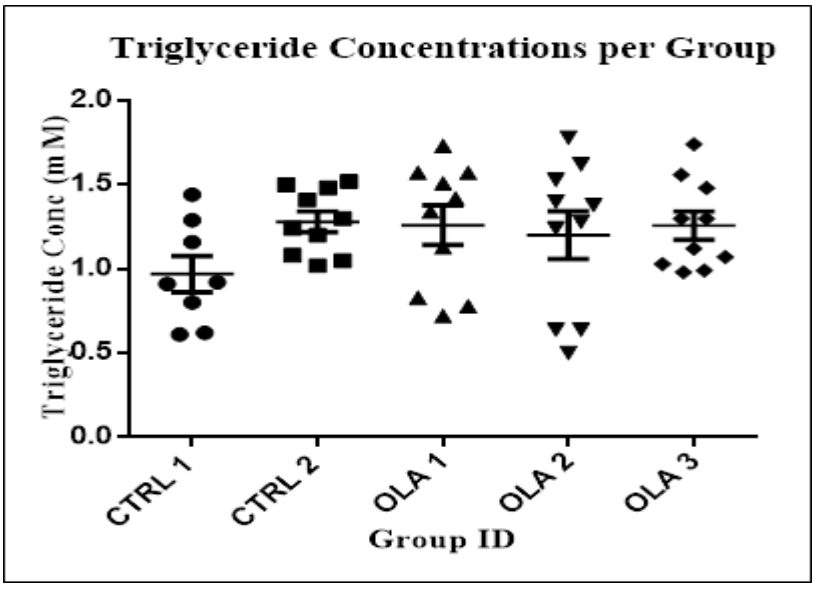

Figure 3-6 Serum triglyceride concentrations of distinct experimental groups. Conc : concentration. The values indicated as Mean + SEM.

In human studies, serum triglyceride levels were found to significantly increase after atypical antipsychotic treatments in both psychotic patients (Teff & Kim, 2011; Ak *et al.*, 2013) and healthy persons (Fountaine, *et al.*, 2010). On the other hand, metformin is an anti-lipogenic agent and expected to lower the serum triglyceride levels (Zhou, *et al.*, 2001). Although metformin was found to decrease serum triglyceride levels in human trials as expected (Bristol-Mayers Squibb Company, 2013; Wulffele *et al.*, 2004), there are some exceptions. Ranganathan *et al*. 2006 observed that no change in triglyceride levels of 10-week metformin treated human subjects with insulin intolerance occured. Surprisingly, in the 14-week study of Baptista *et al*. in 2006, it was reported that after metformin administration to olanzapine-treated patients, serum triglyceride levels were significantly increased in metformin treated patients compared to placebo given ones. When the animal studies are considered, significant decrease in serum triglyceride levels after 5-day metformin administration was reported in male Sprague-Dawley rats (Zhou *et al*. 2001). Reduced serum triglyceride levels in mice due to increased glycerol clearance from the blood after metformin treatment was also found (Geerling *et al*. 2014). On the other hand, similar to our results, Hu *et al*. 2014 reported that no significant difference was observed in serum triglyceride levels of olanzapine-treated and olanzapine-metformin co-treated rats. However, their study only lasted 2-weeks compared to our 14-week study. In our study, it was expected to observe lower serum triglyceride levels in untreated rats and in metformin-treated rats compared to olanzapine treated ones which was not observed. Although the mean levels were lower in the master controls (CTRL 1), still it did not reached statistical significance. The reason for our results coming out as insignificant may have been due to the genetic heterogeneity of the animal samples (outbred animals) with contribution of differing factors which could clearly be observed by the intragroup variation of the results (Figure 3-4). Nevertheless, when CTRL 2 and olanzapine groups were compared, it could be

that metformin may not have a negative effect on serum triglyceride levels of rats in the presence or absence of olanzapine treatment.

3.2.2 Serum Leptin Levels

Since serum leptin levels directly correlates with the adipose mass in the body (Lee & Bishop, 2011), it was measured to estimate the changes in adiposity due to drug administrations (Figure 3-6). Overall, the difference between OLA 1 and CTRL 2 was found to be significant (Figure 3-6.A). That was plausible since it was expected for the CTRL 2 group to have the lowest while OLA 1 group to have the highest serum leptin levels. However, since the true control for the OLA 2 group was CTRL 2 group, those 2 groups analyzed separately by unpaired t-test which yielded no significant difference with CTRL 2 group 164.4 $\pm$ 16.20 pg/mL and OLA 2 group 165.7 $\pm$ 23.38 pg/mL serum leptin (Figure 3-6.B). In other words, olanzapine treatment did not change serum leptin levels under metformin treatment. In addition, in order to observe effect of early metformin administration compared to late administration, olanzapine groups were analyzed by taking the non-metformin administered ones as the control (Figure 3-6.C). Interestingly, when olanzapine treated rats started to receive metformin at 7^{th} week, serum leptin levels significantly decreased compared to just olanzapine treated ones (281.8 $\pm$ 27.45pg/mL). Although there was no significant difference between body weights of OLA 1 and OLA 2 groups, the significantly reduced leptin levels in OLA2 group implies decreased adiposity in metformin-treated olanzapine rats compared to olanzapine-treatment only which was also visually observed (Figure 3-4). However, the olanzapine group with 14-week metformin administration (203.3 $\pm$ 23.79 pg/mL) showed no significant difference from just olanzapine treated ones. It may imply that initial effect of metformin on serum leptin levels may be more pronounced compared to the latter effect. Besides, even though no difference was detected between CTRL 1 group (239.4 $\pm$ 47.33pg/mL) and OLA 1 group, fat

accumulation around the internal organs of OLA 1 group animals were observed to be quite high compared CTRL 1 animals (Figure 3-4).

In general, leptin levels are elevated in patients treated with antipsychotics which are thought to be due to increased weight as an outcome of the treatment (Lee & Bishop, 2011; Jin *et al.*, 2008). On the other hand, from different rat studies differing results were reported. After chronic olanzapine administration for 20 days on mice (Albaugh *et al*., 2006), and following olanzapine administration for 9 weeks to Wistar rats (Zugno *et al*., 2011), circulatory leptin levels were reported to rise significantly. In contrast, it was reported that no significant increase observed in serum leptin levels of rats following 6-day olanzapine treatment (Ferno *et al*. 2011). Similarly, Cooper *et al*. 2005 found no difference in circulating leptin levels in olanzapine-treated female Wistar rats after a 3-week period. In addition, study conducted by Sezlev *et al*. 2012 with male Wistar rats with 4-weeks olanzapine administration also resulted in no difference in leptin levels compared to controls. In this study, olanzapine administered rats have higher leptin levels compared to metformin and olanzapine co-administered ones. The variation observed among the reported results most probably due to differences in drug amounts, durations and animal types. Metformin treatment significantly decreases leptin levels in human which was confirmed by several studies (Kadhim *et al*., 2012; Fruehwald-Schultes, *et al.*, 2002; Glueck, *et al.*, 2001), even though some observed no change (Adamia *et al.*, 2007). It was also observed that metformin treatment of rat primary adipocytes resulted in inhibition of leptin secretion (Mick *et al*. in 2000). Moreover, it was shown that serum leptin levels were reduced by metformin treatment in HFD received rats compared to controls (Kim *et al*. 2006). The findings in our study related to metformin treatment were in accordance with the previous studies. Statistical significance in OLA1 vs OLA 2 group but not in CTRL 1 vs CTRL 2 group might have implied that the potency of metformin action on leptin levels was higher in olanzapine treatment than only metformin treatment. It may be also said that olanzapine related increase in circulating leptin

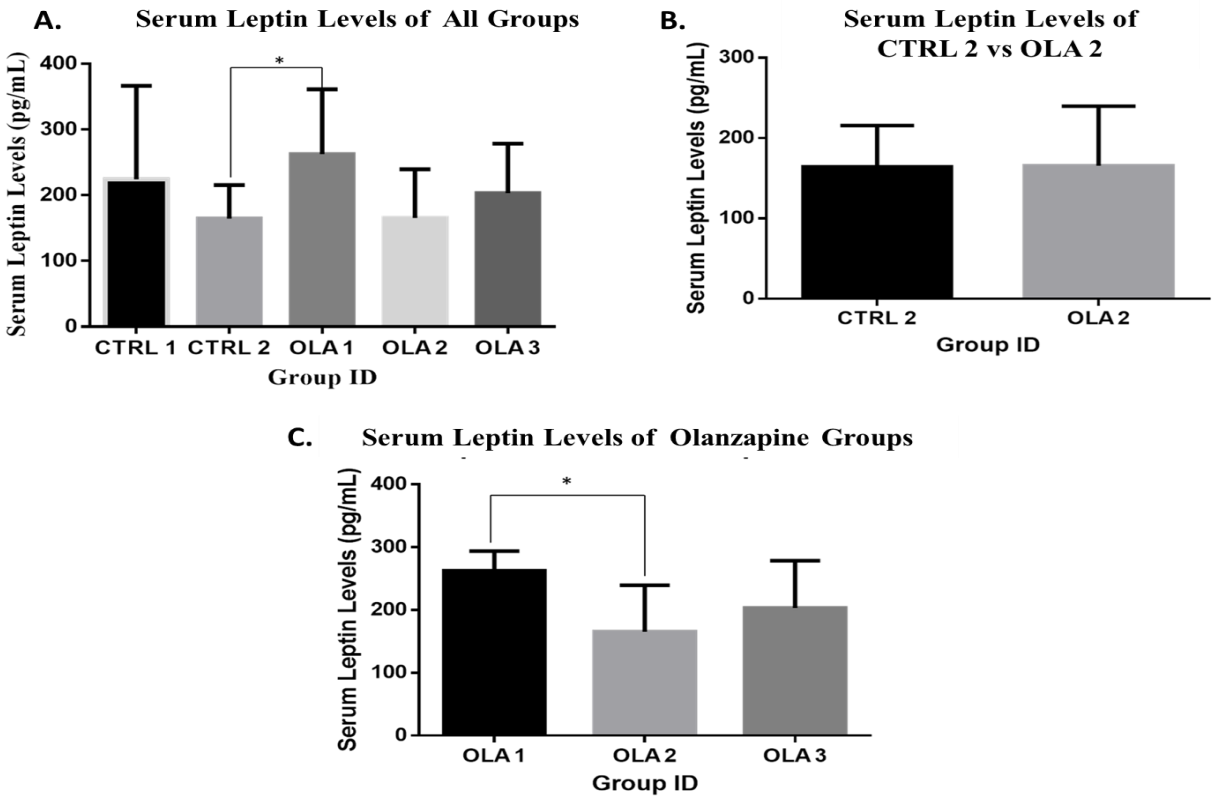

Figure 3-7 Serum leptin levels. A. Analysis results of one-way ANOVA applied to all groups. B. Analysis results of unpaired t-test applied to CTRL 2 and OLA 2. C. Analysis results of one-way ANOVA applied to all olanzapine groups. * $p < 0.05$. The values indicated as Mean + SEM.

amount was reduced back to the original levels by the action of metformin (Figure 3-6.B/C).

3.3 EXPRESSION STUDIES

3.3.1 RNA Sample Concentrations and Qualities

Nucleic acid concentrations and absorbance ratios of RNA samples were recorded as in Table C-1 and C-2 (Appendix C). All the RNA samples' 260/280 and 260/230 absorbance ratios indicated that the samples were pure and free from contamination or proteins, phenol, or other contaminants except C4R3 and C6R2. Those 2 samples' 260/230 ratios were lower than expected. That was probably indicated presence of carry over solutions such as phenol, ethanol and other contaminants etc.

As mentioned earlier in the section 2.3.5, measurement of concentrations and the absorbance ratios of the samples were not enough to assess integrity of the RNA and gDNA contamination of the samples; therefore, qualities of samples were also checked by running in agarose gels and visualization (Appendix D). In general, what is expected from an agarose gel result of the total RNA sample of a eukaryotic organism is to observe the most abundant mRNAs as descriptive bands for the RNA quality. Since the most abundant RNA type of in all cells were ribosomal RNA (rRNA), 28S, 18S and 5S rRNA bands were used to assess the integrity of eukaryotic RNA samples. Specifically, 28S band is expected to be 2 times more intense compared to 18S band when visualized for an intact RNA sample. The integrity of the rat samples for this study was evaluated to be in desired shape except 1 sample from CTRL 2 group which was highly degraded (C6R2) (Figure D-3 in Appendix D) which was removed from the experimental

group. Another important point was to evaluate gDNA contamination for the quality of the total RNA samples. Since gDNA is heavier than the RNAs, in the gel it was expected to be either closer to or stuck in the wells. In the gels, DNA bands were present in the RNA samples when run immediately after the isolation (Figure D-1 – D-6 upper lanes); therefore, a rigorous DNase treatment was applied to clean DNA contamination (Figure D-1 – D-6 lower lanes). In addition, since a heavy DNA contamination was observed in some samples, every sample was treated with DNase. Except C6R2 all RNA samples were considered as having good quality and used in RT-qPCR experiments.

3.3.2 RT-qPCR Results

3.3.2.1 Standard Curves

Figure E-1, shows the standard curve constructed for rat *GAPDH* reaction. The efficiency of the reaction was found to be 0.99 at 1/50 – 1/800 dilution interval. In all gene expression experiments standard curve graphs X axis shows concentration and Y axis shows CT values. In addition, Figure E-2 shows the reaction curves and melt curves. The melt curve (Figure E-2.B) shows a sharp peak around 82.5 ^{o}C indication of the target species of cDNA being amplified. However, looking at the background noise and merged shoulder at lower Tm values, possibility of presence of minor non-specific amplifications or primer dimer formations were considered. If the wave-like peaks at lower temperatures were due to primer-dimer formations, those broad peaks should be much higher in NTC samples owing to the lack of a cDNA template to compete with binding. Nevertheless, the melt curve of the NTC showed that background was almost absent. On the other hand, if it was due to gDNA contamination and non-specific amplification, then the higher waves would have been observed in the no RT control, again due to absence of competing

cDNA. Furthermore, since primers were intron-spanning, it would be unfavorable for the *Taq* polymerase to amplify them due to quite long product sizes. To observe whether there was specific amplification of the target region or nonspecific products, the RT-qPCR products were run in the agarose gel (Figure E-3), only a single type of band at the expected target amplicon size (92bp) from each reaction was observed which confirm the specific amplification. Although it was not detected in the gel image, the observed shoulder may have been due to the background coming from the possible non-specific or/and undetectable amplifications. Also, the noRT control did not give any peak in the melt curve or cross the threshold during the reaction which implies no gDNA amplification occurred even if it had been present. Similarly, the NTC control did not show a detectable amplification or a melt peak indicating there was not DNA contamination in the used reagents and water.

Standard curve constructed for the rat *POMC* reaction was shown in Figure E-4. The efficiency of the reaction was found to be 0.97 at 1/50 – 1/200 dilution interval. Figure E-5 shows the reaction curves and melt curves. The single peak around 85^{o}C in melt curve showed one type of DNA being amplified, which was proven in the agarose gel image of the RT-qPCR products which matched the expected amplicon size of 80bp (Figure E-6). However, the same background peaks were also observed on the melt curve as in *GAPDH*, but again, the band around expected target amplicon size in the agarose gel image was found to be specific enough. In addition, there was no peak for noRT and NTC controls during the melt analysis and no Ct value during the reaction so that it can be concluded no detectable amplicon for gDNA was present.

Figure E-7 shows standard curve constructed for the rat *NPY* reaction. The efficiency of the reaction was found to be 0.95 at 1/50 – 1/800 dilution interval. Figure E-8 shows the reaction curves and melt curves. The melting temperature of the target product was around 83 ^{o}C; however, as in other melt curves, the

background peaks were observed. The single amplicon bands around the expected amplicon size, 89bp, were detected (Figure E-9). Neither no RT control nor NTC did give peaks in melt curve nor Ct values during the reaction which indicated no DNA contamination of gDNA contribution.

The reaction and melt curves for *GAPDH, POMC* and *NPY* of all the samples were depicted in Appendix E.

3.3.2.2 *NPY* and *POMC* Expression Results

Fold change analysis results of the *NPY* gene expression and the *POMC* gene expression are presented on Figure 3-7 and Figure 3-8, respectively. In addition, all of the Ct values can be found in Appendix E. The *NPY* levels were unexpectedly found to be significantly down regulated for all groups (Figure 3-7.A). On the other hand, *POMC* expressions were significantly down regulated in all olanzapine groups compared to CTRL 1 (Figure 3-8.A) since olanzapine may induce feeding through inhibition of POMC neuron action.

In Figures 3-7.B/C and 3-8. B/C, each group was compared with their own controls. Specifically, olanzapine caused 2.2 fold increase of the NPY expression in combination with metformin treatment (OLA2) compared to only metformin treatment (CTRL 2). That was parallel to the findings of Huang et al.2006, Ferno et al.2011 and Weston-Green et al.2012, but oppose to the unchanged NPY levels reported by Davoodi et al.2009 and Guesdon et al.2010. However, the longest studies were up to 2-weeks (Weston-Green et al. 2012 and Gueston et al.2010). Based on our data, olanzapine may act on the NPY neurons to stimulate the NPY expression and protein levels so that the food intake may increase. However, it might also imply that metformin cannot normalize the olanzapine-induced increase

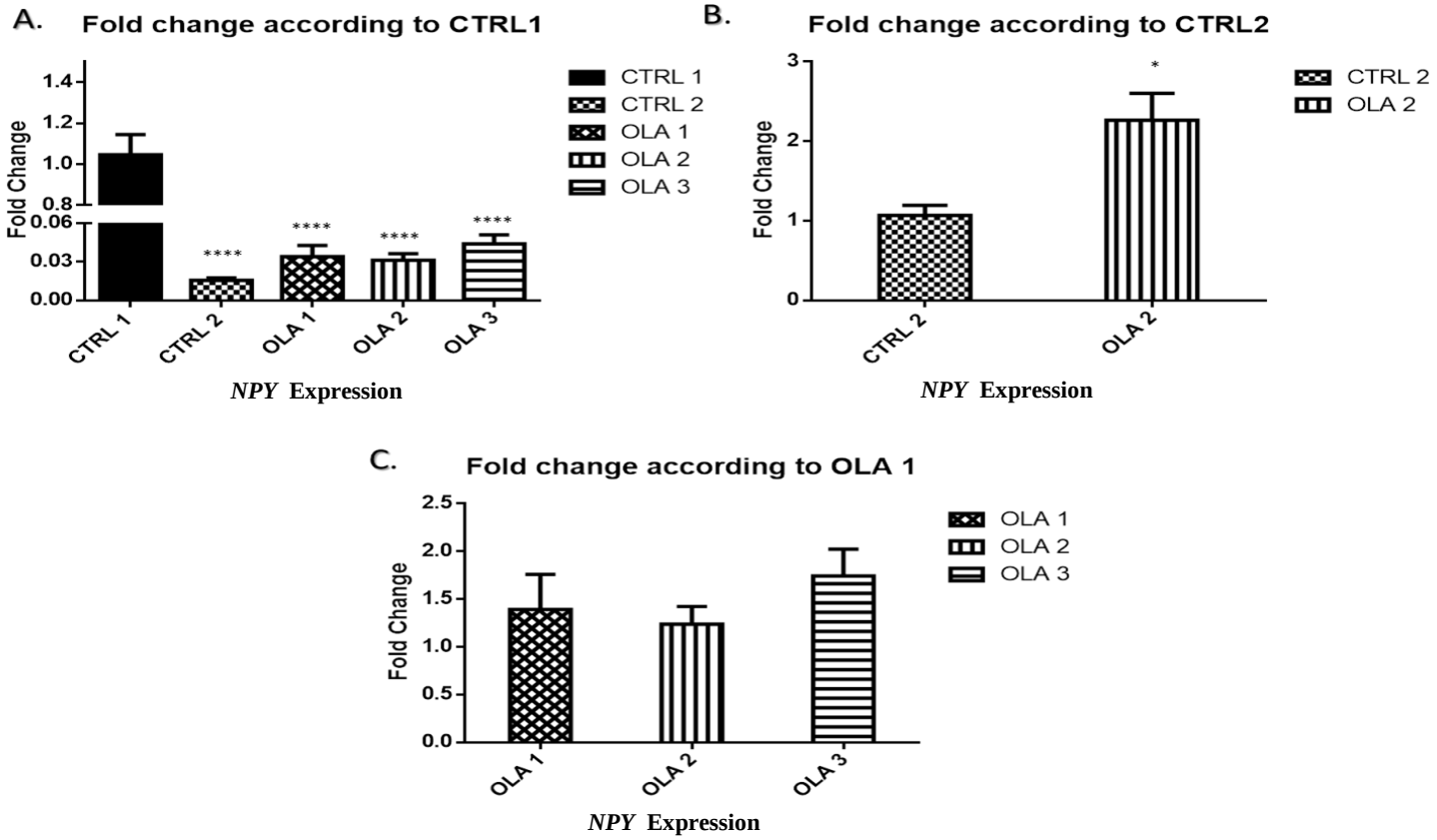

Figure 3-9 Fold change of the *NPY* expressions in all groups A. Analysis results of one-way ANOVA applied to all groups. B. Analysis results of unpaired t-test applied to CTRL 2 and OLA 2 groups. C. Analysis results of one-way ANOVA applied to all olanzapine groups. * $p<0.05$, **** $p<0.0001$. The values indicated as Mean $\pm$ SEM.

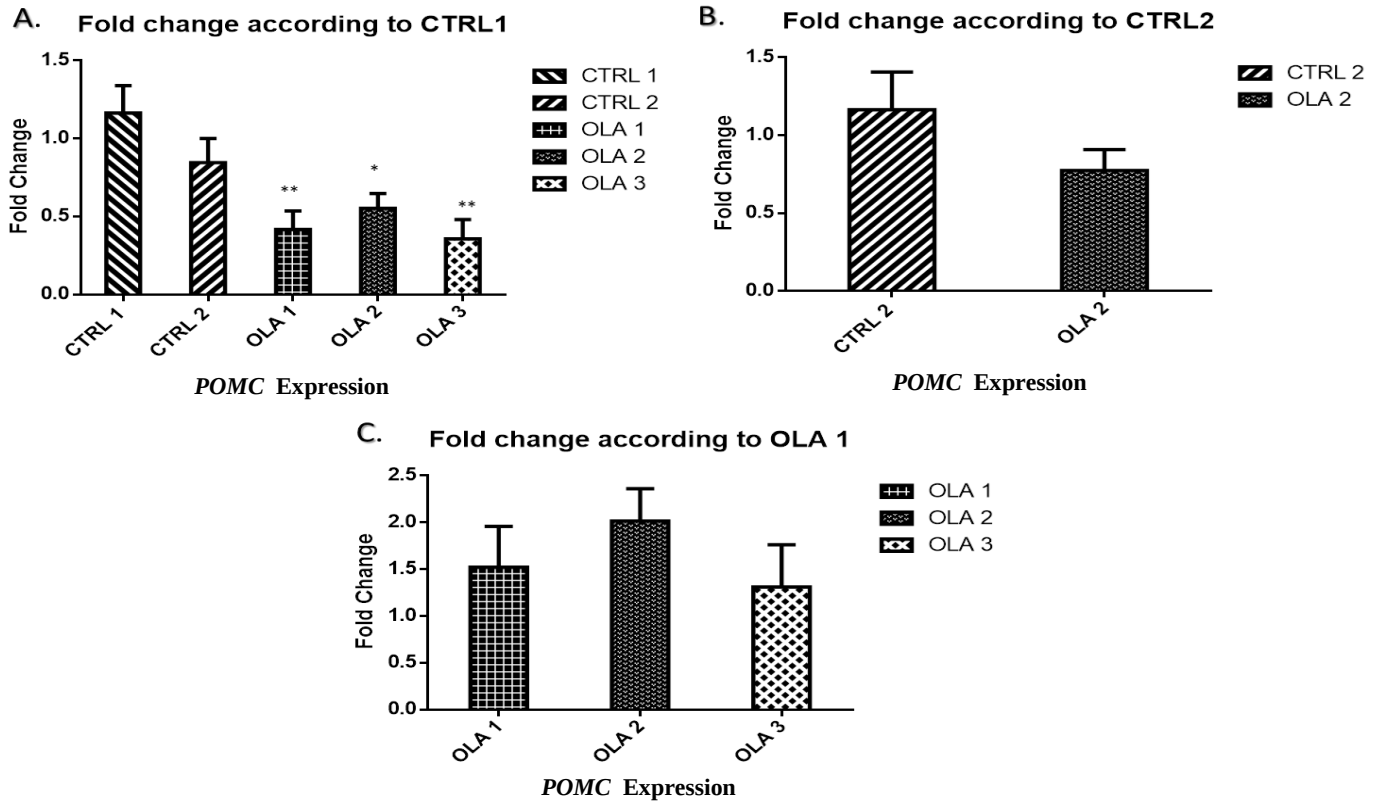

Figure 3-8 Fold change of *POMC* expressions in all groups. A. Analysis results of one-way ANOVA applied to all groups. B. Analysis results of unpaired t-test applied to CTRL 2 and OLA 2 groups. C. Analysis results of one-way ANOVA applied to all olanzapine groups * $p<0.05$, ** $p<0.005$. The values indicated as Mean $\pm$ SEM

in the *NPY* levels. That could also be observed clearly when olanzapine groups were compared to each other, which yielded no significant change in the *NPY* expression (Figure 3-8.C). When the grouped analysis results of *POMC* levels were considered, none of the results reached the statistical significance. The interesting point was the tendency of increasing *NPY* and decreasing *POMC* levels in OLA 3 group compared to decreasing *NPY* and increasing *POMC* levels in OLA 2 which might indicate that in the long term metformin exposure, the inhibitory effect of metformin on appetite could be lost. That observation also correlated with the meal size results with the sharper decrease observed in the OLA 2 group compared to OLA 3 group (Figure 3-1) as well as the circulating leptin levels (Figure 3-6). On the other hand, significant result obtained from the comparison of *NPY* levels of OLA 2 and CTRL 2 did not correlate with the meal size difference (Figure 3-2) and weight gain results (Figure 3-3) which did not differ from each other. It is possible that the expressed gene levels might have not been reflected to NPY and POMC protein levels so that no difference was seen in the overall phenotype. Another possibility was the peripheral actions of metformin may have cope with the effect of increased NPY and decreased POMC levels on appetite. In addition, body fat and muscle composition did not evaluated in this study changes of which might be another reason for uncorrelated expression and body weight results.

Animal studies conducted on the metformin treatment of olanzapine-induced weight gain were quite recent. In addition, although there are implications of the metformin action on CNS in the literature, the researches up to now only focused on the peripheral actions of metformin treatment opposing the weight gain side effect of olanzapine. In the current study, a potential angle for the direct opposing action of metformin on CNS to olanzapine was investigated for the first time. It is possible that metformin action on POMC/CART and NPY/AgRP neurons in the ARC opposes the olanzapine action on the same neurons so that it can inhibit stimulation of food intake by olanzapine. In this study, 2 focuses, hypothalamic

NPY and *POMC* expression levels were chosen due to the fact that after the integration of triggered potential intracellular signal pathways by metformin and olanzapine, the final response of those neuron populations to control the appetite is expression and release of those neuropeptides. In addition, although the changes in expression levels were determined, protein levels of them are under investigation to confirm changed expression levels at the protein level.

There were significant outcomes related to metformin administration time during olanzapine treatment. In order to understand mechanisms acting in those neurons to result in *NPY* and *POMC* expression level changes, the expression and protein levels as well as the activation/inhibition modifications of possible molecules in the triggered pathways by metformin and olanzapine may be further studied. For instance, it was shown that metformin increases leptin receptor expression in the ARC (Aubert *et al.*, 2011), which could be one of the contributing actions. Moreover, since metformin is known to increase STAT3 phosphorylation which is also at the downstream of the leptin signaling pathway could be another path for future directions. Furthermore, AMPK is a strong candidate for investigation because not only it is known to activated by metformin (Duan, *et al.*, 2013), but also sub-chronic administered olanzapine was shown to inhibit AMPK (Ferno, *et al.*, 2011). Moreover, metformin may mimic the ghrelin-induced activation of AMPK in NPY neurons (Andrews, 2011) so that it may decrease NPY levels which are stimulated by olanzapine. In addition, the pathway may also merged at the level of PKA as it is present in downstream pathway of 5-HT1B receptor (Ohno *et al.*, 2013) and metformin is known to decrease activity of PKA in liver (Pernicova & Korbonits, 2014). Another possibility is interaction at downstream of 5-HT2C receptor downstream, since there are indications of 5-HT2C receptor relation to drug-induced weight gain (Reynolds & Kirk, 2010), especially in terms of polymorphisms (Zhang & Malhotra, 2011). To sum up, there are several possible molecules that might be investigated and involved in intracellular

pathways for the total impact of olanzapine and metformin in the hypothalamus in the preceding studies.

To our knowledge, it was the first animal study to compare the impact of the starting time of metformin intake on efficacy of its action. As can be interpreted from the overall results, metformin prescription following the chronic olanzapine administration could have more pronounced effects on appetite compared to co-administration with olanzapine from the start. On the other hand, abdominal fat accumulation was observed to be less when metformin was co-administration with olanzapine from the start. Nevertheless, since the significant weight gain side effect was not observed in all patients (Teff & Kim, 2011; Zhang & Malhotra, 2011) it might better to follow up olanzapine treatment for a short while and then prescribe metformin if the weight gain is observed.

There were some limitations in the study. First of all, total body adiposity of the animals could not be determined, which could have been found out by use of nuclear magnetic resonance (NMR) spectroscopy. However, instead of that, it was tried to be estimated by the serum parameters and subjective observations. That was because of the instrument unavailability for the animal scanning purpose. In addition, the only available food was standard chow diet. However, the food choice may be another contributed factor for the increase in weight due to elevated appetite (van der Zwaal *et al.*, 2014) and, in fact, it was reported that when the rats were supplied with food choices, they preferred both carbohydrate rich and fat rich food upon continues NPY injection into the brain (Beck, 2006). Since the ARC is merely a subgroup of neurons in the hypothalamus, the contribution from other hypothalamic nuclei could not be ruled out from the results. However, the main populations of hypothalamic NPY and POMC neurons are located in the ARC and send projections to the other parts and brain regions (King, Hentges, & ST, 2011) (van den Heuvel, *et al.*, 2014); therefore, it was assumed that the isolated *POMC* and *NPY* mRNAs came from the ARC. Another limitation lies in the number of

animals and high intragroup variations as also observed in other studies (van der Zwaal *et al.*, 2014). In order for the results to reflect changes in humans, rats were bought as outbreeds. Although that was the most plausible choice, the used numbers might have not been enough for the power of the test.

CHAPTER 4

CONCLUSIONS AND FUTURE DIRECTIONS

- Metformin was found to be effectively decreasing the appetite and that effect may be more pronounced when co-administered with olanzapine. However, that effect was not reflected on the total body weights, but observed as decreased abdominal fat in olanzapine groups treated with metformin. On the other hand, olanzapine was found to have no effect on appetite. In accordance with that, the total body weight results did not differ between olanzapine and the main control group, but only olanzapine treated animals were observed to have increased abdominal fat compared to the control groups.

- Serum triglyceride levels were found to be unaffected by both olanzapine and metformin treatments. On the other hand, circulating leptin levels implies that effect of metformin on leptin levels under chronic olanzapine treatment may be more pronounced initially and that effect might be lost with the prolonged metformin administration. That was also supported by meal size results with the sharper decrease observed in the OLA 2 group compared to OLA 3 group, and by the reverse pattern observed in *NPY* and *POMC* levels in OLA 2 and OLA 3. Moreover, metformin administration

might decrease the olanzapine-related increase of leptin levels to the control levels which may be due to the decreased adiposity by metformin action. However, the abdominal fat depositions were observed to be the least in the longer metformin administered group (OLA 3). Therefore, the decision to start metformin at which point should be thought thoroughly. Nevertheless, since the weight gain side effect was not observed in all patients, it might better to follow up olanzapine treatment for a short while and then prescribed metformin if the weight gain is observed.

- Olanzapine has a high affinity for 5-HT2C receptors (Eli Lilly, 2013) which are also found on POMC neurons in the ARC (Berglund, *et al.*, 2013). In addition, serotonin acts on POMC neurons resulting in increased α-MSH levels and inhibit food intake (Berglund, *et al.*, 2013). In addition, 5-HT2C antagonists were shown to increase feeding (Reynolds & Kirk, 2010) and systemic KO of 5-HT2C resulted in increased feeding and weight gain (Tecott, *et al.*, 1995). Therefore, the olanzapine antagonism for 5-HT2C receptors on POMC neurons could also interfere with the intracellular signaling so that *POMC* expressions may decrease which might diminish the POMC-control on feeding. 5-HT1B receptors are found on NPY neurons in the ARC and agonists of them inhibit NPY neurons while antagonists have positive impact on food consumption (Heisler, *et al.*, 2006). Hence, although the affinity of olanzapine to 5-HT1B receptors is low (Eli Lilly, 2013), still antagonism on 5-HT1B may also contribute to olanzapine-induced weight gain. Those possibilities may be investigated in the future studies.

- Since POMC and NPY are not the only hypothalamic neuropeptides involve in energy regulation, other potent peptides, namely AgRP and CART, may be studied, too. In addition, protein levels of the studied peptides should be

determined to accurately estimate the total impact of metformin-olanzapine co-treatment on the ARC neurons.

- There may be many possible players of metformin action in the brain to reverse food intake induction by olanzapine. Still an overall model was hypothesized from the results of the current study (Figure 4-1).

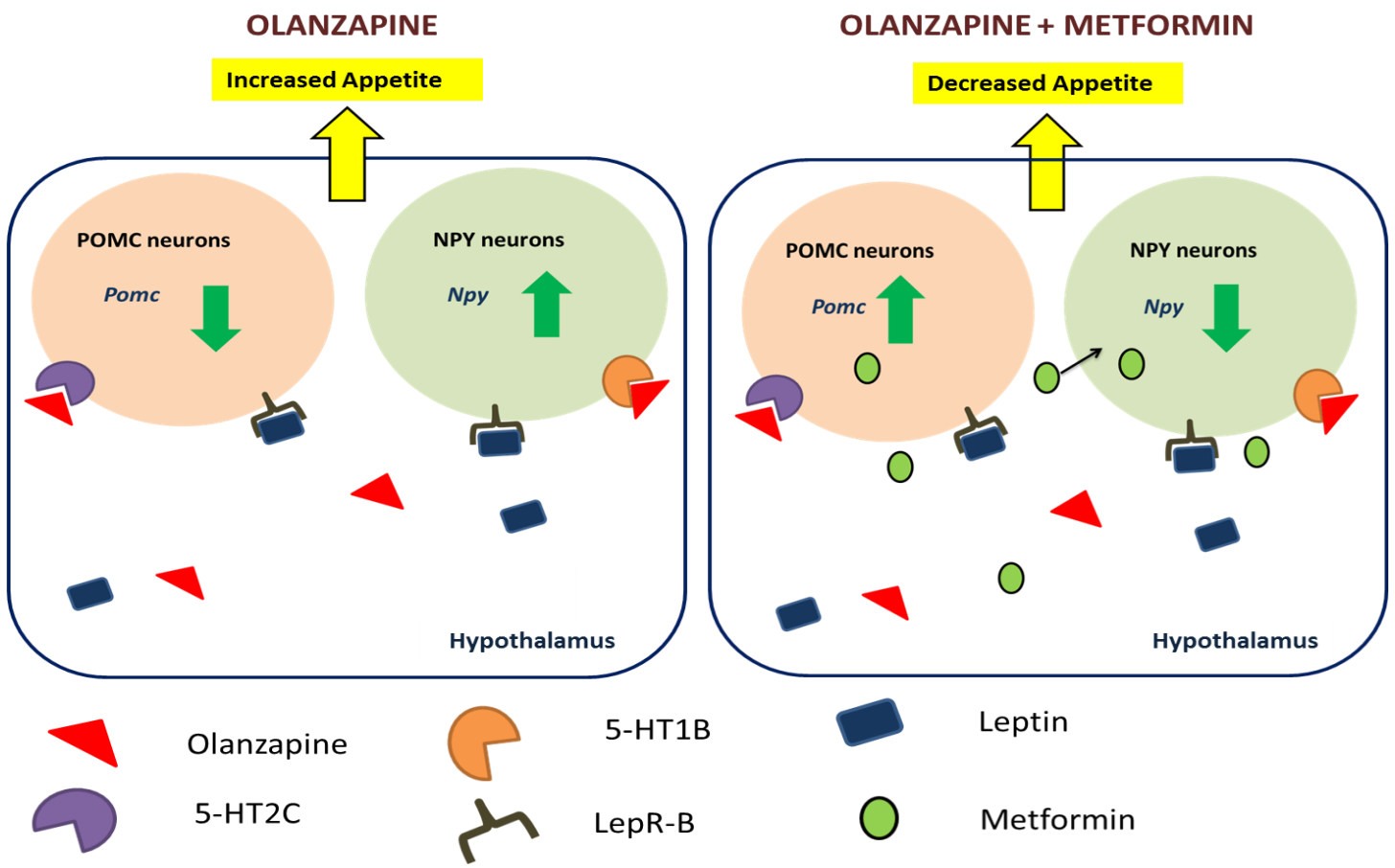

Figure 4-1 Proposed effects of olanzapine and metformin co-administration on hypothalamic POMC and NPY neurons

REFERENCES

Adamia, N., Virsaladze, D., Charkviani, N., Skhirtladze, M., & Khutsishvili, M. (2007). Effect of metformin therapy on plasma adiponectin and leptin levels in obese and insulin resistant postmenopausal females with type 2 diabetes. *Georgian Medical News*, 52-55.

Ak, M., Sezlev, D., Sutcigil, L., Akarsu, S., Ozgen, F., & Yanik, T. (2013). The investigation of leptin and hypothalamic neuropeptides role in first attack psychotic male patients: Olanzapine monotherapy. *Psychoneuroendocrinology*, 341-347.

Albaugh, V., Henry, C., Bello, N., Hajnal, A., Lynch, S., Halle, B., *et al.* (2006). Hormonal and metabolic effects of olanzapine and clozapine related to body weight in rodents. *Obesity*, 36-51.

Andino, L., Ryder, D., Shapiro, A., Matheny, M., Zhang, Y., Judge, M., *et al.* (2011). POMC overexpression in the ventral tegmental area ameliorates dietry obesity. *Journal of Endocrinology*, 199-207.

Andrews, Z. (2011). Central mechanisms involved in the orexigenic actions of ghrelin. *Peptides*, 2248-2255.

Aravagiri, M., Teper, Y., & Marder, S. (1999). Pharmacokinetics and tissue distribution of Olanzapine in rats. *Biopharmaceutics and Drug Disposition*, 369-377.

Aubert, G., Mansuy, V., Voirol, M.-J., Pellerin, L., & Pralong, F. P. (2011). The anorexigenic effects of metformin involve increases in hypothalamic leptin receptor expression. *Metabolism Clinical and Experimental*, 327-334.

Baptista, T., Martinez, J., Lacruz, A., Rangel, N., Beaulieu, S., Serrano, A., *et al.* (2006). Metformin for prevention of weight gain and insulin resistance with olanzapine: a double-blind placebo-controlled trial. *Canadian Journal of Psychiatry*, 192-196.

Baptista, T., Rangel, N. F., El Fakih, Y., Uzcátegui, E., Galeazzi, T., Gutiérrez, M., *et al.* (2007). Metformin as an adjunctive treatment to control body weight and metabolic dysfunction during olanzapine administration: a multicentric, double-blind, placebo-controlled trial. *Schizophrenia Research*, 99–108.

Beck, B. (2006). Neuropeptide Y in normal eating and in genetic and dietary-induced obesity. *Philosophical Transactions of the Royal Society Biological Sciences*, 1159-185.

Belgardt, B. F., Okamura, T., & Brüning, J. C. (2009). Hormone and glucose signalling in POMC and AgRP neurons. *The Journal of Physiology*, 5305-5314.

Berglund, E., Liu, C., Sohn, J., Liu, T., Kim, M., Lee, C., *et al.* (2013). Serotonin 2C receptors in pro-opiomelanocortin neurons regulate energy and glucose homeostasis. *The Journal of Clinical Investigation*, 5061-5070.

Block, L., Schemling, L., Couto, A., Mourao, S., & Bresolin, T. (2008). Pharmaceutical equivalance of metformin tablets with various binders. *Journal of Basic and Applied Pharmaceutical Sciences*, 29-35.

Borgers, A., Koopman, K., Bisschop, P., Serlie, M., Swaab, D., Fliers, E., *et al.* (2014). Decreased serotonin transporter imminoreactivity in the human hypothalamic infundibular nucleus of overweight subjects. *Frontiers in Neuroscience*, 8:106; doi: 10.3389/ fnins.2014.00106.

Boyda, H., Procyshyn, R., Asiri, Y., Wu, C., Wang, C., Lo, R., *et al.* (2014). Antidiabetic drug combination treatment for glucose intolerance in adult female rats treated acutely with olanzapine. *Progress in Neuro-Physchopharmacology & Biological Physchiatry*, 170-176.

Boyda, H., Procyshyn, R., Tse, L., Hawkes, E., Jin, C., Pang, C., *et al.* (2012). Differential effects of 3 classes of antidiabetic drugs on olanzapine-induced glucose dysregulation and insulin resistance in female rats. *Journal of Psychiatry & Neuroscience*, 407-415.

Bristol-Mayers Squibb Company. (2013, November 13). *US Food and Drug Administration (FDA).* Retreived on June 23, 2014 from FDA Approved Drug Products - Glucophage (metformin hydrocloride) Label Information:

http://www.accessdata.fda.gov/scripts/cder/drugsatfda/index.cfm?fuseaction=Search.Label_ApprovalHistory#labelinfo

Brown, L., & Clegg, D. (2010). Central effects of estradiol in the regulation of adiposity. *The Journal of Steroid Biochemistry and Molecular Biology*, 65-73.

Burcelin, R., Brunner, H., Seydoux, J., Thorens, B., & Pedrazzini, T. (2001). Increased insulin concentrations and glucose storage in neuropeptide Y Y1 receptor-deficient mice. *Peptides*, 421-427.

Bustin, S. B., Garson, J., Hellemans, J., Huggett, J., Kubista, M., Mueller, R., *et al.* (2009). The MIQE guidelines: minimum information for publication of quantitative real-time PCR experiments. *Clinical Chemistry*, 611-622.

Chau-Van, C., Gamba, M., Salvi, R., Gaillard, R. C., & Pralong, F. P. (2007). Metformin inhibits Adenosine 5'-Monophosphate-Activated Kinase activation and prevents increases in Neuropeptide Y expression in cultured hypothalamic neurons. *Endocrinology*, 507-511.

Chen, X., Margolis, K., Gershon, M., Schwartz, G., & Sze, J. (2012). Reduced serotonin reuptake transporter function causes insulin resistance and hepatic steatosis independent of food intake. *PLOS ONE*, 7(3): e32511; doi: 10.1371/journal.pone.0032511.

Cittadini, A., Napoli, R., Monti, M., Rea, D., Longobardi, S., Netti, P., *et al.* (2012). Metformin prevents the development of chronic heart failure in the SHHF rat model. *Diabetes*, 944-953.

Cooper, G., Pickavance, L., Wilding, J., Halford, J., & Goudie, A. (2005). A parametric analysis of olanzapine-induced weight gain in female rats. *Psychopharmacology*, 80-89.

Correll, C., Lencz, T., & Malhotra, A. (2011). Antipsychotic drugs and obesity. *Trends in Molecular Medicine*, 97-107.

Cota, D., Proulx, K., Smith, K. A., Kozma, S. C., Thomas, G., Woods, S. C., *et al.* (2006). Hypothalamic mTOR signaling regulates food intake. *Science*, 927-930.

Cowley, M., Smart, J., Rubinstein, M., Cerdan, M., Diano, S., Horvath, T., *et al.* (2001). Leptin activates anorexigenic POMC neurons through a neural network in the arcuate nucleus. *Letters to Nature*, 480-484.

Crespo, S. C., Cachero, A. P., Jimenez, L. P., Barrios, V., & Ferreiro, E. A. (2014). Peptides and food intake. *Frontiers in Endocrinology*, 5:58.

Dann, S. G., Selvaraj, A., & Thomas, G. (2007). mTOR complex1-S6K1 signaling: at the crossroads of obesity, diabetes and cancer. *Trends in Molecular Medicine*, 252-259.

Davoodi, N., Kalinichev, M., Korneev, S., & Clifton, P. (2009). Hyperphagia and increased meal size are responsible for weight gain in rats treated sub-chronically with olanzapine. *Psychopharmacology*, 693-702.

De Jonghe, B., Hayes, M. R., & Bence, K. K. (2011). Melanocortin control of energy balance: Evidence from rodent models. *Cellular and Molecular Life Sciences*, 2569-2588.

Delgado, T. (2013). Glutamate and GABA in appetite regulation. *Frontiers in Endocrinology*, 4:103; doi: 10.3389/fendo.2013.00103.

Dorak, M. (2006). *Real-Time PCR.* New York: Taylor & Francis Group.

Dores, R. M., Londraville, R. L., Prokop, J., Davis, P., Dewey, N., & Lesinski, N. (2014). Melanocortin/melanocortin receptors. *Journal of Molecular Endocrinology*, T29-T42.

Duan, Y., Zhang, M., Sun, L., Dong, S., Wang, G., Zhang, J., *et al.* (2013). Metformin inhibits food intake and Neuropeptide Y gene expression in the hypothalamus. *Neural Regeneration Research*, 2379-2388.

Eli Lilly. (2013, July 26). *US Food and Drug Administration (FDA).* Retrieved on June 23, 2014 from FDA Approved Druf Products - Zyprexa (Olanzapine) label information: http://www.accessdata.fda.gov/scripts/cder/drugsatfda/index.cfm?fuseaction=Search.Label_ApprovalHistory

FDA Center for Drug Evaluation and Research. (1999). *Office of Clinical Pharmacology and Biopharmaceutics Review(s) - Olanzapine / Zyprexa.* Silver Spring: US Food and Drug Administration (FDA).

Fernandez, E., Carrizo, E., Fernandez, V., Connell, L., Sandia, I., Prieto, D., *et al.* (2010). Polymorphisms of the LEP and LEPR genes, metabolic profile after prolonged clozapine administration and response to antidiabetic metformin. *Schizophrenia Research*, 213-217.

Ferno, J., Varela, L., Skrede, S., Vazquez, M., Nogueiras, R., Dieguez, C., *et al.* (2011). Olanzapine-induced hyperphagia and weight gain associate with orexigenic hypothalamic neuropeptide signaling without concomitant AMPK phosphorylation. *PLOS ONE*, 6(6): e20571; doi: 10.1371/journal.pone.0020571.

Fleige, S., & Pfaffl, M. (2006). RNA integrity and the effect on the real-time qRT-PCR performance. *Molecular Aspects of Medicine*, 126-139.

Fountaine, R., Taylor, A., Mancuso, J., Greenway, F., Byerley, L., Smith, S., *et al.* (2010). Increased food intake and energy expenditure following administration of olanzapine to healthy men. *Obesity*, 1646-1651.

Fruehwald-Schultes, B., Oltmanns, K., Toschek, B., Sopke, S., Kern, W., Born, J., *et al.* (2002). Short-term treatment with metformin decreases serum leptin concentration without affecting body weight and body fat content in normal-weight healthy men. *Metabolism*, 531-536.

Gantz, I., & Fong, T. M. (2003). The melanocortin system. *American Journal of Physiology Endocrinology and Metabolism*, E468-474.

Geerling, J., Boon, M., van der Zon, G., van den Berg, S., van den Hoek, A., Lombes, M., *et al.* (2014). Metformin lowers plasma triglycerides by promoting VLDL-triglyceride clearance by brown adipose tissue in mice. *Diabetes*, 880-891.

Genne-Bacon, E. (2014). Thinking evolutionarily about obesity. *Yale Journal of Biology and Medicine*, 99-112.

Glueck, C., Fontaine, R., Wang, P., Subbiah, M., Weber, K., Illig, E., *et al.* (2001). Metformin reduces weight, centripetal obesity, insulin, leptin, and low-density lipoprotein cholesterol in nondiabetic, morbidly obese subjects with body mass index greater than 30. *Metabolism - Clinical and Experimental*, 856–861.

Gonzalez-Campoy, J., Richardson, B., Richardson, C., Gonzalez-Cameron, D., Ebrahim, A., Strobel, P., *et al.* (2014). Bariatric endocrinology: principles of medical practice. *International Journal of Endocrinology*, [Epub] 12 pages.

Guesdon, B., Denis, R., & Richard, D. (2010). Additive effects of olanzapine and melanin-concenrating hormone agonism on energy balance. *Behavioral Brain Research*, 14-20.

Harvey, J., & Ogden, D. (2014). Obesity treatment in disadvantaged population groups: where do we stand and what can we do? *Preventive Medicine*, [in Press / Epub] 5 pages.

Heiling, M. (2004). The NPY system in stress, anxiety and depression. *Neuropeptides*, 213-224.

Heisler, L., Jobst, E., Sutton, G., Zhou, L., Borok, E., Thornton-Jones, Z., *et al.* (2006). Serotonin Reciprocally Regulates Melanocortin Neurons to Modulate Food Intake. *Neuron*, 239-249.

Hinney, A., Vogel, C., & Hebebrand, J. (2010). From monogenic to polygenic obesity: recent advances. *Child and Adolescent Psychiatry*, 297-310.

Hu, Y., Young, A., Ehli, E., Nowotny, D., Davies, P., Droke, E., *et al.* (2014). Metformine and berberine prevent olanzapine-induced weight gain in rats. *PLOS ONE*, 9(3): e93310; doi: 10.1371/journal.pone0093310.

Huang, X., Deng, C., & Zavitsanou, K. (2006). Neuropeptide Y mRNA expression levels following chronic olanzapine, clozapine and haloperidol administration in rats. *Neuropeptides*, 213-219.

Hummon, A., Lim, S., Difilippantonio, M., & Ried, T. (2007). Isolation and solubilization of proteins after TRIzol extraction of RNA and DNA from patient material following prolonged storage. *BioTechniques*, 467-472.

Ito, Y., Banno, R., Shibata, M., Adachi, K., Hagimoto, S., Hagiwara, D., *et al.* (2013). GABA type B receptor signaling in proopiomelanocortin neurons protects against obesity, insulin resistance, and hypothalamic inflammation in male mice on high-fat diet. *The Journal of Neuroscience*, 17166-17173.

Jablonski, K., McAteer, J., de Bakker, P., Franks, P., Pollin, T., Hanson, R., *et al.* (2010). Common variants in 40 genes assessed for diabetes incidence and response to metformin and lifestyle intervention in the diabetes prevention program. *Diabetes*, 2672-2681.

Jin, H., Meyer, J., Mudaliar, S., & Jeste, D. (2008). Impact of atypical antipsychotic therapy on leptin, ghrelin and adiponectin. *Schizophrenia Research*, 70-85.

Jonghe, B. C., Matthew, R. H., & Bence, K. K. (2011). Melanocortin control of energy balance: evidence from rodent models. *Cellular and Molecular Life Sciences*, 2569-2588.

Kadhim, K., Ismael, D., Khalaf, B., Hussein, K., Zalzala, M., & Hussain, S. (2012). Dose-dependent relationship between serum metformin levels and glycemic control, insulin resistance and leptin levels in females newly diagnosed with type 2 diabetes mellitus. *Journal of Diabetes Mellitus*, 179-185.

Kalariya, N., Shoeb, M., Ansari, N., Srivastava, S., & Ramana, K. (2012). Antidiabetic drug metfromin suppresses endotoxin-induced uveitis in rats. *Investigative Opthalmology & Visual Science*, 3431-3440.

Kim, J., Shon, E., Kim, C., & Kim, J. (2012). Renal podocyte injury in a rat model of type 2 diabetes is prevented by metformin. *Expermental Diabetes Research*, 9 pages; doi: 10.1155/2012/210821.

Kim, Y.-W., Kim, J.-Y., Park, Y.-H., Park, S.-Y., Won, K.-C., Choi, K.-H., *et al.* (2006). Metformin restores leptin sensitivity in high-fat-fed obese rats with leptin resistance. *Diabetes*, 716-724.

King, C., Hentges, & ST. (2011). Relative Number and Distribution of Murine Hypothalamic Proopiomelanocortin Neurons Innervating Distinct Target Sites. *PLOS ONE*, 6(10): e25864; doi:10.1371/journal.pone.0025864.

Klein, D., Cottingham, E., Sorter, M., Barton, B., & Morrison, J. (2006). A randomized, double-blind, placebo-controlled trial of metformin treatment of weight gain associated with initiation of atypic antipsychotic therapy in children and adolescents. *American Journal of Psychiatry*, 2072-2079.

Kravchuk, E., Grineva, E., Bairamov, A., Galagudza, M., & Vlasov, T. (2011). The effect of metformin on myocardial tolerance to ischemia-reperfusion injury in the rat model of diabetes mellitus type II. *Experimental Diabetes Research*, 5 pages; doi: 10.1155/2011/907496.

Kruger, N. (2002). The Bradford Method for Protein Quantitation. J. Walker in, *The Protein Protocols Handbook* (pg. second edition;15-21). New Jersey: Humana Press Inc.

Kurşungöz, C. (2012, August). Determination of hypothalamic neuropeptide levels involved in appetite regulation in atypical antipsychotic drug, Risperidone treatment. *Master Thesis submitted to Graduate School of Natural and Applied Sciences, METU*. Ankara, Turkey.

Lee, A., & Bishop, J. (2011). Pharmacogenetics of leptin in antipsychotic-associated weight gain and obesity-related complications. *Pharmacogenomics*, 999-1016.

Lee, C. K., Choi, Y. J., Park, S. Y., Kim, J. Y., Won, K. C., & Kim, Y. W. (2012). Intracerebroventricular injection of metformin induces anorexia in rats. *Diabetes and Metabolism Journal*, 293-299.

Lee, Y., & Jeong, J. (2011). A systematic review of metformin to limit weight-gain with atypical antipsychotics. *Journal of Clinical Pharmacy and Therapeutics*, 537-545.

Life Technologies Corporation. (2010). *Life Technologies.* Retreived on February 1, 2014 from Ambion, TRIzol Reagent : http://tools.lifetechnologies.com/content/sfs/manuals/trizol_reagent.pdf

Likhite, N., & Warawdekar, U. (2011). A unique method for isolation and solubilization of proteins after extraction of RNA from tumor tissue using trizol. *Journal of Biomolecular Techniques*, 37-44.

Livak, K., & Schmittgen, T. (2001). Analysis of relative gene expression data using real time quantitative PCR and the 2^-deltadelta Ct method. *Methods*, 402-408.

Lv, W.-s., Wen, J.-p., Li, L., Sun, R.-x., Wang, J., Xian, Y.-x., *et al.* (2012). The effect of metformin on food intake and its potential role in hypothalamic regulation in obese diabetic rats. *Brain Research*, 11-19.

Maayan, L., & Correll, C. (2010). Management of antipsychotic-related weight gain. *Expert Review of Neurotherapeutics*, 1175-1200.

Martire, M., Pistritto, G., Mores, N., Agnati, L., & Fuxe, K. (1995). Presynaptic A2-adrenoceptors and neuropeptide Y Y2 receptors inhibit [3H]noradrenaline release from rat hypothalamic synaptosomes via different mechanisms . *Neuroscience Letters*, 9-12.

Mick, G., Wang, X., Fu, C., & McCormick, K. (2000). Inhibition of leptin secretion by insulin and metformin in cultured rat adipose tissue. *Biochimica et Biophysica Acta*, 426-432.

Millington, G. W. (2007). The role of proopiomelanocortin (POMC) neurons in feeding behaviour. *Nutrient & Metabolism*, 4:18.

Mori, H., Inoki, K., Münzberg, H., Opland, D., Fauozi, M., Villanueva, E. C., *et al.* (2009). Critical role for hypothalamic mTOR activity in energy balance. *Cell Metabolism*, 362-374.

Morris, M., & Hansen, M. (2009). Orexigenic Peptides. G. Frühbeck in, *Peptides in Energy Balance and Obesity* (pg. 1-33). Oxfordshire; Cambridge: CAB International.

Morrison, J., Cottingham, E., & Barton, B. (2002). Metformin for weight loss in pediatric patients taking pschotropic drugs. *American Journal of Psychiatry*, 655-657.

Morton, G., Cummings, D., Baskin, D., Barsh, G., & Schwartz, M. (2006). Central nervous system control of food intake and body weight. *Nature Reviews*, 289-295.

Münzberg, H., Björnholm, M., Bates, S., & Mayers Jr, M. (2005). Leptin receptor action and mechanims of leptin resistance. *Cellular and Molecular Life Sciences*, 642-652.

Naftolin, F., Garcia-Segura, L., Keefe, D., Leranth, C., Maclusky, N., & Brawer, J. (1990). Estrogen effects on the synaptology and neural membranes of the rat hypothalamic arcuate nucleus. *Biology of Reproduction*, 21-28.

Nguyen, D., & El-Serag, H. (2010). The epidemiology of obesity. *Gastroenterology Clinics of North America*, 1-7.

Nogueiras, R., Weidmer, P., Perez-Tilve, D., Veyrat-Durebex, C., Keogh, J., Sutton, G., *et al.* (2007). The central melanocortin system directly controls peripheral lipid metabolism. *The Journal of Clinical Investigaton*, 3475-3488.

Ohno, Y., Shimizu, S., & Tokudome, K. (2013). Recent advances in 5-hydroxytryptamine (5-HT) receptor research: how many pathophysiological roles does 5-HT play via its multiple receptor subtypes? *Biological & Pharmaceutical Bulletin*, 1396-1400.

Papanastasiou, E. (2013). The prevalence and mechanisms of metabolic syndrome in schizophrenia: a review. *Theurapeutic Advances in Psychopharmacology*, 33-51.

Perboni, S., Ueno, N., Mantovani, G., & Inui, A. (2009). Anorexigenic Peptides. G. Frühbeck in, *Peptides in Energy Balance and Obesity* (pg. 33-61). Oxfordshire; Cambridge: CAB International.

Pernicova, I., & Korbonits, M. (2014). Metformin - mode of action and clinical implications for diabetes and cancer. *Nature Reviews Endocrinology*, 143-156.

Pfaffl, M. (2006). Relative Quantfication. M. Dorak in, *Real-Time PCR* (pg. 63-82). New York: Taylor & Francis Group.

Phizer. (2011, December 5). Olanzapine Phizer prospectus. Kent, United Kingdom: Pfizer Limited.

Picciotto, M. R., & Mineur, Y. S. (2013). Nicotine, food intake, and activation of POMC neurons. *Neuropsychopharmacology Reviews*, 245.

Pol, A. N. (2012). Nneuropeptide transmission in brain circuits. *Neuron*, 98-115.

Qiagen. (2009, November). Rotor-Gene Q User Manual. Germany: Qiagen.

Ranganathan, G., Unal, R., Pokrovskaya, I., Yao-Borengasser, A., Phanavanh, B., Lecka-Czernik, B., *et al*. (2006). The lipogenic enzymes DGAT1, FAS, and LPL in adipose tissue: effects of obesity, insulin resistance, and TZD treatment. *Journal of Lipid Research*, 2444-2450.

Reynolds, G., & Kirk, S. (2010). Metabolic side effects of antipsychotic drug treatment - pharmacological mechanisms. *Pharmacology & Therapeutics*, 169-179.

Sachdanandam, K., Hutchinson, J., Elgebaly, M., Mezzetti, E., Dorrance, A., Motamed, K., *et al.* (2009). Glycemic control prevents microvascular remodeling and increased tone in type 2 diabetes: link to endothelin-1. *American Journal of Physiology Regulatory Integrative and Comparative Physiology*, R952-R959.

Sasaki, T., & Kitamura, T. (2010). Roles of FoxO1 and Sirt1 in the central regulation of food intake. *Endocrine Journal*, 939-946.

Savontaus, E., Breen, T. L., Kim, A., Yang, L. M., Chua, S. C., & Wardlaw, S. L. (2004). Metabolic effects of transgenic melanocyte-stimulating hormone overexpression in lean and obese mice. *Endocrinology*, 3881-3891.

Schleimer, S., Johnston, G., & Henderson, J. (2005). Novel oral drug administration in an animal model of neuroleptic therapy. *Journal of Neuroscience Methods*, 159-164.

Schwartz, M. W., Woods, S. C., Porte Jr, D., Seeley, R. J., & Baskin, D. G. (2000). Central nervous system control of food intake. *Nature*, 661-671.

Sezlev, D. (2012, September 3). Alterations of hypothalamic neuropeptides involved in food intake and appetite in Olanzapine monotherapy. *Master Thesis submitted to Graduate School of Natural and Applied Sciences, METU*. Ankara, Turkey.

Sherafat-Kazemzadeh, R., Yanovski, S., & Yanovski, J. (2013). Pharmacotherapy for childhood obesity: present and future prospects. *International Journal of Obesity*, 1-15.

Sherson, E., Yakes, J., & Katalonos, N. (2014). A review of the use of the 5 A's model for weight loss counselling: differences between physician practice and patient demand. *Family Practice*, [Epub ahead of print] 1-10.

Stephenne, X., Foretz, M., Taleux, N., van der Zon, G., Sokal, E., Hue, L., *et al.* (2011). Metformin activates AMP-activated protein kinase in primary human hepatocytes by decreasing cellular energy status. *Diabetologia*, 3101-3110.

Taylor, B., Fu, W., Kuphal, K., Stiller, C., Winter, M., Chen, W., *et al.* (2014). Inflammation enhances Y1 receptor signaling, neuropeptide Y-mediated inhibition of hyperalgesia, and substance P release from primary afferent neurons. *Neuroscience*, 178-194.

Tecott, L., Sun, L., Akana, S., Strack, A., Lowenstein, D., Dallman, M., *et al.* (1995). Eating disorder and epilepsy in mice lacking 5-HT2C serotonin receptors. *Letters to Nature*, 542-546; doi: 10.1038/374542a0.

Teff, K., & Kim, S. (2011). Atypical antipsychotics and the neural regulation of food intake and peripheral metabolism. *Physiology & Behavior*, 590-598.

Thermo Fisher Scientific Inc. (2012). *Thermo Scientific.* Retreived on April 5, 2014 from Pierce Protein Biology Products: http://www.piercenet.com/guide/protein-assay-selection-guide

Thermo Scientific. (2009). NanoDrop 2000/2000c Spectrophotometer V1.0 User Manual. Wilmington, DE, the USA: Thermo Scientific Fisher Inc; accessible at http://www.nanodrop.com.

van den Heuvel, J., Eggels, L., van Rozen, A., Luijendijk, M., Fliers, E., Kalsbeek, A., *et al.* (2014). Neuropeptide Y and leptin sensitivity is dependent on diet composition. *Journal of Neuroendocrinology*, 377-385.

van der Zwaal, E., SK, J., la Fleur, S., & Adan, R. (2014). Modeling olanzapine-induced weight gain in rats. *International Journal of Neuropsychopharmacology*, 169-186.

Varela, L., & Horvath, T. L. (2012). Leptin and insulin pathways in POMC and AgRP neurons that modulate energy balance and glucose homeostasis. *EMBO Reports*, 1079-1086.

von Bohlen und Halback, O., & Dermietzel, R. (2006). Neuromodulators. O. von Bohlen und Halback, & R. Dermietzel in, *Neurotransmitters and Neuromodulators: Handbook of Receptors and Biological Effects* (pg. 2nd edition; 144-149, 315-319). Weinheim: WILEY-VCH Verlag GmbH & Co.KGaA.

von Buhlen und Halback, O., & Dermietzel, R. (2006). Neurotransmitters. O. von Buhlen und Halback, & R. Dermietzel in, *Neurotransmitters and Neuromodulators* (pg. 46-142; 2nd edition). Weinheim: Wiley VCH Verlag GmbH & Co.

Vong, L., Ye, C., Yang, Z., Choi, B., Chua Jr, S., & Lowell, B. (2011). Leptin action on GABAergic neurons prevents obesity and reduce inhibitory tone to POMC neurons. *Neuron*, 142-154; doi: 10.1016/j.neuron.2011.05.028.

Wang, O., & Majzoub, J. A. (2011). Adrenocorticotropin. S. Melmed in, *The Pituitary* (pg. 3rd edition, 49-75). London; Burlington; San Diego: Elsevier Inc.

Wardlaw, S. L. (2011). Hypothalamic proopiomeanocortin processing and the regulation of energy balance. *European Journal of Pharmacology*, 213-219.

Weston-Green, K., Huang, X., & Deng, C. (2012). Alterations to melanocortinergic, GABAergic and cannabinoid neurotransmission associated with olanzapine-induced weight gain. *PLOS ONE*, 7(3): e33548; doi: 10.1371/journal.pone.0033548.

World Health Organization (WHO). (2014, May). *WHO media center*. on Retrieved June 23, 2014 from Obesity and Overweight: http://www.who.int/mediacentre/factsheets/fs311/en/

Wu, R., Zhao, J., Guo, X., He, Y., Fang, M., Guo, W., *et al.* (2008). Metformin addition attenuates olanzapine-induced weight gain in drug-naive first episode schizophrenia patients. *American Journal of Pscyhiatry*, 352-358.

Wulffele, M., Kooy, A., De Zeeuw, D., Stehouwer, C., & Gansevoort, R. (2004). The effect of metformin on blood pressure, plasma cholesterol and triglycerides in type 2. *Journal of Internal Medicine*, 1-14.

Xu, Y., O'Brien III, W., Lee, C., Myers Jr, M., & Tong, Q. (2012). Role of GABA release from leptin receptor- expressing neurons in body weight regulation. *Endocrinology*, 2223-2233; doi: 10.1210/en.2011-2071.

Yanik, T., Sezlev, D., & Ak, M. (2013, July 6-11). Change of hypothalamic and peripheral levels of appetite related hypothalamic neurohormones in olanzapine treated male Wistar rats. *The Federation of European Biochemical Societies (FEBS) poster presentation*. St. Petersburg, Russia.

Zhang, H., Kranzler, H. R., Weiss, R. D., Luo, X., Brady, K. T., Anton, R. F., *et al.* (2009). Pro-opiomelanocortin gene variation related to alcohol or drug dependence: Evidence and replications across family- and polulation-based studies. *Biological Psychiatry*, 128-136.

Zhang, J., & Malhotra, A. (2011). Pharmacogenetics and antipsychotics: therapeutic efficacy and side effects prediction. *Expert Opinion on Drug Metabolism & Toxicology*, 9-37.

Zhou, G., Myers, R., Li, Y., Chen, Y., Shen, X., Fenyk-Melody, J., *et al.* (2001). Role of AMP-activated protein kinase in mechanism of metformin action. *Journal of Clinical Investigation*, 1167-1174.

Zugno, I., Barcelos, M., de Oliveira, L., Canever, L., de Luca, R., Fraga, D., *et al.* (2011). Energy metabolism, leptin, and biochemical parameters are altered in rats subjected to the chronic administration of olanzapine. *Revista Brasileira de Psiquiatria*, 168-175.

APPENDIX A

PREPARATION AND COMPONENTS OF BUFFERS AND SOLUTIONS

10% Sucrose Solution (w/v)

10 g of sucrose (Sigma-Aldrich, Germany) was dissolved in 100mL dH_2O by the help of the magnetic stirrer. It was used freshly without storage.

1X Phosphate Buffered Saline

Commercially available tablets for preparation of 0.01 M phosphate buffer with 0.0027 M potassium chloride (KCl) and 0.137 M sodium chloride (NaCl) at pH 7.4 was purchased from Sigma-Aldrich (Germany). According to manufacturer's instructions, 1 tablet was dissolved in 200mL DEPC-treated water and filtered into DEPC-treated glass bottle and stored at $+4^{o}C$.

50X Tris-Acetate EDTA (TAE) Buffer, pH 8,0

Table A-1 Prescription for 50X TAE Buffer

Ingredient	**Amount**
Trizma Base (Sigma-Aldrich, Germany)	121 g
Glacial Acetic Acid	28,55 mL
Ethylenediaminetetraacetic acid (EDTA)	37,2 g
Final Volume	500 mL

The indicated amount of Trizma base and EDTA were weighted and about 400mL dH_2O was added onto them. After that, glacial acetic acid was added and all the components were mixed until fully dissolved by the help of magnetic stirrer. Then pH was adjusted with 2M NaOH (Applichem, Germany) and the volume was added up to 500mL by dH_2O. After that, the solution was filtered into sterile glass bottle and stored at $+4^oC$.

1X TAE Buffer

1X TAE was prepared by 50 fold dilution from the 50X stock buffer by dH_2O.

1% Agarose Gel Preparation (for RNA samples)

0,5 g agarose (Sigma-Aldrich, Germany) was weighted and dissolved in 50mL 1X TAE buffer by heating in the microwave about 2 min (until it was fully dissolved). Then, waited to cool a little bit and 1,5 µL ethidium bromide (EtBr) (Sigma-Aldrich, Germany) from 10mg/mL stock solution was added. It was mixed immediately and poured to the electrophoresis gel tank (EasyCast OWL mini - Thermo Scientific, USA). The appropriate combs were placed and left to jellify. After that, 2 µL 1:1 diluted RNA samples were mixed with 2 µL 2X RNA loading dye and loaded into the wells. RNA ladder was loaded into 1 well and the samples were run at 80V for 50 min. The results were visualized by Vilber Lourmat UV Imager (Belgium).

3% Agarose Gel Preparation

It was prepared similar to 1% Agarose gel with only difference in agarose amount (1,5g agarose /50mL).

RevertAid First Strand cDNA Synthesis Kit - 5X Reaction Buffer (Thermo Scientific , USA)

- 250 mM Tris-HCl, pH 8,3
- 250 mM KCl
- 20 mM $MgCl_2$
- 50 mM Dithiothreitol (DTT)

SYBR Green JumpStart *Taq* ReadyMix without $MgCl_2$ (Sigma-Aldrich, Germany)

- 20 mM Tris-HCl, pH 8,3
- 100 mM Potassium Chloride (KCl)
- 0,4 mM deoxyadenosine triphosphate (dATP)
- 0,4 mM deoxythymidine triphosphate (dTTP)
- 0,4 mM deoxycytidine triphosphate (dCTP)
- 0,4 mM deoxyguanosine triphosphate (dGTP)
- SYBR Green I dye
- JumpStart *Taq* Antibody
- 0,05 u/µL *Taq* DNA Polymerase
- Glass passivator
- Stabilizers

APPENDIX B

STANDARD CURVES

Triglyceride Standard Curves

Table B-1 Triglyceride standards' concentrations

Triglceride standards	Concentration (mM or µmol/mL)
standard 0	0.00
standard 1	0.04
standard 2	0.08
standard 3	0.12
standard 4	0.16
standard 5	0.20

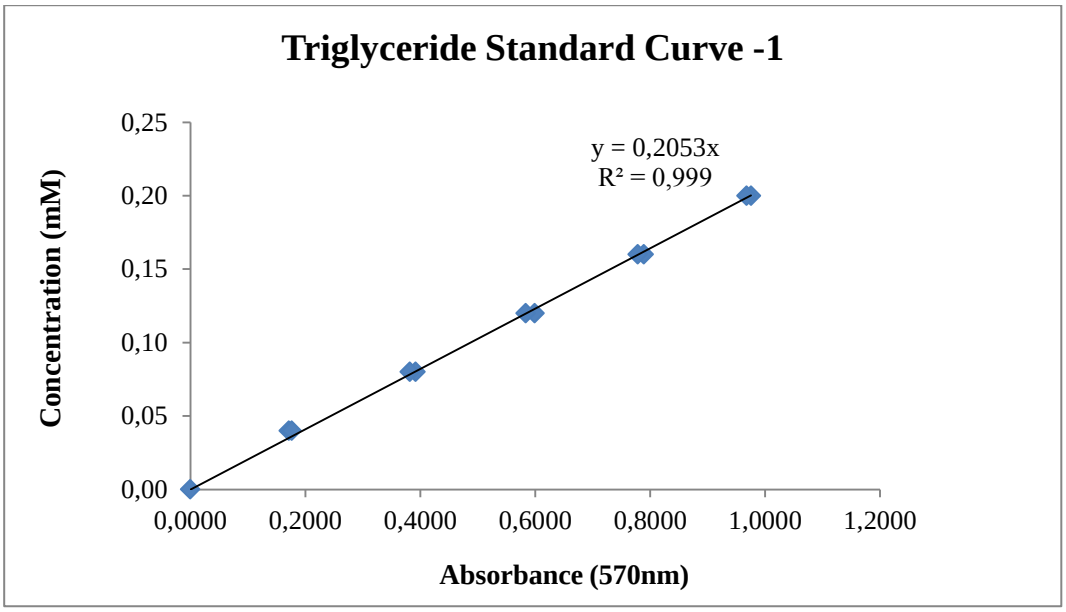

Figure B-1 Triglyceride standard curve 1

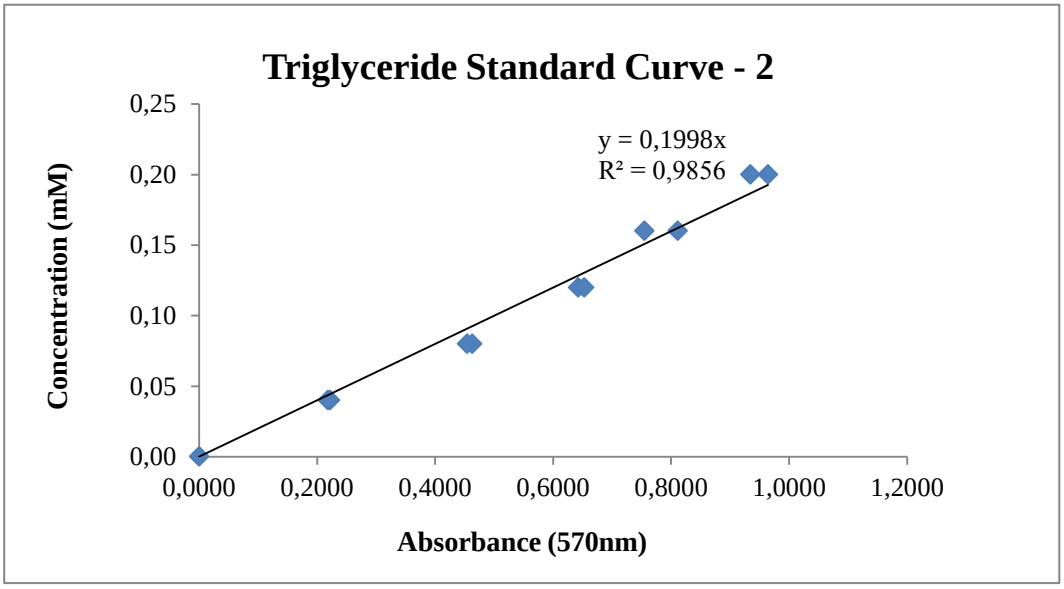

Figure B-2 Triglyceride standard curve 2

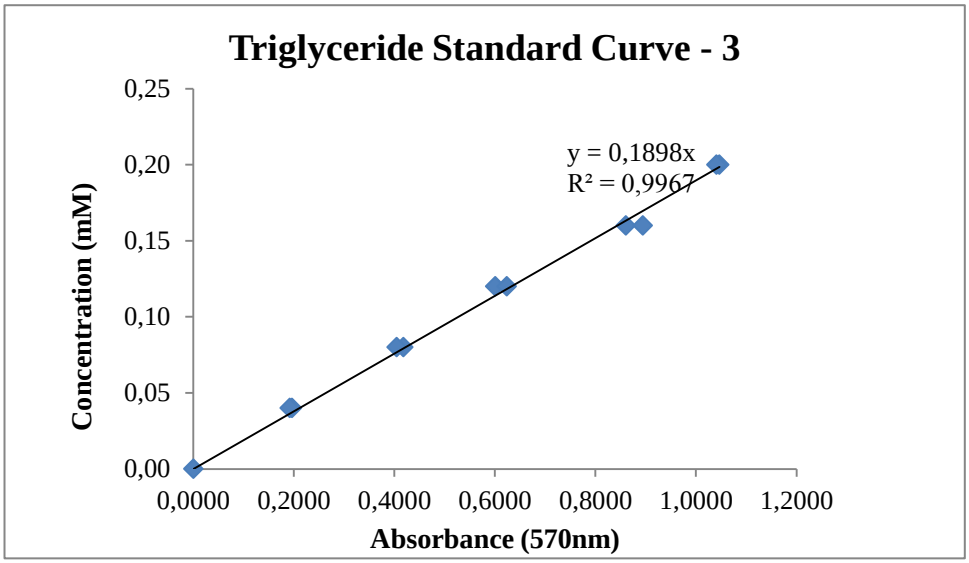

Figure B-3 Triglyceride standard curve 3

Leptin ELISA Standard Curve

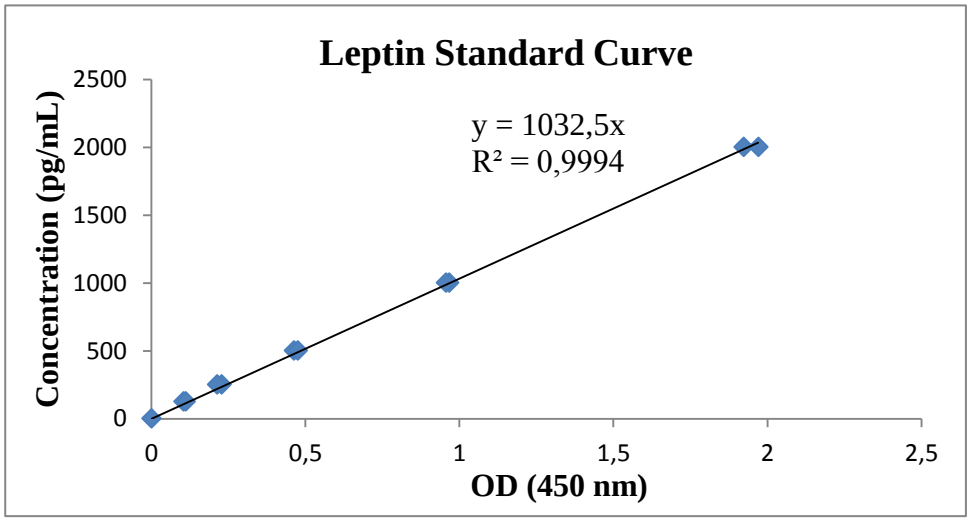

Figure B-4 Leptin ELISA standard curve

Table B-2 Rat leptin standards concentrations for ELISA

Leptin standards	Concentration (pg/mL)
standard 0	2000
standard 1	2000
standard 2	1000
standard 3	1000
standard 4	500
standard 5	500

APPENDIX C

RNA CONCENTRATIONS

Total RNA Concentrations Before DNase Treatment and Cleanup Protocol

Table C-1 RNA concentrations and absorbance ratios measured immediately after isolation (*) Taken out of the study due to low RNA integrity observed in agarose gel.

Group ID	Sample ID	Concentration (ng/µL)	OD_{260} / OD_{280}	OD_{260} / OD_{230}
CTRL1	**C1R1**	1058,45	2,03	2,1
	C1R2	856,4	2,04	2,13
	C1R3	780,75	1,98	1,94
	C1R4	813,85	2,02	1,91
	C2R1	1181,2	1,98	2,14
	C2R2	1261,35	2,02	2,22
	C2R3	898,7	1,95	2,21
	C3R1	3041,35	1,98	2,04
	C3R2	1167,5	2,05	2,16
	C3R3	1100,8	2,05	2,09

Table C-1 (Continued)

CTRL2	**C4R1**	484,8	2,06	1,95
	C4R2	160,15	2,02	1,06
	C4R3	534,75	2,08	2,03
	C4R4	790,2	2,03	1,87
	C5R1	1044,2	2,07	2,09
	C5R2	869,75	2,06	2,04
	C5R3	518,05	2,1	1,97
	C6R1	1154,75	2,03	2,16
	C6R2 (*)	374	2,06	1,18
	C6R3	996,2	2,02	2,1
OLA 1	**C7R1**	1090,95	1,98	2,21
	C7R2	787,7	2,07	1,98
	C7R3	926,85	2,03	2,05
	C7R4	394,1	2,02	1,71
	C8R1	722,5	2,03	2,13
	C8R2	823,05	2,03	2,02
	C8R3	843,25	2,06	2,11
	C9R1	715,3	2,04	2,01
	C9R2	548,55	1,92	1,97
	C9R3	603,95	2,04	2,07
OLA 2	**C10R1**	876	2	2,13
	C10R2	843,6	2,07	2,09
	C10R3	889,1	1,97	2,19
	C10R4	763,4	2,06	1,88
	C11R1	955,3	2,01	1,98
	C11R2	661,7	2,08	2,02
	C11R3	734,2	1,96	1,73
	C12R1	1015,7	1,98	2,1
	C12R2	700,3	1,97	1,99
	C12R3	1081,5	2,04	2,15

Table C-1 (Continued)

OLA 3	**C13R1**	823,8	2,01	2,12
	C13R2	645,7	1,99	2,06
	C13R3	655,6	1,99	2,12
	C13R4	2165,4	1,96	1,81
	C14R1	666,1	1,99	1,66
	C14R2	434	2,02	1,84
	C14R3	910,9	1,96	2,19
	C15R1	548,2	1,98	1,95
	C15R2	1234,7	2,01	1,95
	C15R3	537,8	2,04	1,66

Table C-2 The final concentrations and absorbance ratios of the RNA samples

Group ID	**Sample ID**	**Concentration (ng/µL)**	**OD_{260} / OD_{280}**	**OD_{260} / OD_{230}**
CTRL1	**C1R1**	664,8	2,08	2,18
	C1R2	431,9	2,02	1,98
	C1R3	514,7	2,10	2,00
	C1R4	570,9	2,10	2,05
	C2R1	564,5	2,11	2,13
	C2R2	591,8	2,09	2,12
	C2R3	428,7	2,02	2,13
	C3R1	405	2,04	2,18
	C3R2	594,7	2,08	2,05
	C3R3	559,1	2,10	2,16

Table C-2 (Continued)

CTRL2	**C4R1**	617,8	2,13	2,14
	C4R2	1352,9	2,11	2,02
	C4R3	619,7	2,14	1,60
	C4R4	668,2	2,10	2,10
	C5R1	490,9	2,12	1,84
	C5R2	639,3	2,09	2,22
	C5R3	842,8	2,09	2,20
	C6R1	803,8	2,08	2,15
	C6R2	303,8	1,99	1,68
	C6R3	494,1	2,07	2,01
OLA 1	**C7R1**	484,7	2,07	2,24
	C7R2	474,1	2,08	2,04
	C7R3	604,0	2,10	2,17
	C7R4	582,1	2,09	2,14
	C8R1	697,9	2,14	2,22
	C8R2	717,5	2,12	2,23
	C8R3	724,6	2,11	2,19
	C9R1	1292,9	2,09	2,24
	C9R2	512,1	2,08	2,13
	C9R3	791,1	2,10	2,26
OLA 2	**C10R1**	600,4	2,08	2,18
	C10R2	834,3	2,08	2,10
	C10R3	452,5	2,05	2,08
	C10R4	679,6	2,04	1,89
	C11R1	541,1	2,12	2,04
	C11R2	724,1	2,08	2,19
	C11R3	659,1	2,09	2,14
	C12R1	513,9	2,07	2,17
	C12R2	697,8	2,09	2,11
	C12R3	628,3	2,09	2,19

Table C-2 (Continued)

OLA 3	**C13R1**	540,9	2,13	2,02
	C13R2	555,6	2,05	2,02
	C13R3	527,7	2,08	2,05
	C13R4	332,6	2,06	2,06
	C14R1	574,8	2,11	2,05
	C14R2	1489,5	2,08	2,2
	C14R3	577,2	2,05	1,93
	C15R1	1123,7	2,09	2,21
	C15R2	528	2,08	2,18
	C15R3	1039,6	2,1	2,18

APPENDIX D

AGAROSE GEL IMAGES OF RNA SAMPLES

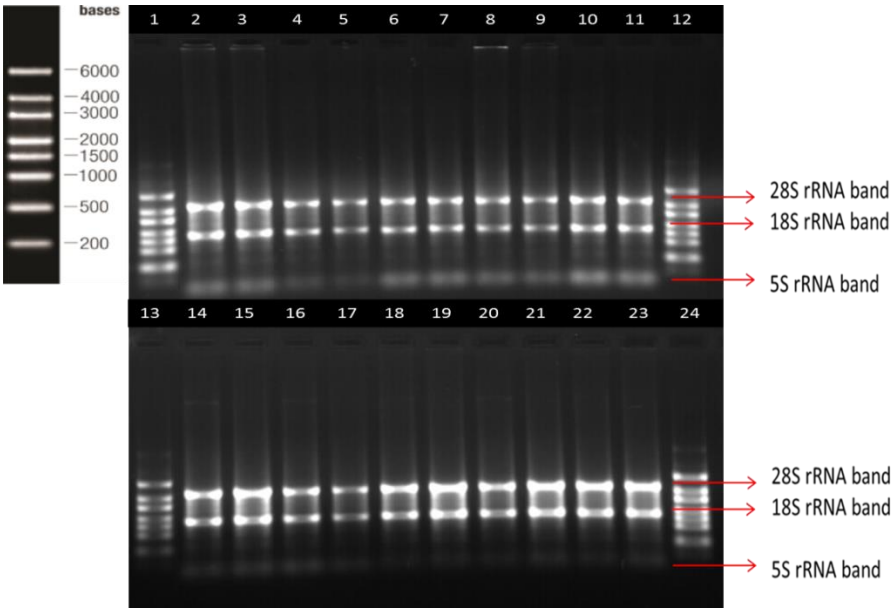

Figure D-1 Agarose gel image of CTRL 1 group RNA samples before and after 1st DNase treatment. The first load of each sample shows immediately after RNA isolation while second load shows after regular DNase treatment. Left figure represents the used RNA ladder bands and their corresponding sizes. 1, 12, 13 & 24: RNA ladder, 2-3: C1R1, 4-5: C1R2, 6-7: C1R3, 8-9: C1R4, 10-11: C2R1, 14-15: C2R2, 16-17: C2R3, 18-19: C3R1, 20-21: C3R2. 22-23: C3R3. rRNA: ribosomal RNA.

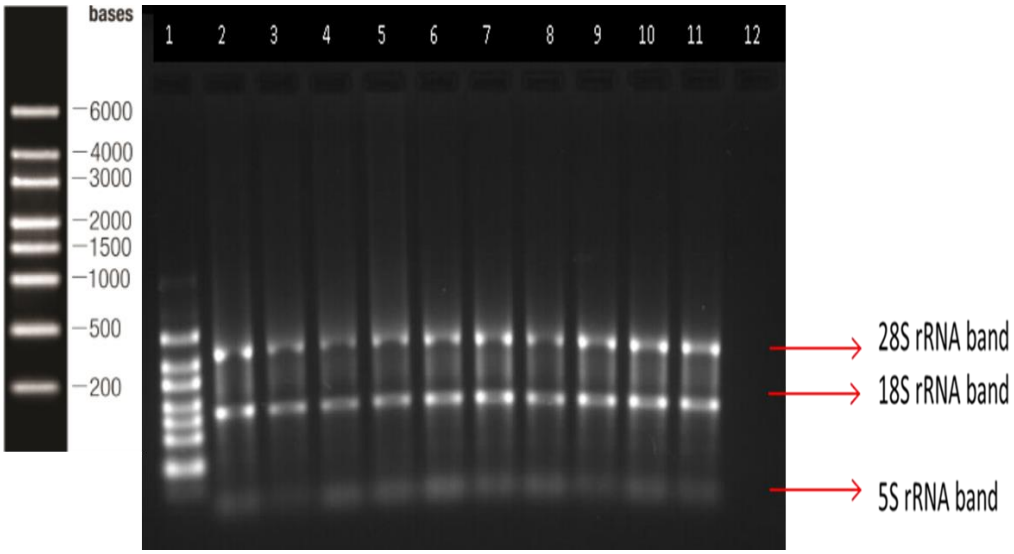

Figure D-2 Agarose gel image of CTRL 1 group RNA samples after 2nd DNase treatment, cleanup and concentration protocol. Left figure represents the used RNA ladder bands and their corresponding sizes. 1: RNA ladder, 2: C1R1, 3: C1R2, 4: C1R3, 5: C1R4, 6: C2R1, 7: C2R2, 8: C2R3, 9: C3R1, 10: C3R2, 11: C3R3, 12: nuclease-free water in which samples were dissolved. rRNA: ribosomal RNA.

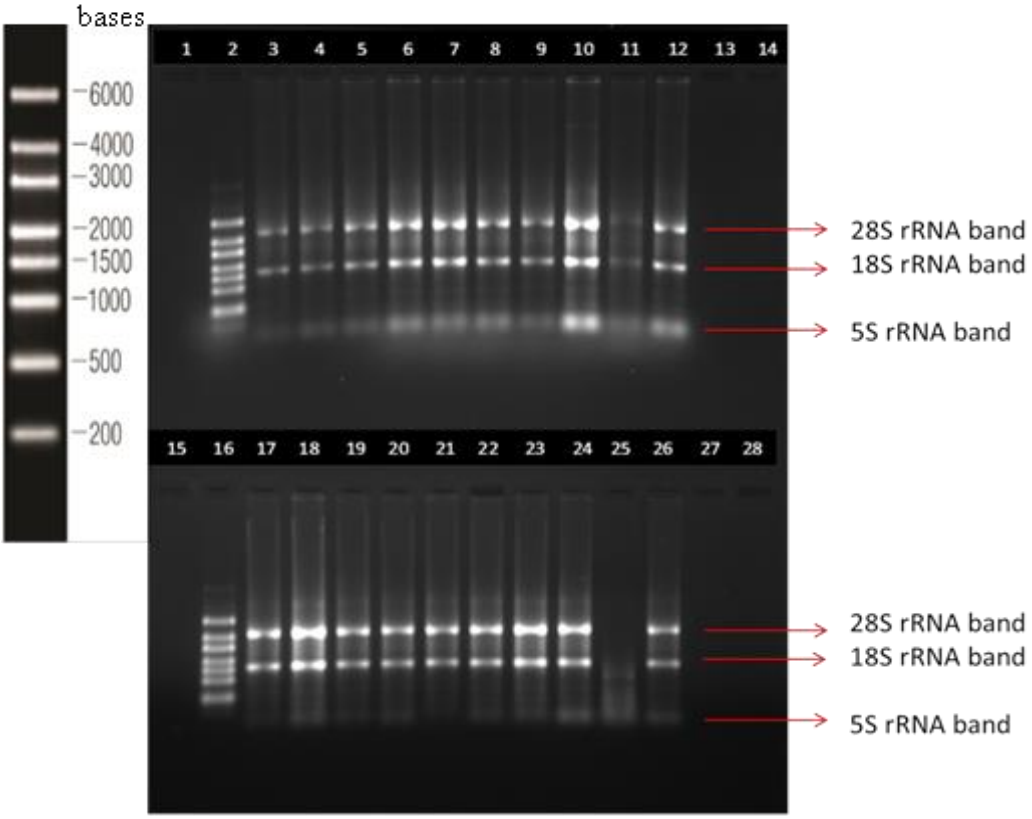

Figure D-3 Agarose gel image of CTRL 2 group RNA samples before and after DNase treatment and cleanup. The upper gel shows all CTRL 2 samples immediately after RNA isolation. The lower gel shows the samples after DNase treatment, RNA cleanup and concentration protocols. Left figure represents the used RNA ladder bands and their corresponding sizes. 2: RNA ladder, 3: C4R1, 4: C4R2, 5: C4R3, 6: C4R4, 7: C5R1, 8: C5R2, 9: C5R3, 10: C6R1, 11: C6R2. 12: C6R3, 16: RNA ladder, 17: C4R1, 18: C4R2, 19: C4R3, 20: C4R4, 21: C5R1, 22: C5R2, 23: C5R3, 24: C6R1, 25: C6R2. 26: C6R3,1, 13, 14, 15, 27 and 28: empty. rRNA: ribosomal RNA.

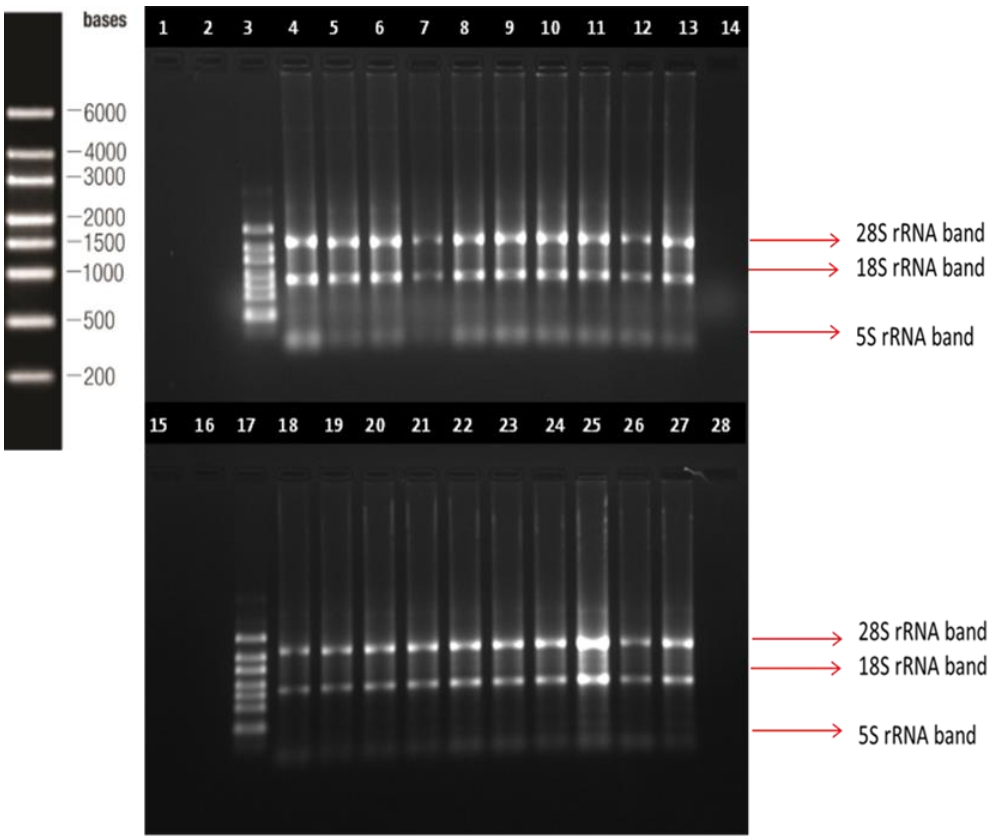

Figure D-4 Agarose gel image of OLA 1 group RNA samples before and after DNase I treatment and cleanup. The upper gel shows all OLA 1 samples immediately after RNA isolation. The lower gel shows the samples after DNase treatment, RNA cleanup and concentration protocols. The left figure represents the used RNA ladder bands and their corresponding sizes. 3 and 17: RNA ladder, 4: C7R1, 5: C7R2, 6: C7R3, 7: C7R4, 8: C8R1, 9: C8R2, 10: C8R3, 11: C9R1, 12: C9R2. 13: C9R3, 18: C7R1, 19: C7R2, 20: C7R3, 21: C7R4, 22: C8R1, 23: C8R2, 24: C8R3, 25: C9R1, 26: C9R2. 27: C9R3, lanes 14 and 28: nuclease-free water in which samples were dissolved and 1, 2, 15 & 16 are empty lanes. rRNA: ribosomal RNA.

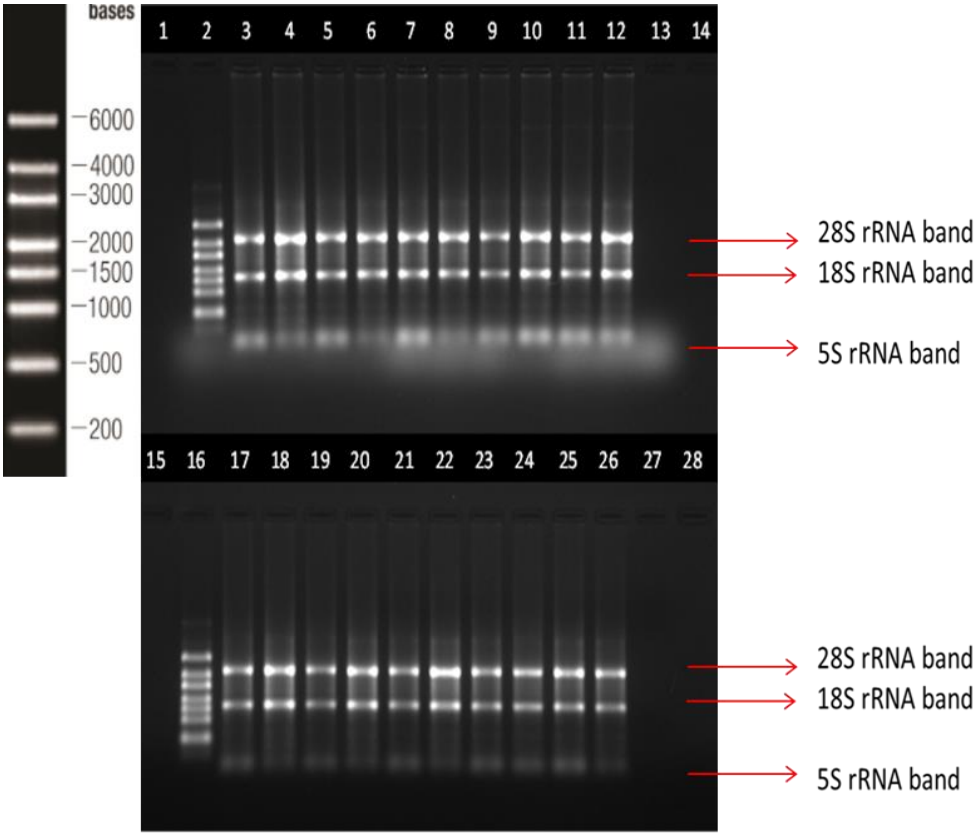

Figure D-5 Agarose gel image of OLA 2 group RNA samples before and after DNase treatment and cleanup. The upper gel shows all OLA 2 samples immediately after RNA isolation. The lower gel shows the samples after DNase treatment, RNA cleanup and concentration protocols. Left figure represents the used RNA ladder bands and their corresponding sizes. 2 & 16: RNA ladder, 3: C10R1, 4: C10R2, 5: C10R3, 6: C10R4, 7: C11R1, 8: C11R2, 9: C11R3, 10: C12R1, 11: C12R2. 12: C12R3, 17: C10R1, 18: C10R2, 19: C10R3, 20: C10R4, 21: C11R1, 22: C11R2, 23: C11R3, 24: C12R1, 25: C12R2. 26: C12R3, 13 & 27: nuclease-free water in which samples were dissolved, 1, 14, 15, 28: empty. rRNA: ribosomal RNA.

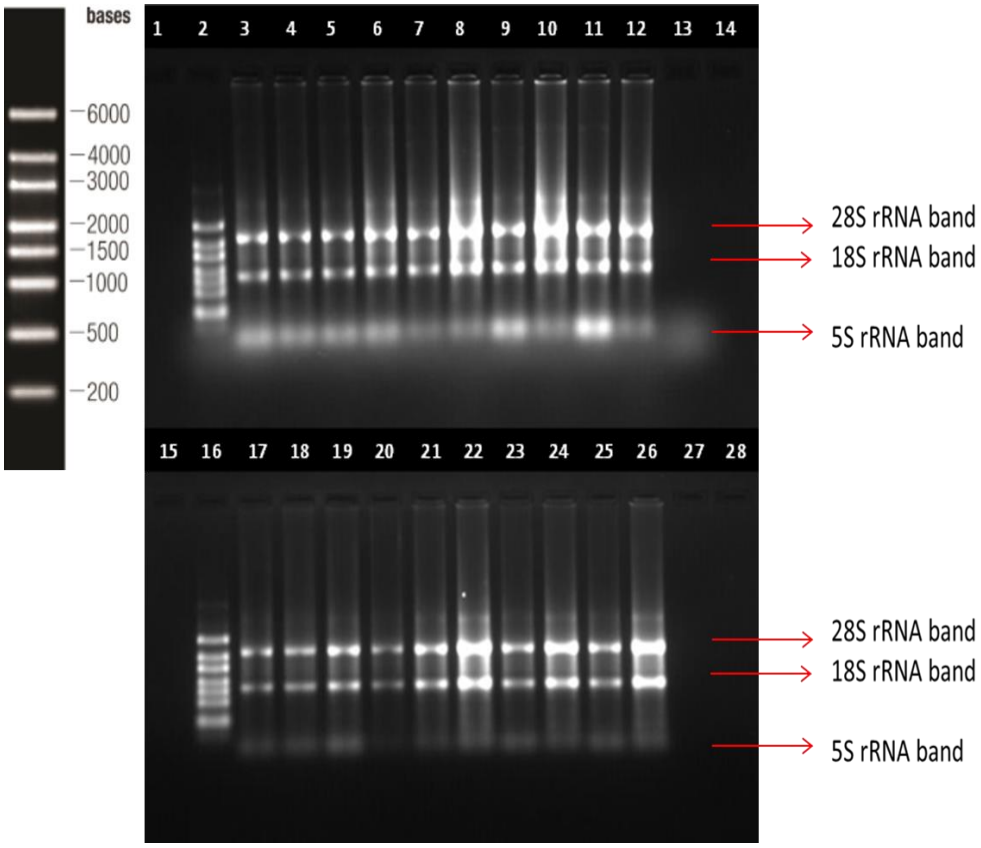

Figure D-6 Agarose gel image of OLA 3 group RNA samples before and after DNase treatment and cleanup. The upper gel shows all OLA 3 samples immediately after RNA isolation. The lower gel shows the samples after DNase treatment, RNA cleanup and concentration protocols. Left figure represents the used RNA ladder bands and their corresponding sizes. 2 & 16: RNA ladder, 3: C13R1, 4: C13R2, 5: C13R3, 6: C13R4, 7: C14R1, 8: C14R2, 9: C14R3, 10: C15R1, 11: C15R2. 12: C15R3, 17: C13R1, 18: C13R2, 19: C13R3, 20: C13R4, 21: C14R1, 22: C14R2, 23: C14R3, 24: C15R1, 25: C15R2. 26: C15R3, 13 & 27: nuclease-free water in which samples were dissolved, 1, 14, 15, 28: empty. rRNA: ribosomal RNA.

APPENDIX E

RT-qPCR STANDARD, REACTION AND MELT CURVES AND AGAROSE GEL IMAGES

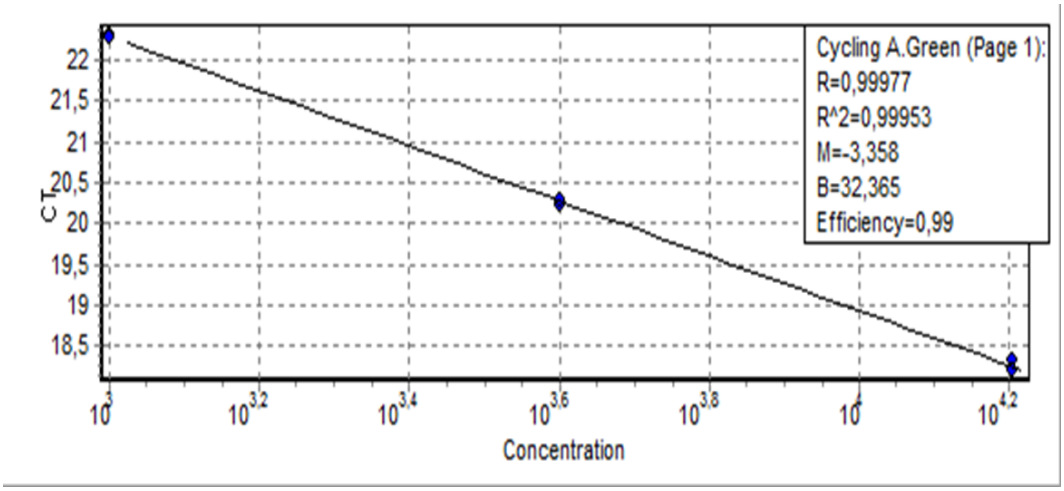

Figure E-1 The *GAPDH* standard curve. Used dilutions were 1/50 and 1/200 with 3 copies and 1/800 with 2 copies from each sample dilution, and 1 copy from noRT and NTC controls.

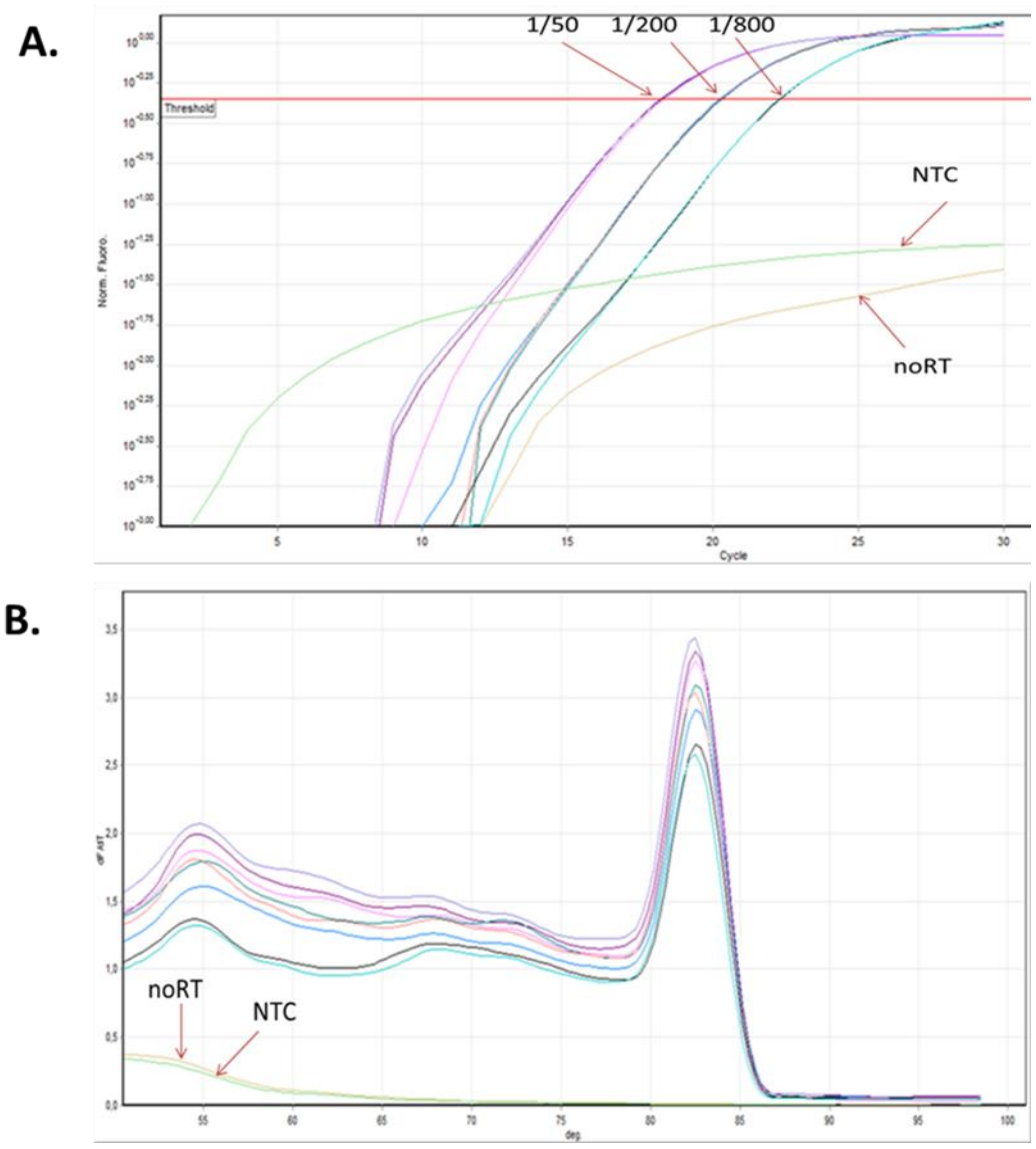

Figure E-2 The *GAPDH* standards RT-qPCR reaction and melt curve. A. Standard curve. B. Melt curve. All give peak at approximately at 82.5^{o}C

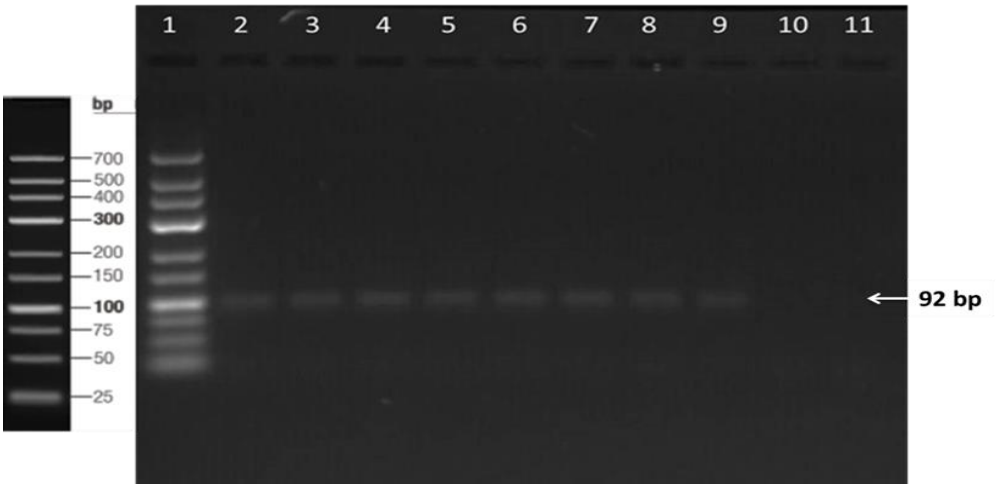

Figure E-3 Agarose gel image of RT-qPCR products from *GAPDH* standard curve reaction. Lanes 1: DNA ladder, 2-4: 1/50 dilution, 5-7: 1/200 dilution, 8-9: 1/800 dilution, 10: noRT control, 11: NTC

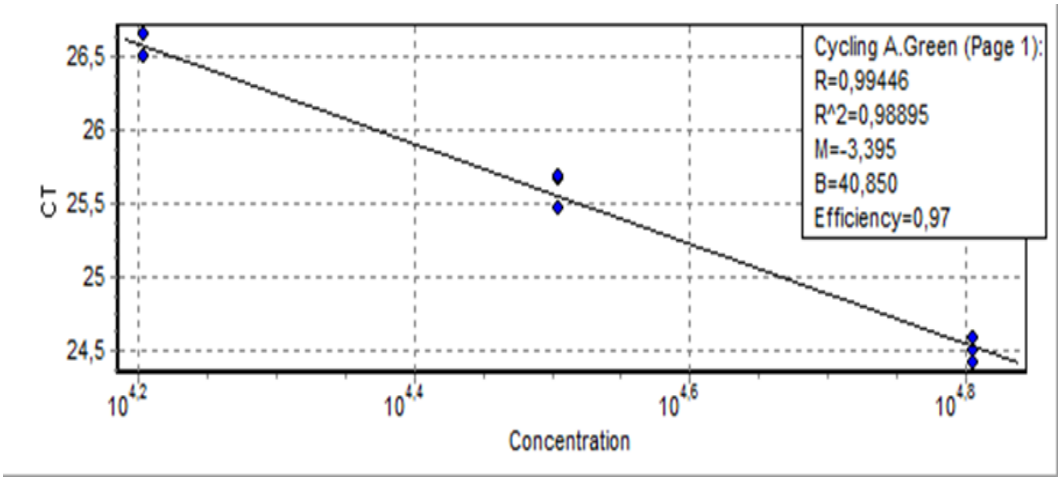

Figure E-4 The *POMC* standard curve. Used dilutions were 1/50, 1/100 and 1/200 with 3 copies from each sample dilution, and 1 copy from noRT and NTC controls.

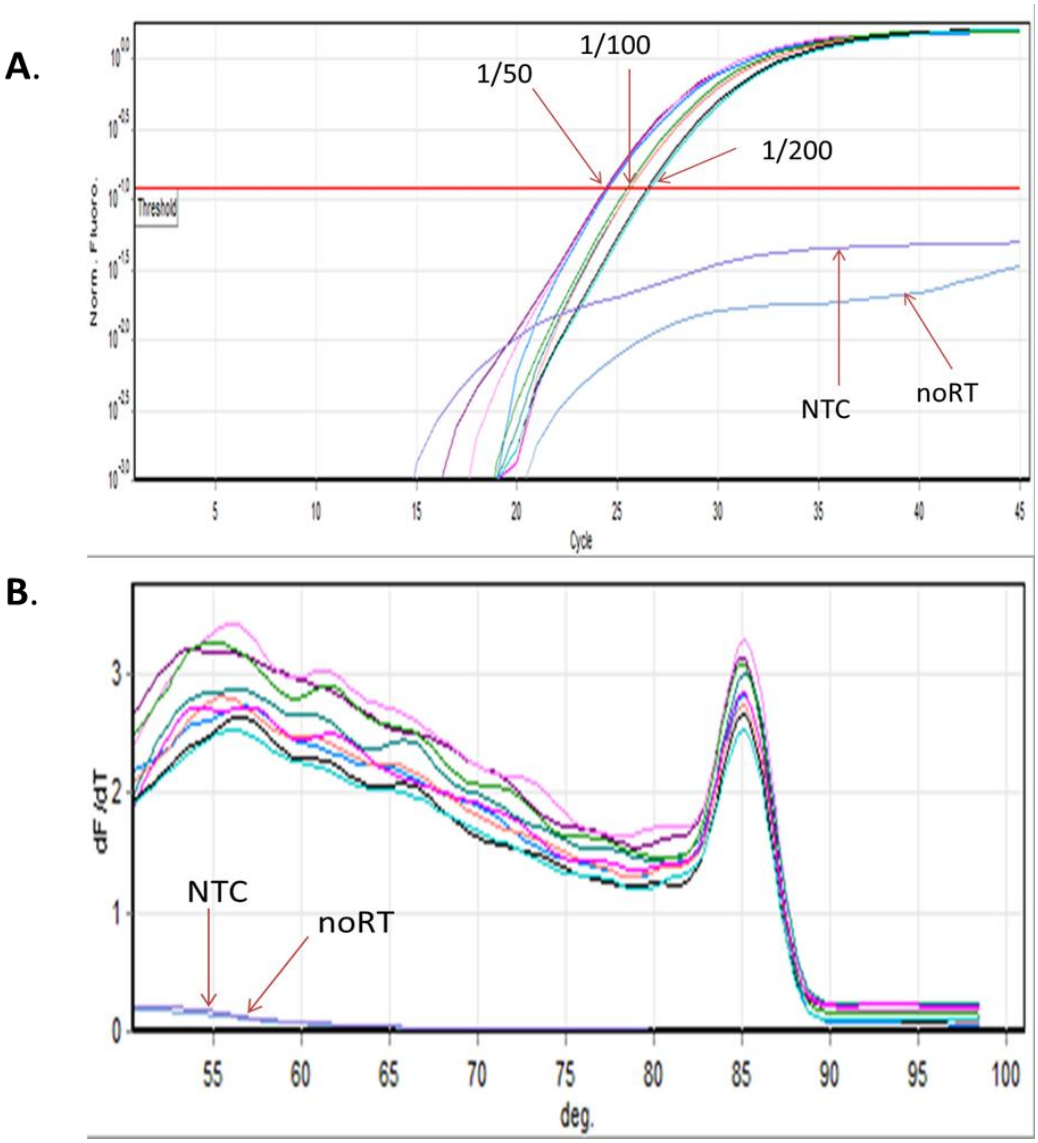

Figure E-5 The *POMC* standards RT-qPCR reaction and melt curve. A. Standard curve. B. Melt curve. All give peak at approximately at 85^{o}C.

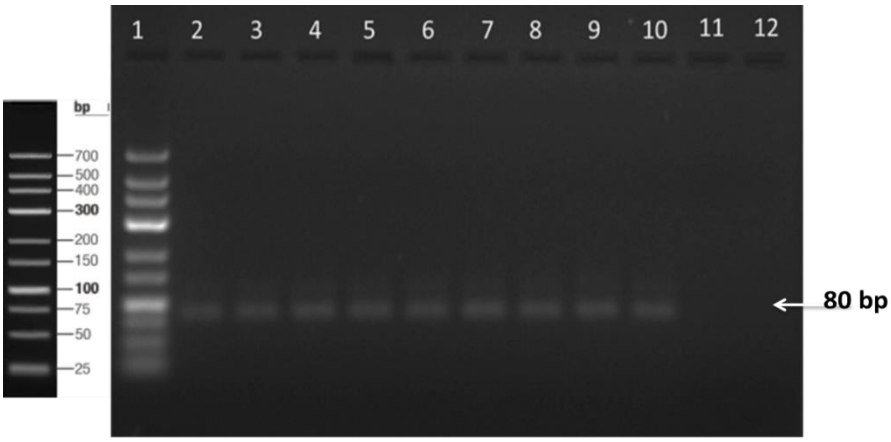

Figure E-6 Agarose gel image of RT-qPCR products from *POMC* standard curve reaction. Lanes 1: DNA ladder, 2-4: 1/50 dilution, 5-7: 1/100 dilution, 8-10: 1/200 dilution, 11: noRT control, 12: NTC

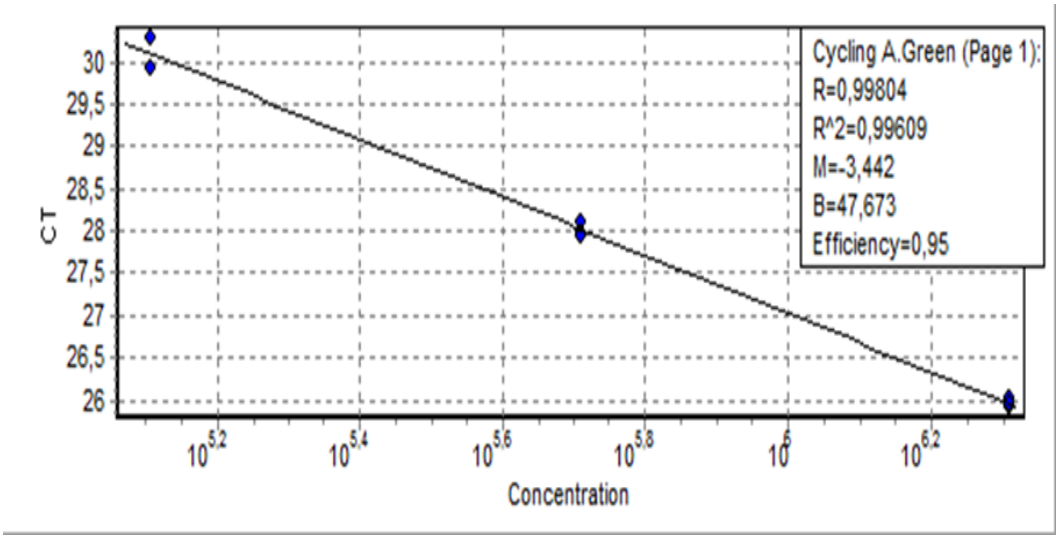

Figure E-7 The *NPY* standard curve. Used dilutions were 1/50, 1/200 and 1/800 with 3 copies from each sample dilution, and 1 copy from noRT and NTC controls.

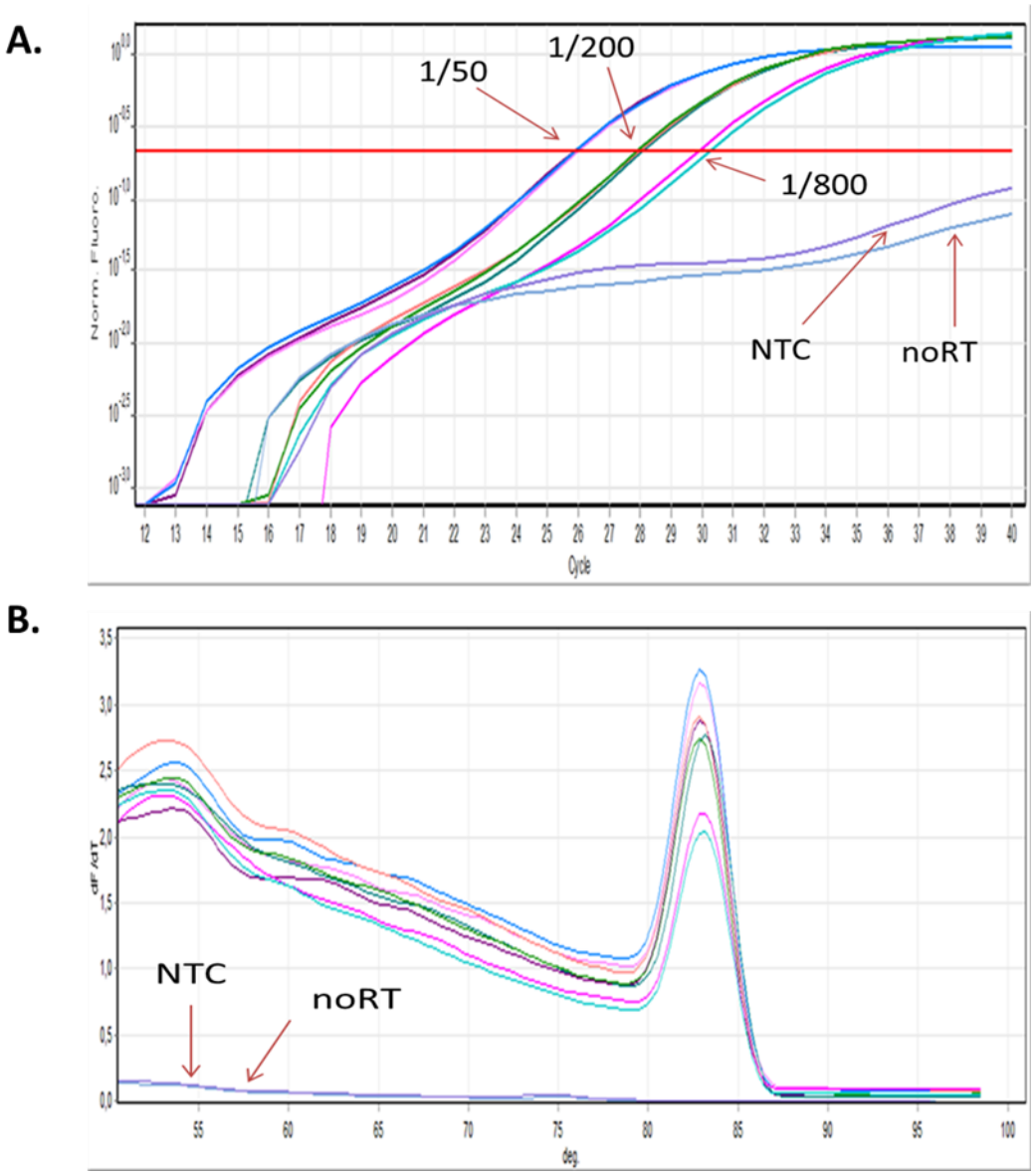

Figure E-8 The *NPY* standards RT-qPCR reaction and melt curve. A. Standard curve. B. Melt curve. All give peak at approximately at 83^{o}C.

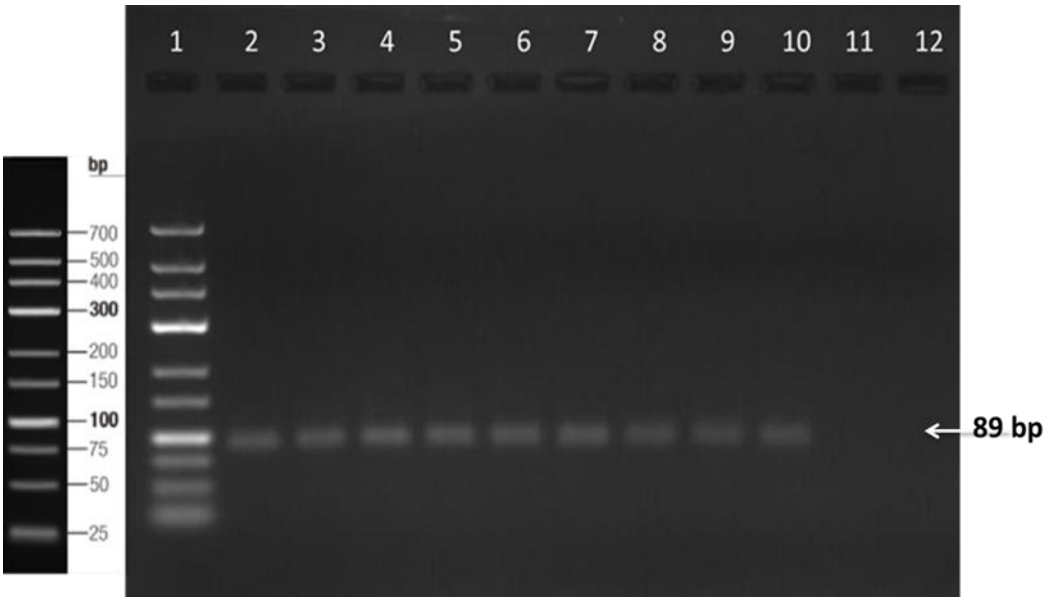

Figure E-9 Agarose gel image of RT-qPCR products from *NPY* standard curve reaction. 1: DNA ladder (can be seen on the left figure), 2-4: 1/50 dilution, 5-7: 1/200 dilution, 8-10: 1/800 dilution, 11: noRT control, 12: NTC.

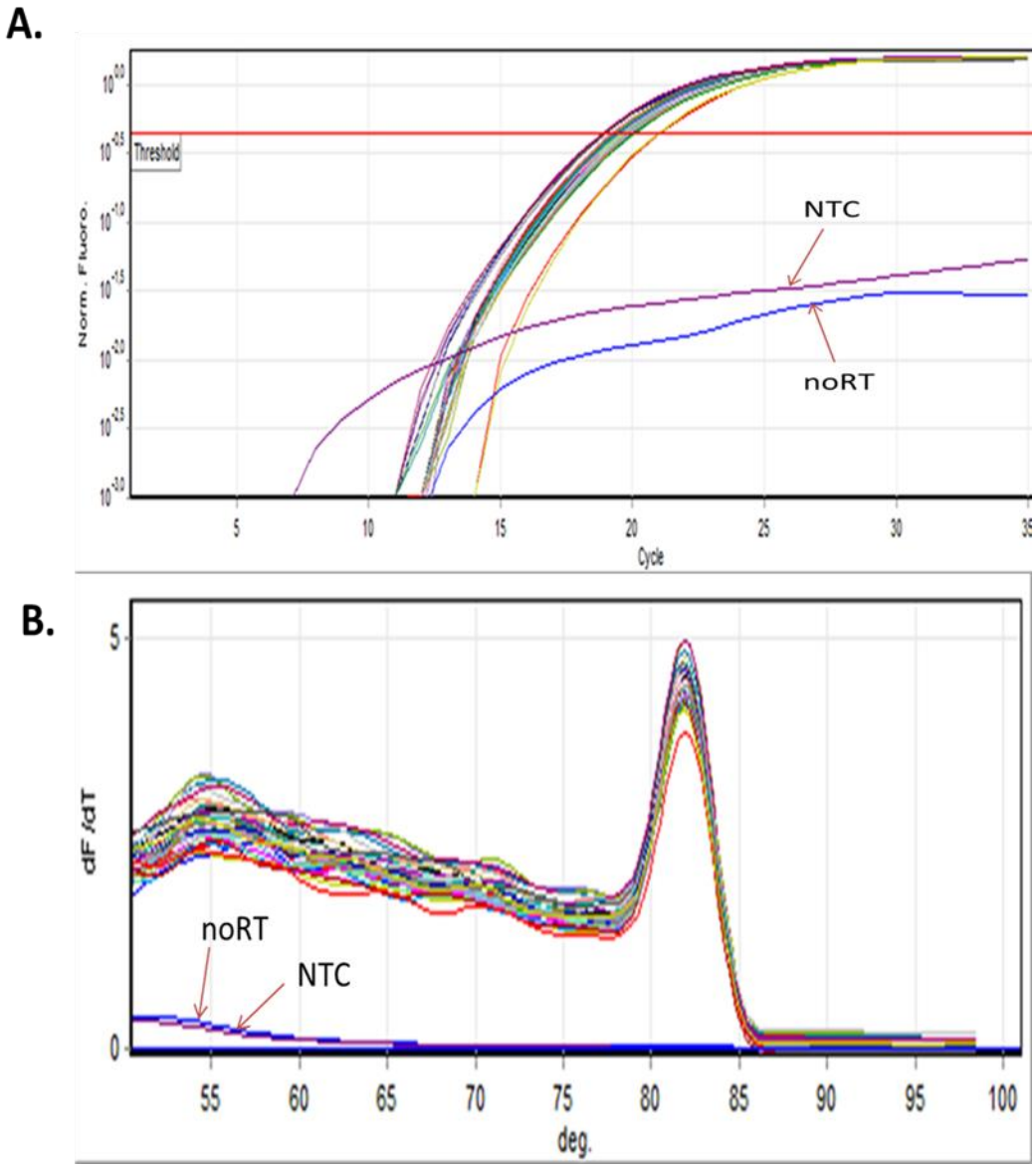

Figure E-10 The *GAPDH* RT-qPCR reaction curve (A) and melt curve (B) of CTRL 1 group.

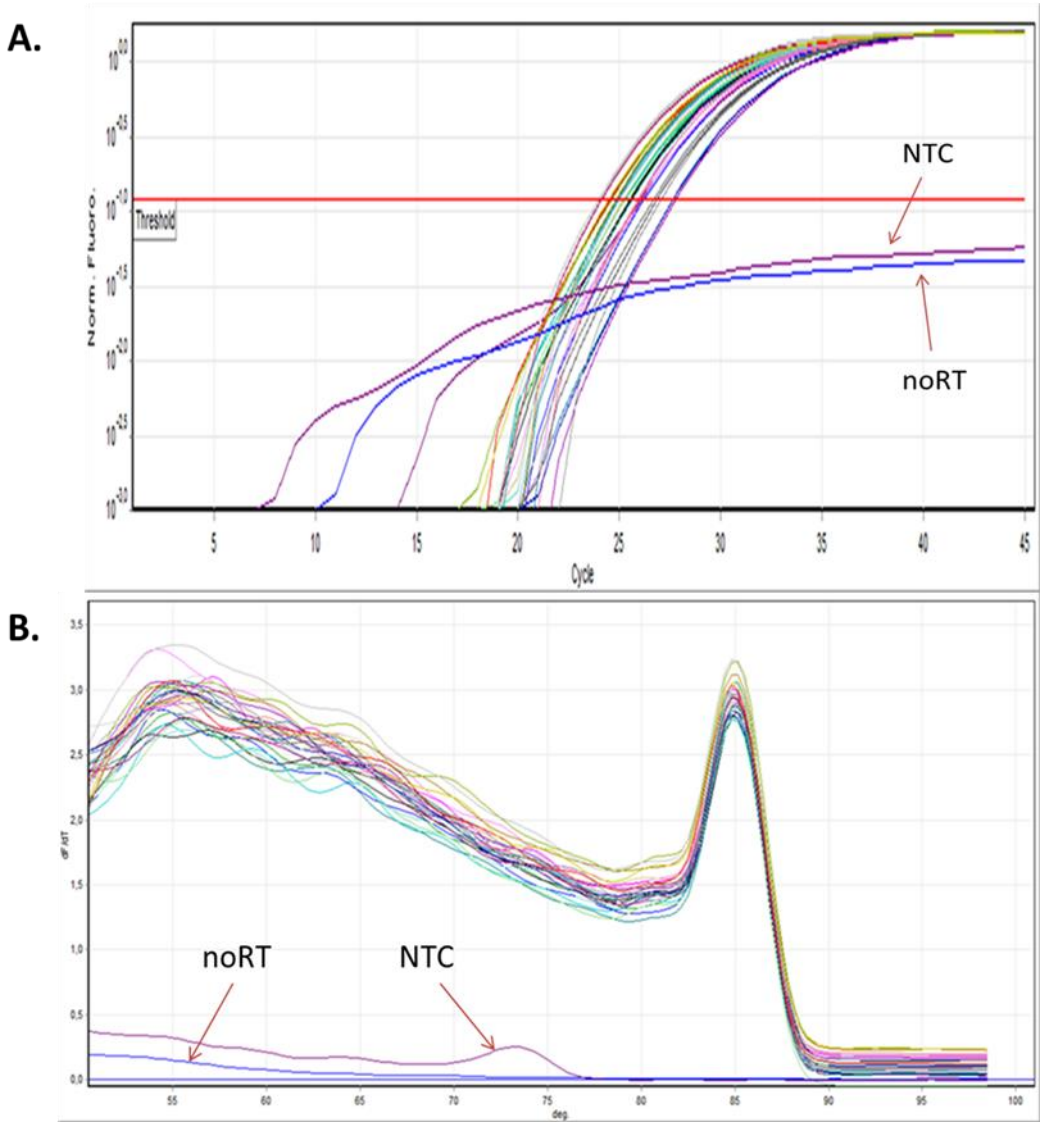

Figure E-11 The *POMC* RT-qPCR reaction curve (A) and melt curve (B) of CTRL 1 group.

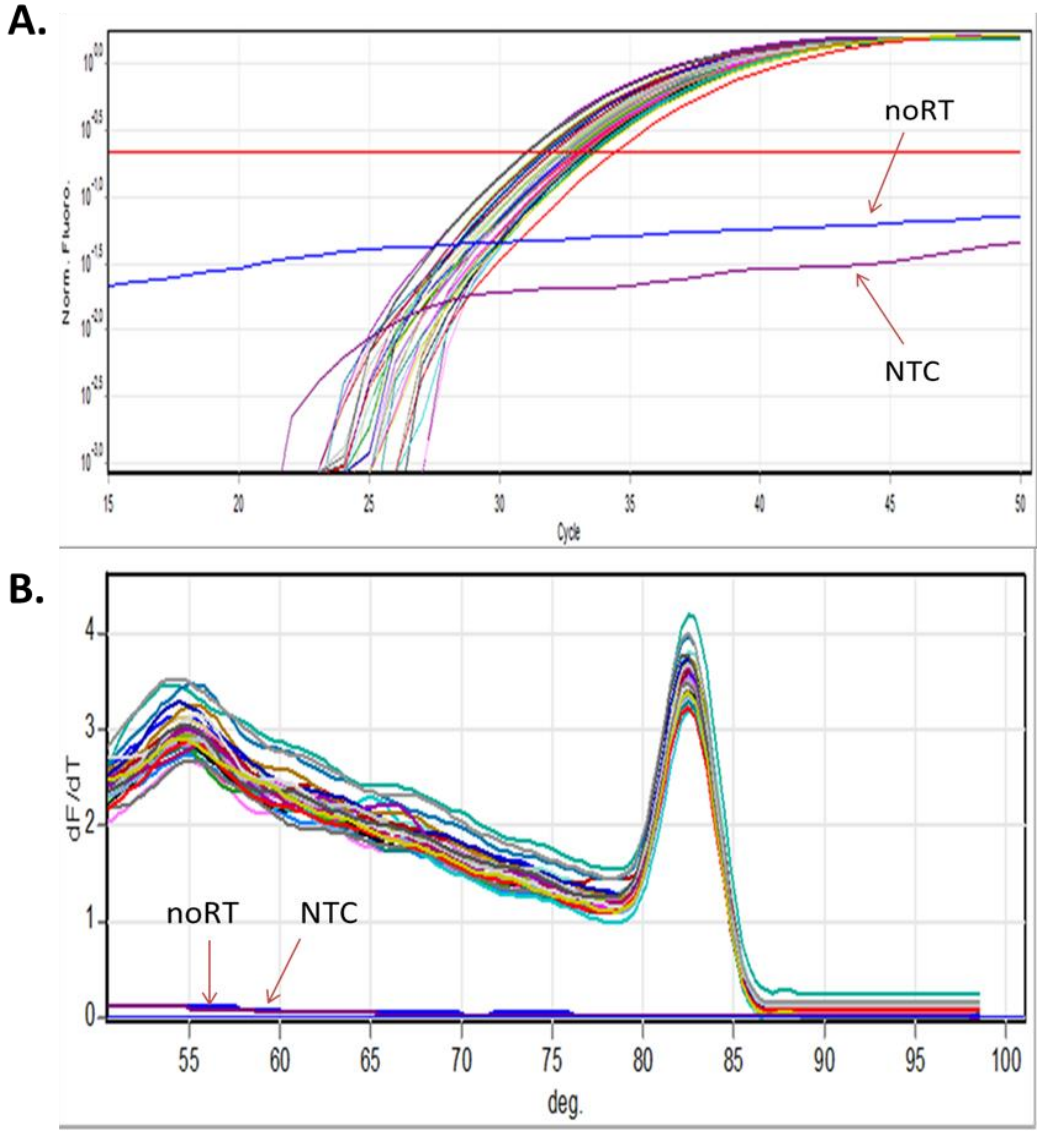

Figure E-12 The *NPY* RT-qPCR reaction curve (A) and melt curve (B) of CTRL 1 group.

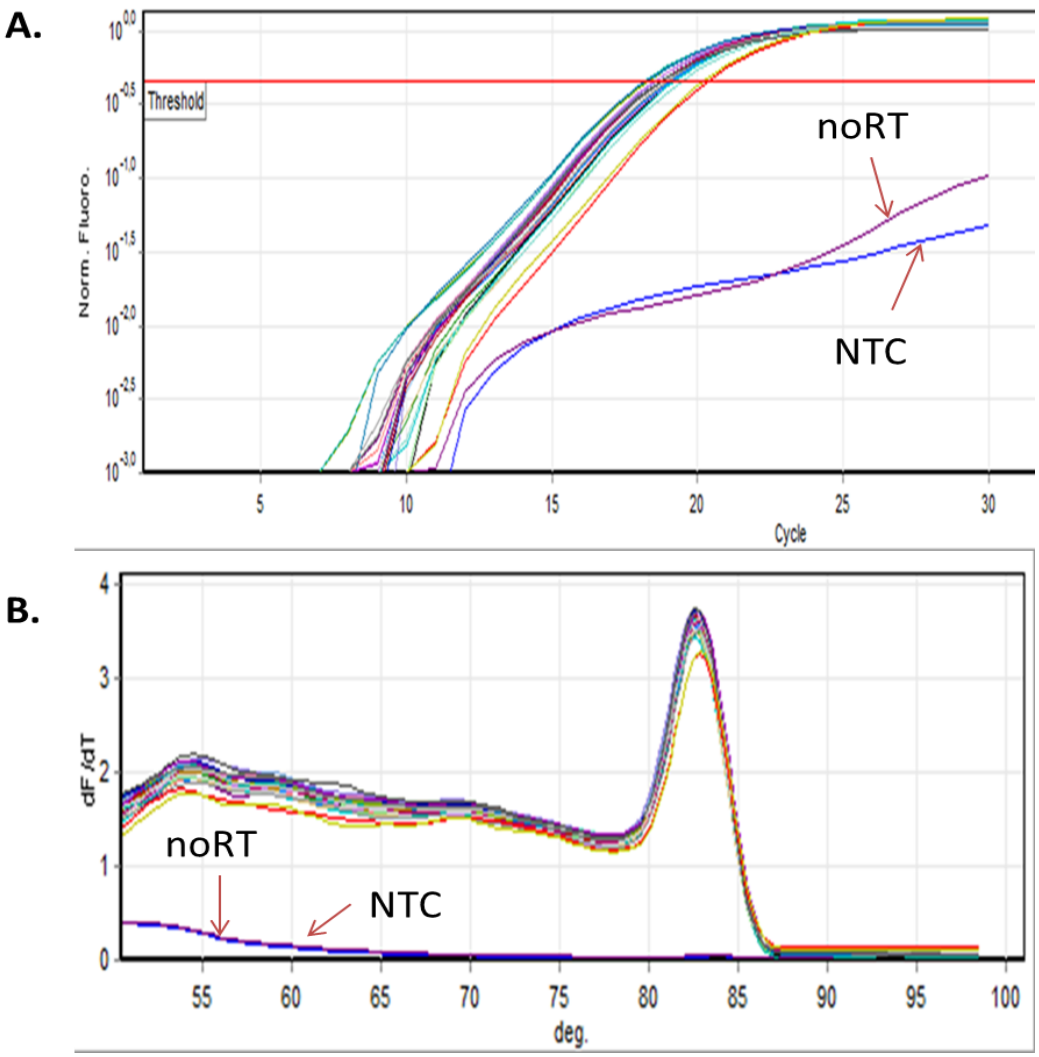

Figure E-13 The *GAPDH* RT-qPCR reaction curve (A) and melt curve (B) of CTRL 2 group.

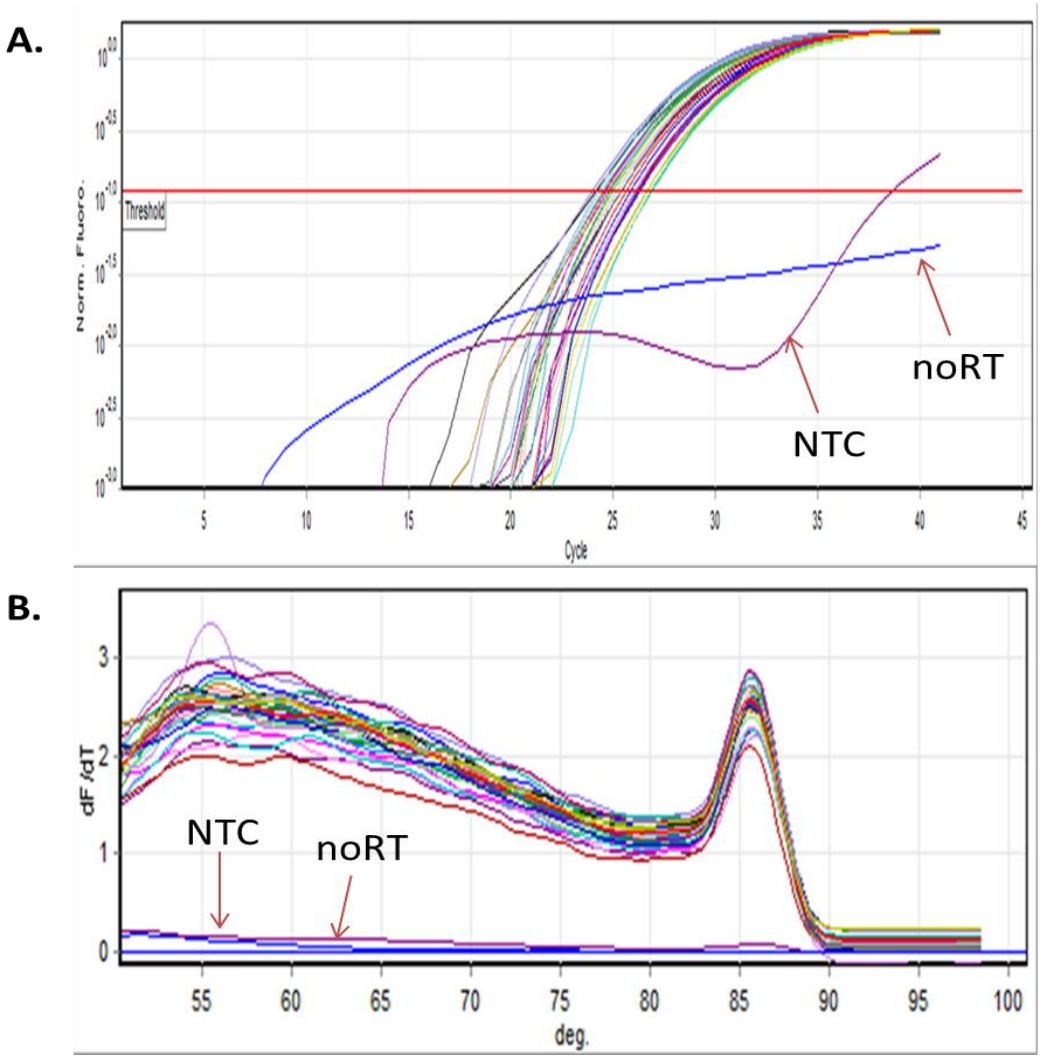

Figure E-14 The *POMC* RT-qPCR reaction curve (A) and melt curve (B) of CTRL 2 group

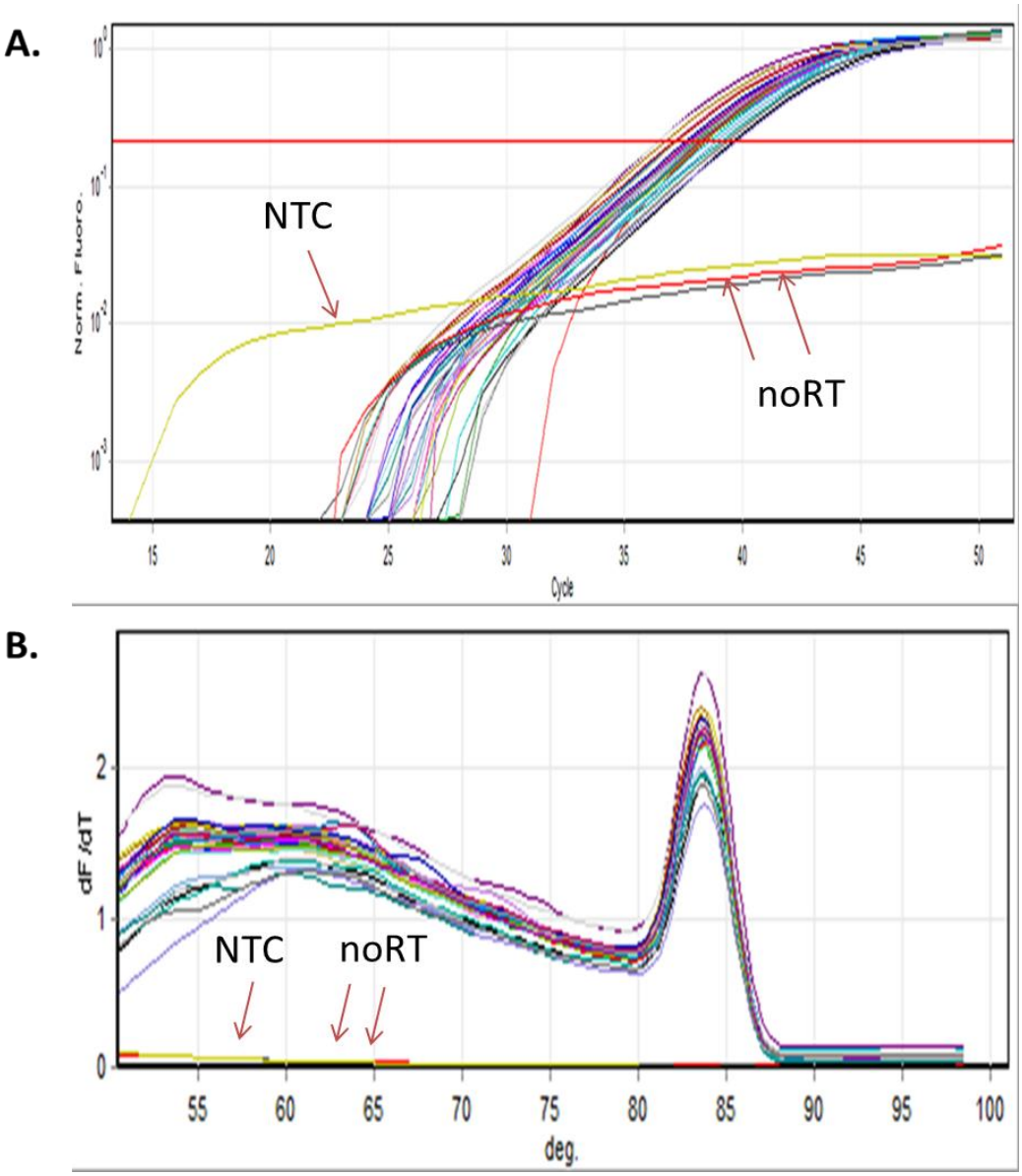

Figure E-15 The *NPY* RT-qPCR reaction curve (A) and melt curve (B) of CTRL 2 group

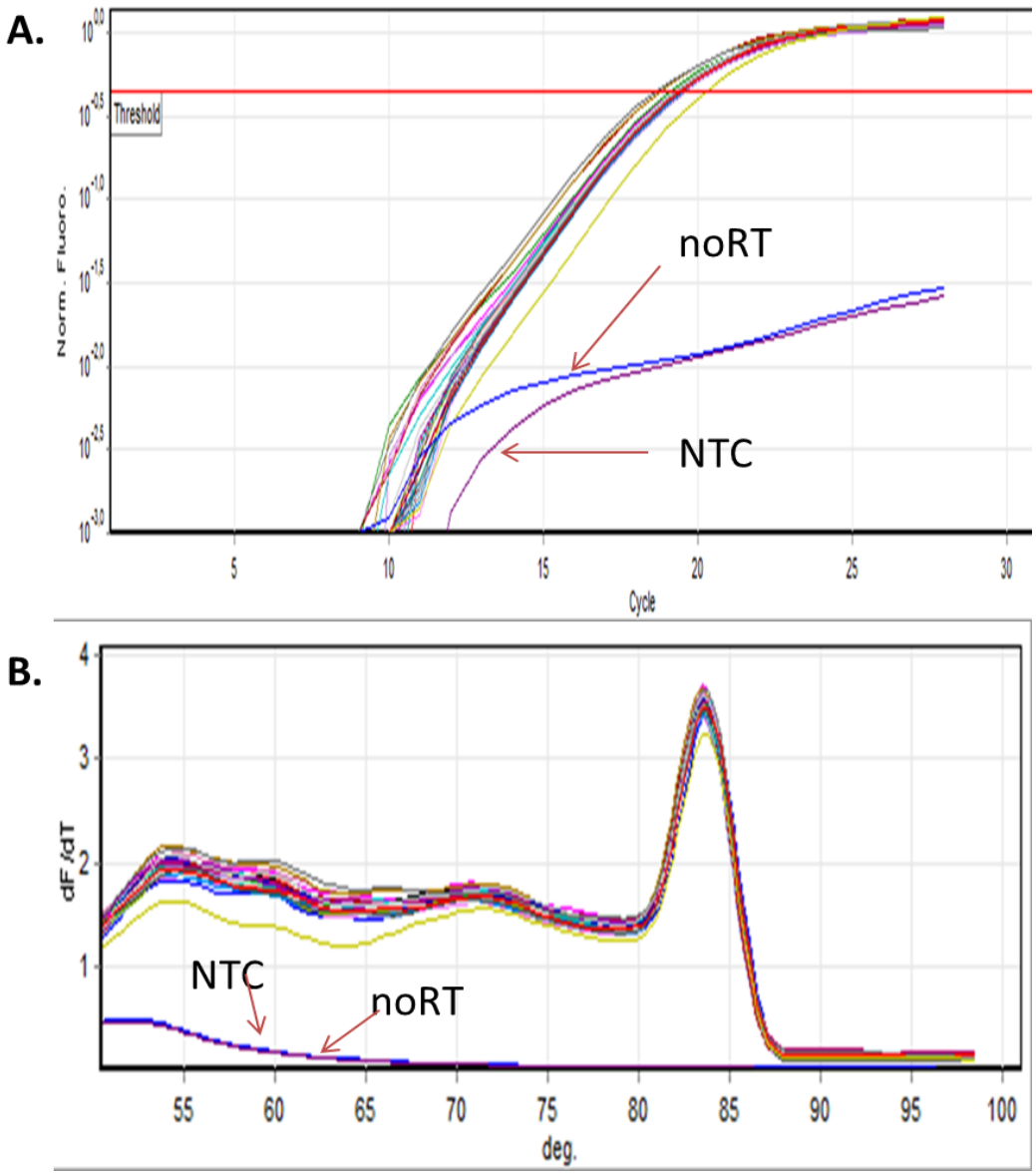

Figure E-16 The *GAPDH* RT-qPCR reaction curve (A) and melt curve (B) of OLA 1 group.

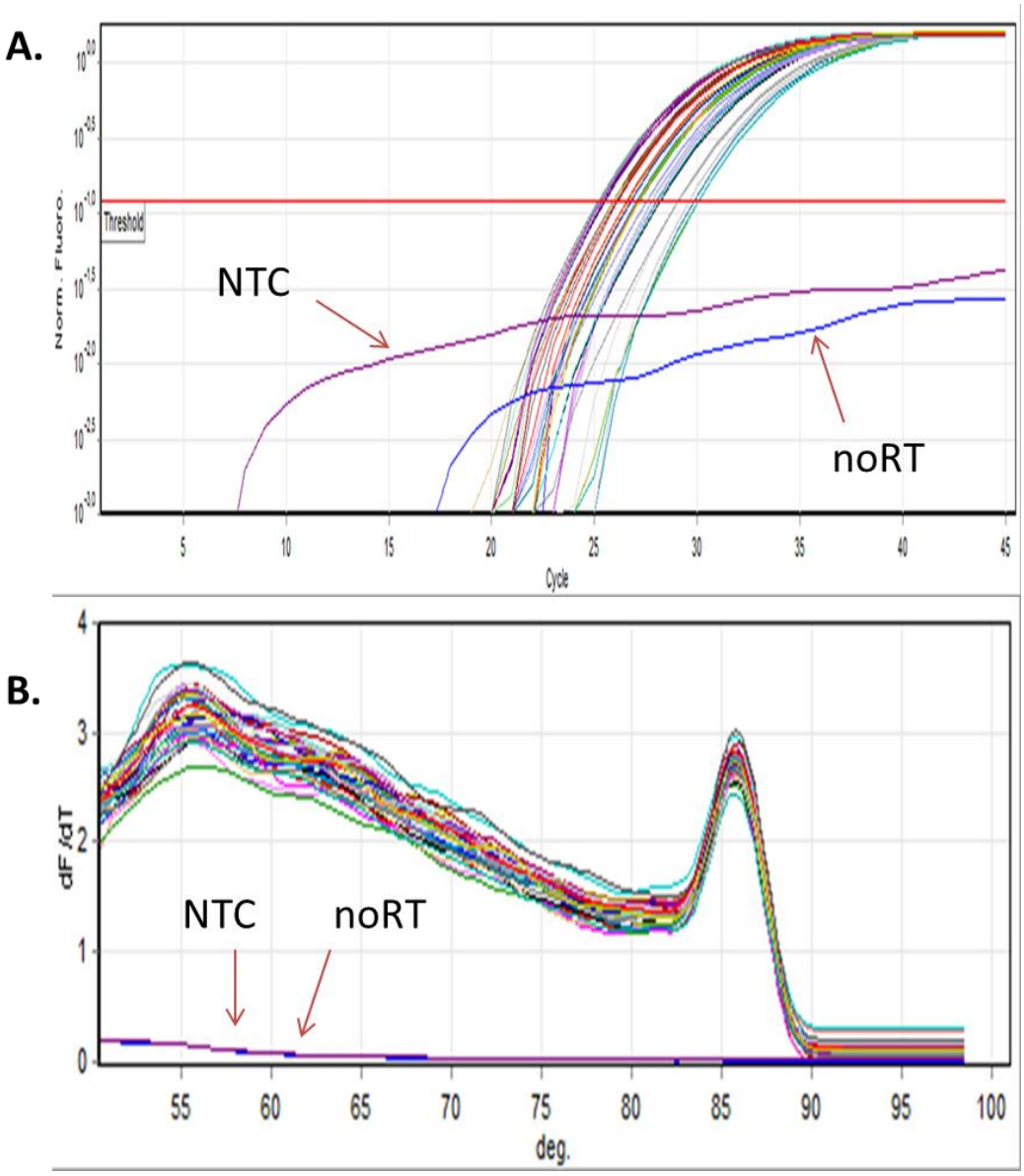

Figure E-17 The *POMC* RT-qPCR reaction curve (A) and melt curve (B) of OLA 1 group

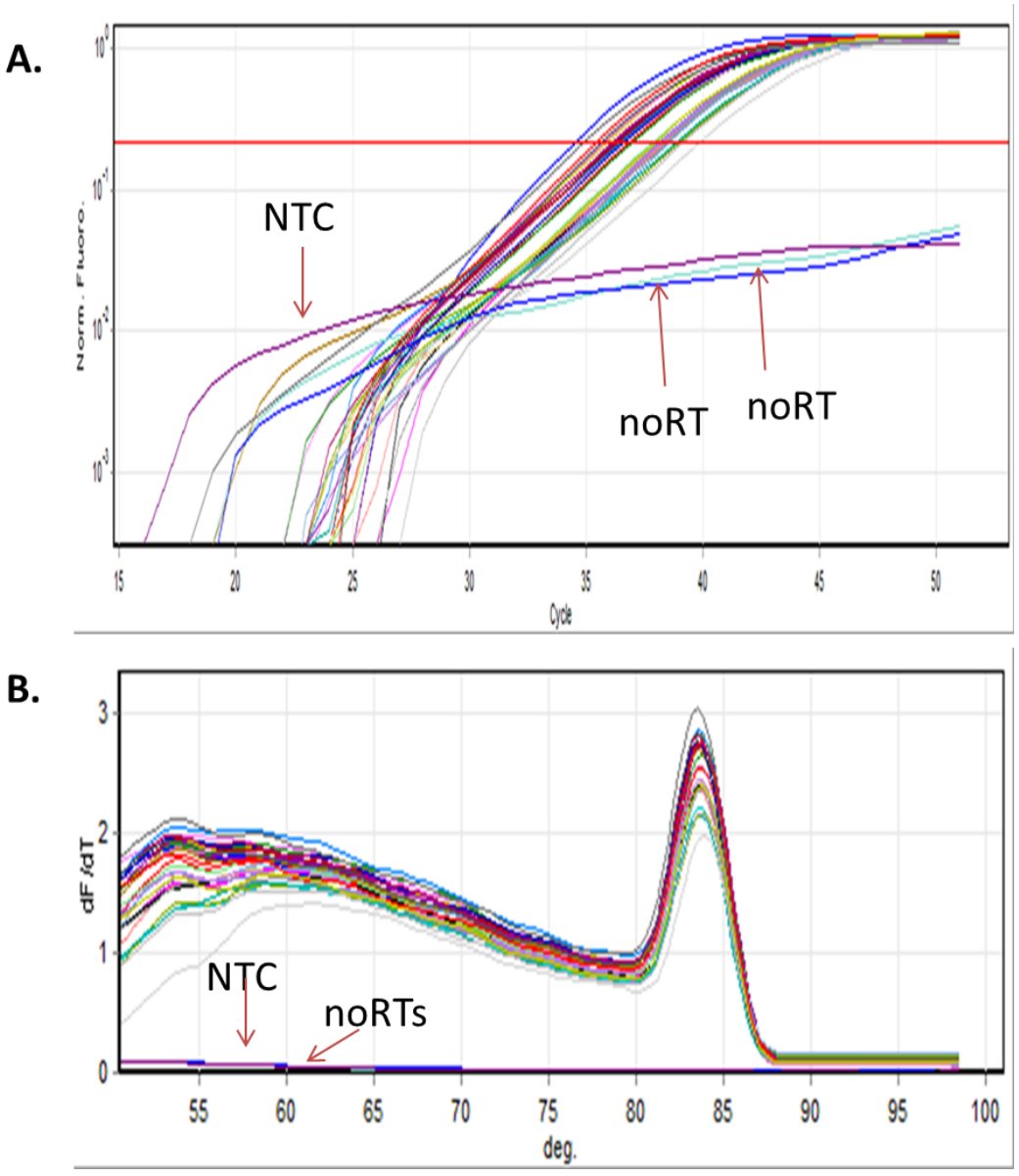

Figure E-18 The *NPY* RT-qPCR reaction curve (A) and melt curve (B) of OLA 1 group.

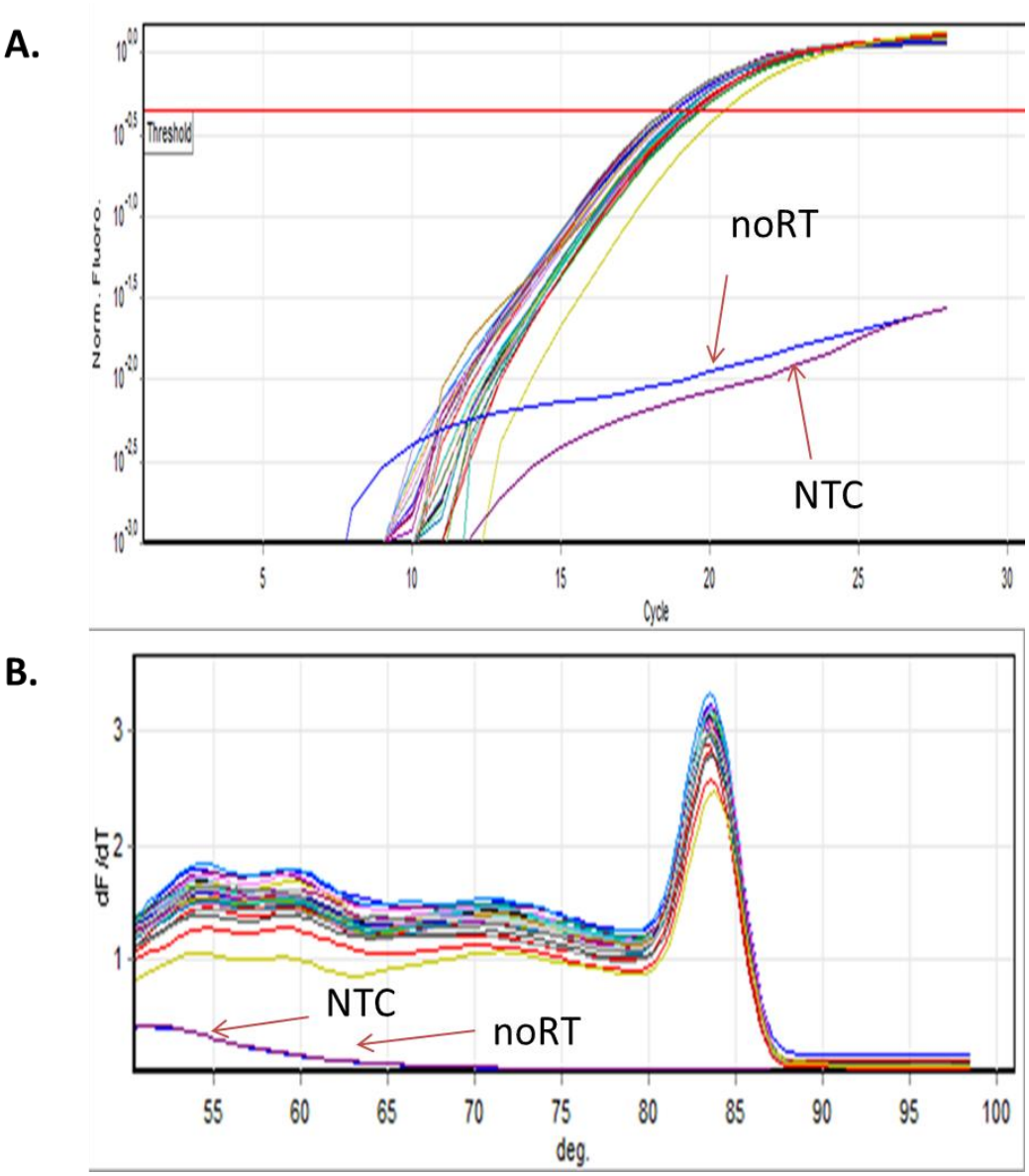

Figure E-19 The *GAPDH* RT-qPCR reaction curve (A) and melt curve (B) of OLA 2 group

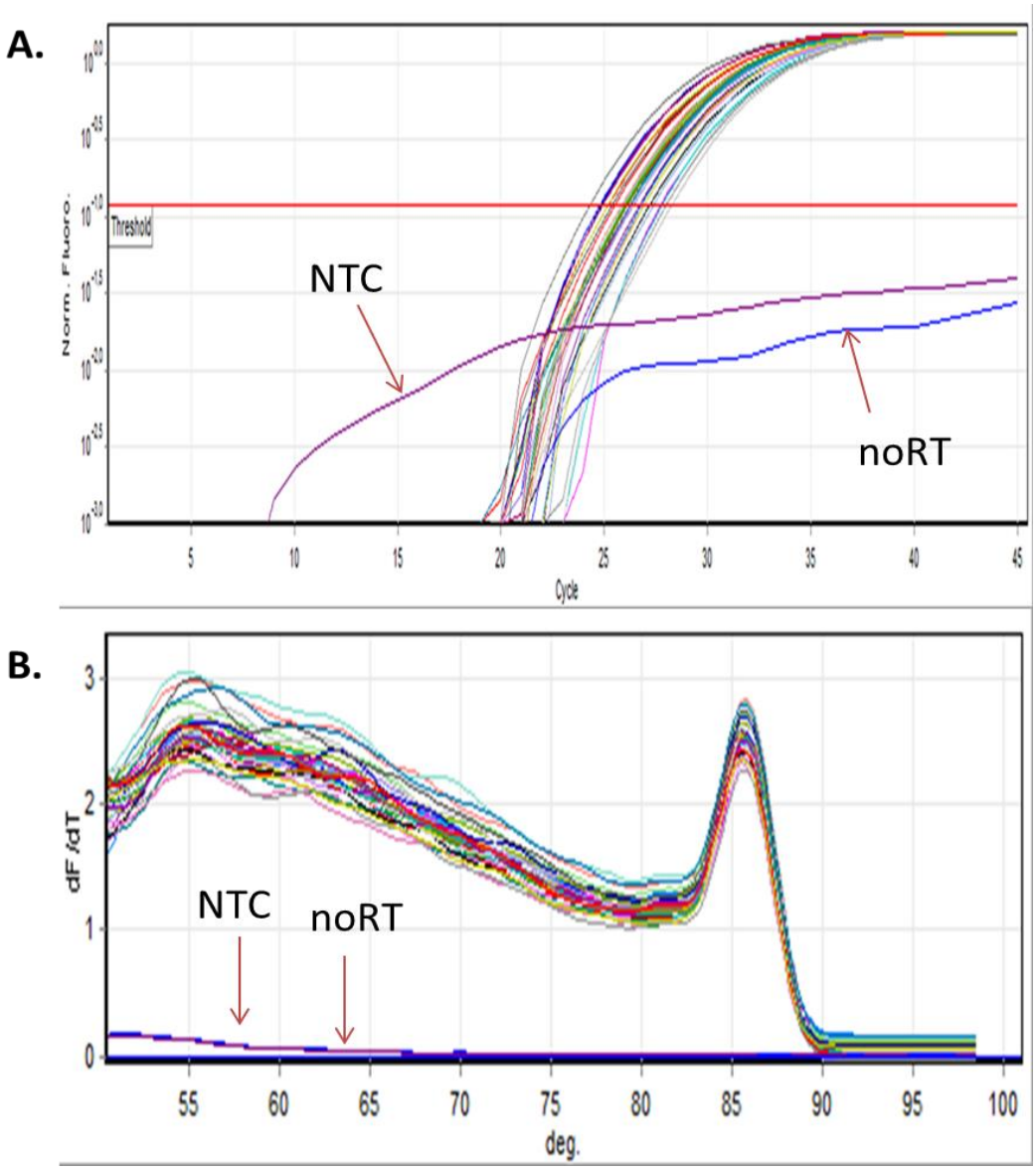

Figure E-20 The *POMC* RT-qPCR reaction curve (A) and melt curve (B) of OLA 2 group.

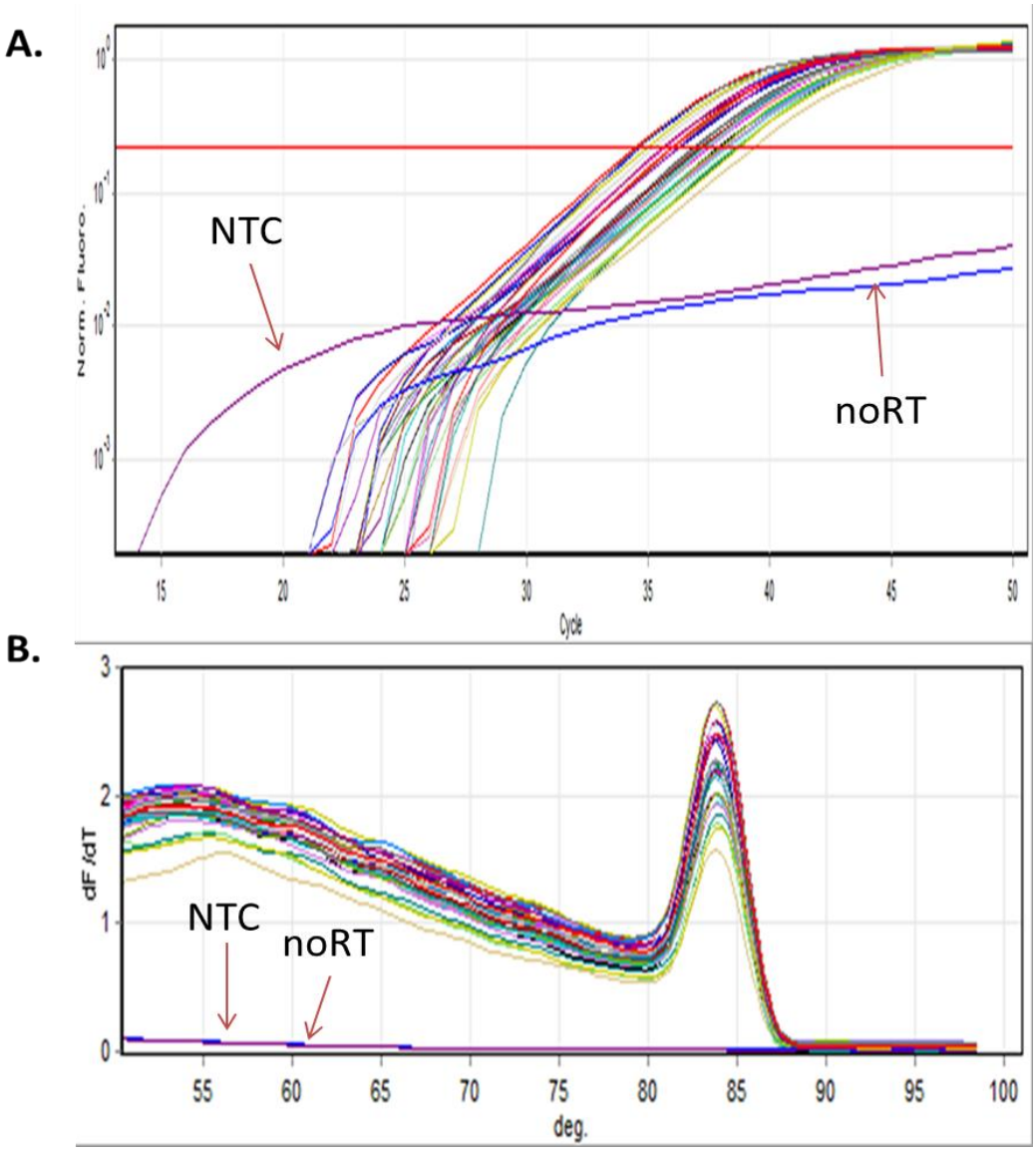

Figure E-21 The *NPY* RT-qPCR reaction curve (A) and melt curve (B) of OLA 2 group.

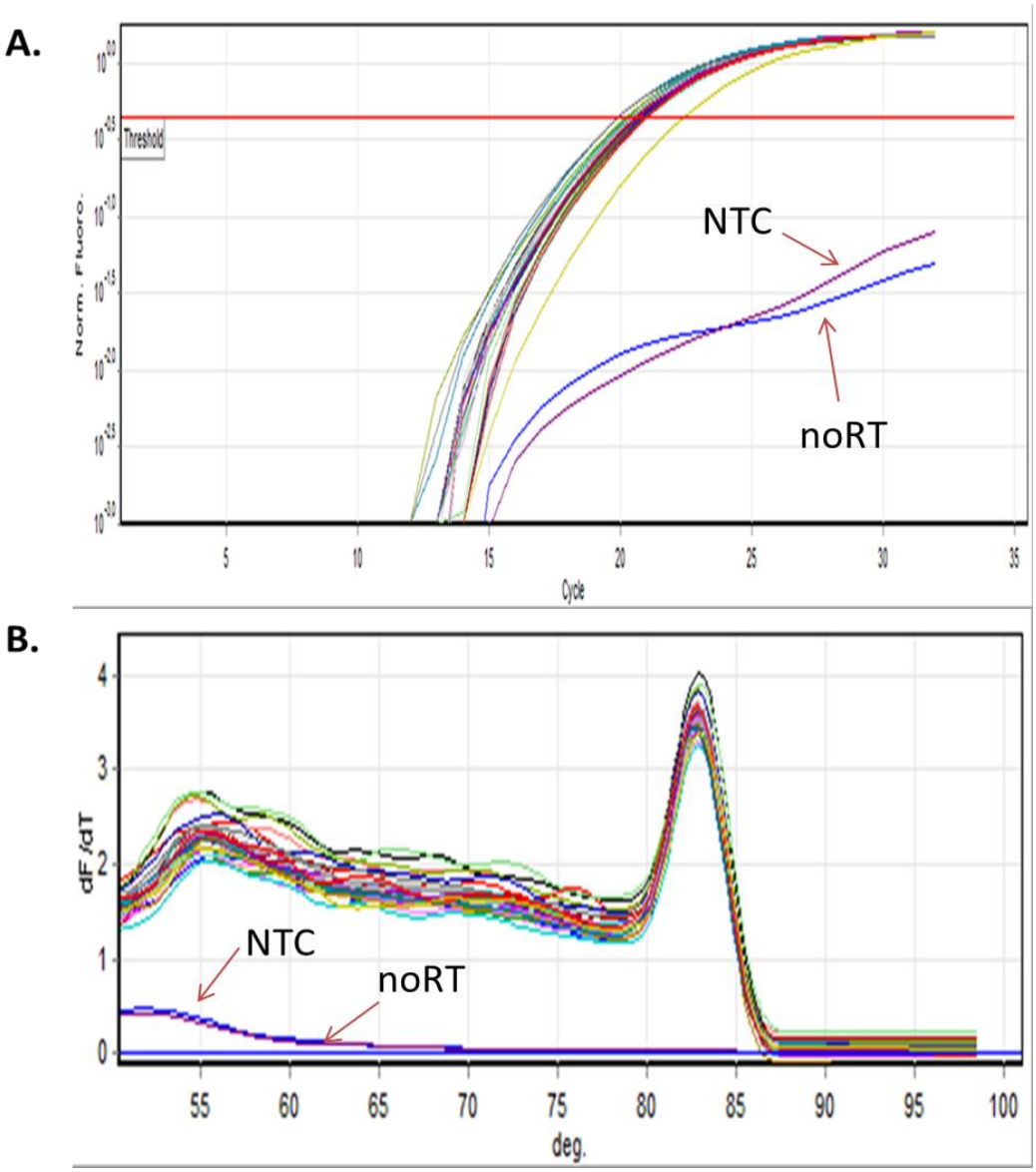

Figure E-22 The *GAPDH* RT-qPCR reaction curve (A) and melt curve (B) of OLA 3 group.

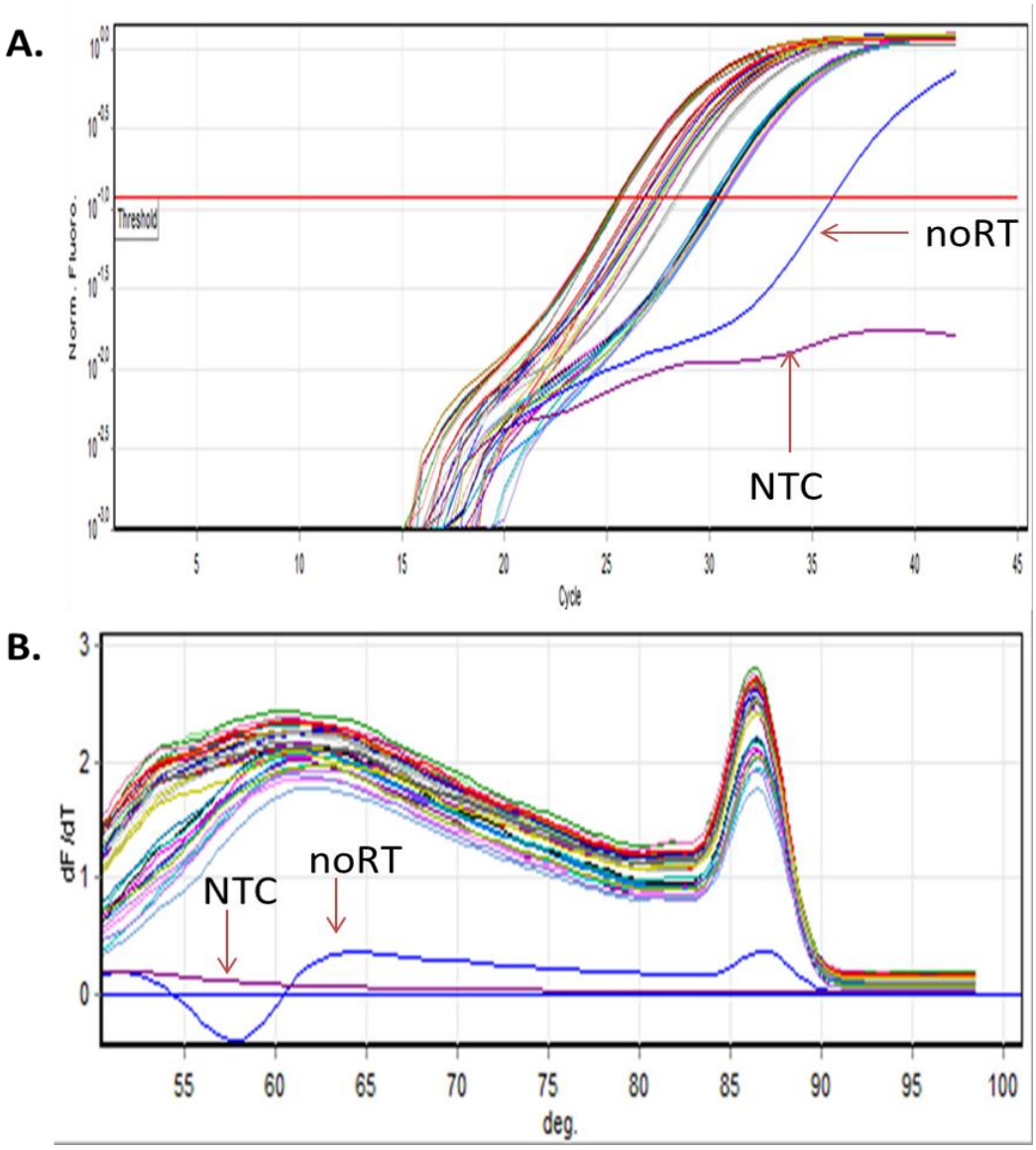

Figure E-23 The *POMC* RT-qPCR reaction curve (A) and melt curve (B) of OLA 3 group.

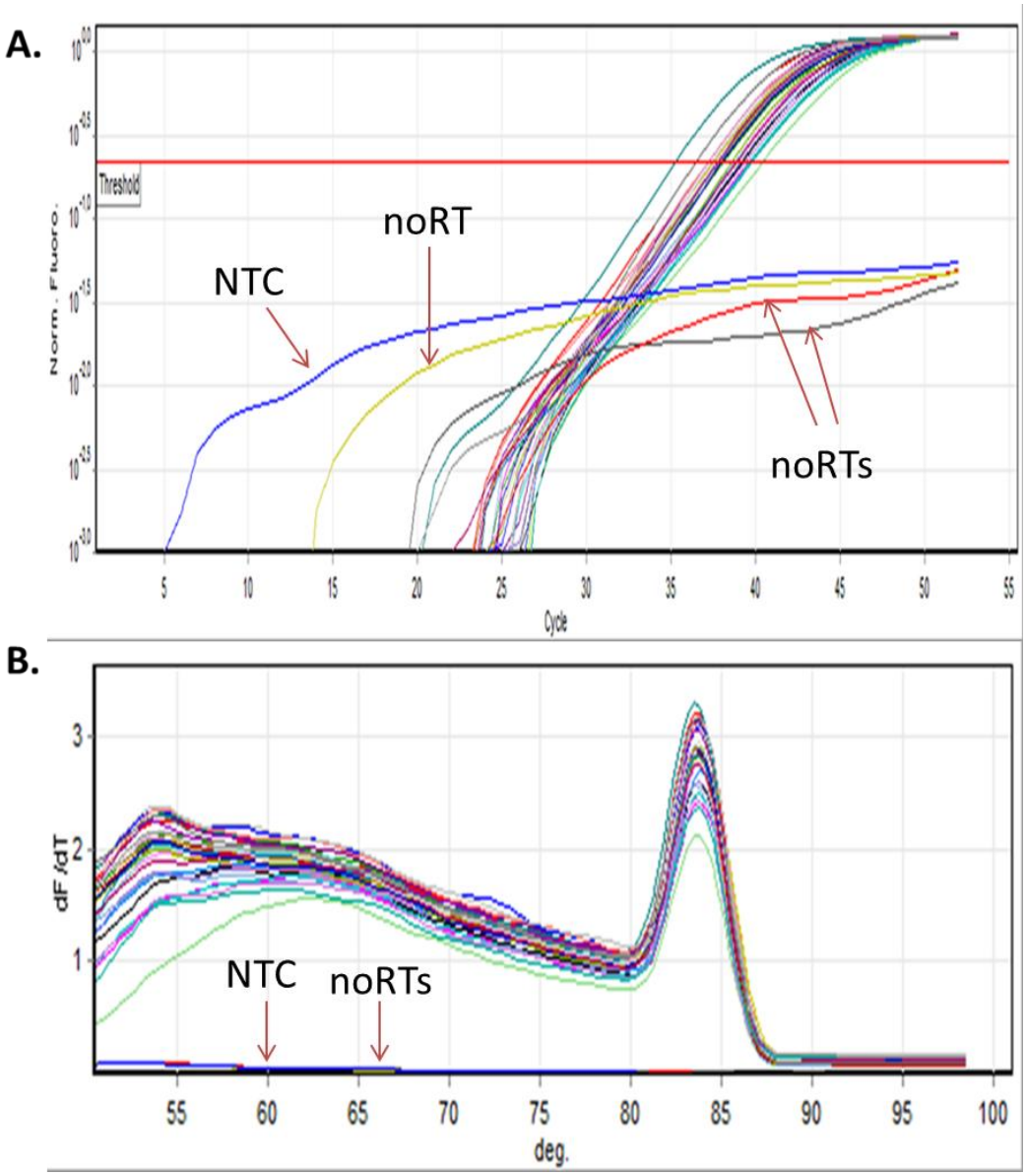

Figure E-24 The *NPY* RT-qPCR reaction curve (A) and melt curve (B) of OLA 3 group.

Table E-1 Mean Ct values of groups

Mean *GAPDH* Ct values of Groups				
CTRL 1	CTRL 2	OLA 1	OLA 2	OLA 3
19,88	19,06	19,41	18,82	20,72
19,68	19,14	19,26	18,61	21,04
20,02	19,35	19,17	19,64	20,75
19,68	19,43	19,26	19,32	20,49
19,72	18,53	19,38	19,44	21,02
19,55	18,77	19,57	19,00	20,61
19,33	18,23	18,77	19,47	20,77
19,47	18,73	19,47	19,16	20,17
18,90	18,93	19,43	18,66	20,81
19,87		19,31	18,65	20,46
Mean *POMC* Ct values of Groups				
CTRL 1	CTRL 2	OLA 1	OLA 2	OLA 3
26,13	26,10	26,67	25,08	26,94
25,84	25,36	27,06	26,82	30,41
25,54	24,50	27,14	25,97	25,67
25,27	26,79	28,09	27,61	30,42
24,99	24,21	25,36	25,97	27,61
25,91	26,15	27,78	26,39	30,72
24,78	24,88	25,93	26,19	25,59
27,70	26,20	29,98	26,21	30,23
24,07	25,26	25,43	24,92	27,52
26,88		29,26	28,12	28,44
Mean *NPY* Ct values of Groups				
CTRL 1	CTRL 2	OLA 1	OLA 2	OLA 3
32,83	37,86	35,77	34,65	37,47
33,31	37,49	36,19	35,65	38,97
32,75	38,09	37,68	37,34	37,60
33,35	38,69	38,48	37,73	39,47
32,27	38,07	37,99	38,38	38,98
32,95	38,91	38,32	37,31	39,08
32,07	37,07	36,40	37,52	37,55
31,82	38,41	38,96	37,49	38,70
31,74	37,77	36,32	36,01	37,85
32,39		39,52	37,15	37,71

APPENDIX F

IDENTIFICATION CODES OF RATS

Table F-1 Identification codes of rats in each group.

Group IDs	CTRL 1	CTRL 2	OLA 3	OLA 4	OLA5
Rat IDs	C1R1	C4R1	C7R1	C10R1	C13R1
	C1R2	C4R2	C7R2	C10R2	C13R2
	C1R3	C4R3	C7R3	C10R3	C13R3
	C1R4	C4R4	C7R4	C10R4	C13R4
	C2R1	C5R1	C8R1	C11R1	C14R1
	C2R2	C5R2	C8R2	C11R2	C14R2
	C2R3	C5R3	C8R3	C11R3	C14R3
	C3R1	C6R1	C9R1	C12R1	C15R1
	C3R2	C6R2	C9R2	C12R2	C15R2
	C3R3	C6R3	C9R3	C12R3	C15R3

APPENDIX G

TESTIS WEIGHTS

Table G-1 Testis and final body weights measured on the sacrifice day. No significant differences were found between groups.

Group ID	Sample ID	Testis Weight (g)	Animal weight (g)	Testis/Body Weight
CTRL 1	C1R1	3,75	465,00	0,008
	C1R2	3,95	473,00	0,008
	C1R3	4,13	543,00	0,008
	C1R4	4,78	620,00	0,008
	C2R1	3,50	515,00	0,007
	C2R2	3,88	582,00	0,007
	C2R3	2,90	574,00	0,005
	C3R1	3,16	493,00	0,006
	C3R2	4,06	644,00	0,006
	C3R3	2,52	522,00	0,005
CTRL 2	C4R1	3,56	472,00	0,008
	C4R2	4,80	470,00	0,010
	C4R3	3,95	482,00	0,008
	C4R4	3,17	479,00	0,007
	C5R1	3,58	510,00	0,007
	C5R2	3,51	462,00	0,008
	C5R3	3,35	506,00	0,007
	C6R1	3,75	525,00	0,007

Figure G-1 (Continued)

CTRL 2	C6R2	3,16	558,00	0,006
	C6R3	3,13	495,00	0,006
OLA 1	C7R1	4,43	512,00	0,009
	C7R2	4,55	492,00	0,009
	C7R3	4,23	498,00	0,008
	C7R4	4,34	523,00	0,008
	C8R1	3,50	548,00	0,006
	C8R2	3,54	528,00	0,007
	C8R3	3,04	610,00	0,005
	C9R1	4,41	540,00	0,008
	C9R2	3,25	434,00	0,007
	C9R3	2,85	577,00	0,005
OLA 2	C10R1	3,16	394,00	0,008
	C10R2	3,81	425,00	0,009
	C10R3	3,51	550,00	0,006
	C10R4	4,72	465,00	0,010
	C11R1	4,86	498,00	0,010
	C11R2	3,98	572,00	0,007
	C11R3	2,98	498,00	0,006
	C12R1	3,16	480,00	0,007
	C12R2	3,13	473,00	0,007
	C12R3	4,33	486,00	0,009
OLA 3	C13R1	3,56	480,00	0,007
	C13R2	3,10	354,00	0,009
	C13R3	3,50	495,00	0,007
	C13R4	3,25	470,00	0,007
	C14R1	3,80	512,00	0,007
	C14R2	3,07	432,00	0,007
	C14R3	3,86	497,00	0,008
	C15R1	3,67	438,00	0,008
	C15R2	3,45	472,00	0,007
	C15R3	3,18	450,00	0,007